RECLAMATION

Managing Water in the West

Sediment Model for the Middle Rio Grande – Phase 1

San Acacia Diversion Dam to Elephant Butte Reservoir

U.S. Department of the Interior
Bureau of Reclamation

December 2004

U.S. Department of the Interior
Mission Statement

The mission of the Department of the Interior is to protect and provide access to our Nation's natural and cultural heritage and honor our trust responsibilities to Indian tribes and our commitments to island communities.

Mission of the Bureau of Reclamation

The mission of the Bureau of Reclamation is to manage, develop, and protect water and related resources in an environmentally and economically sound manner in the interest of the American public.

Sediment Model for the Middle Rio Grande – Phase 1

San Acacia Diversion Dam to Elephant Butte Reservoir

Authored by

Christopher L. Holmquist-Johnson
Hydraulic Engineer
Sedimentation and River Hydraulics Group, D-8540
Technical Service Center
Denver, CO

Peer Reviewed by

Christi Young, P.E., Blair Greimann, Ph.D., P.E., and Paula Makar, P.E.
Hydraulic Engineers
Sedimentation and River Hydraulics Group, D-8540
Technical Service Center
Denver, CO

Outside Peer Reviewed by

Jianchun Haung
Research Scientist
Colorado State University
Fort Collins, CO

U.S. Department of the Interior
Bureau of Reclamation
Technical Service Center
Denver, Colorado

December 2004

Acknowledgements

The following persons contributed to this report:

Field Data Collection:
Travis Bauer, Kent Collins, Robert Hilldale, Walter Johnson, Paula Makar, Tony Shanahan, Socorro Field Office, and Albuquerque Area Office. Contractors: Tetra Tech Inc.

Aerial Photography/Planform Interpretation:
Jan Oliver.

Figure Preparation:
Travis Bauer, Blair Greimann, and Paula Makar.

Data Analysis Checking:
Travis Bauer, Jianchun Huang, Blair Greimann, and Robert Hilldale.

Report Writing:
Travis Bauer, Jaci Gould, Blair Greimann, and Paula Makar.

Software Development and Support:
Blair Greimann, and Jianchun Huang.

Technical Consultation:
Ted Yang, Drew Baird, and Tim Randle.

Report Reviews:
Blair Greimann, Jianchun Huang, Paula Makar, and Christi Young.

Funding:
Science Subcommittee of the Middle Rio Grande Endangered Species Act Collaborative Program, Albuquerque Area Office, and New Mexico Interstate Stream Commission.

Sediment Model for the Middle Rio Grande – Phase 1

San Acacia Diversion Dam to Elephant Butte Reservoir

Authored by

_____ DATE:_____

Christopher L. Holmquist-Johnson, Hydraulic Engineer
Sedimentation and River Hydraulics Group, D-8540

Peer Reviewed by

_____ DATE:_____

Christi Young, P.E., Hydraulic Engineer
Sedimentation and River Hydraulics Group, D-8540

_____ DATE:_____

Blair Greimann, Ph.D., P.E., Hydraulic Engineer
Sedimentation and River Hydraulics Group, D-8540

_____ DATE:_____

Paula Makar, P.E., Hydraulic Engineer
Sedimentation and River Hydraulics Group, D-8540

Outside Peer Reviewed by

_____ DATE:_____

Jianchun Haung, Research Scientist
Colorado State University

Executive Summary

The Rio Grande is not in equilibrium and continues to evolve in response to reduced peak flows, incoming sediment loads, and available floodplain. Geomorphology studies document a significant overall reduction in active channel width with accompanying vegetation encroachment; channel incision and loss of floodplain connectivity in some reaches, aggradation in others; general bed material coarsening with an increasing amount of the river changing from sand-bedded to gravel-bedded; river planform changing from a wide, multi-thread channel to a single-thread channel; and a general reduction in slope. All of these trends impact water delivery, valley drainage, and flood protection in addition to habitat for endangered species. A viable maintenance program that includes long-term strategies in addition to short-term emergency fixes is essential to reduce and potentially reverse many of these trends.

The Generalized Sediment Transport for Alluvial Rivers - One Dimension (GSTAR-1D) computer program, developed by Reclamation, and customized specifically for the Middle Rio Grande, was used to develop a sediment transport model from San Acacia Diversion Dam (Agg/Deg#1208) to Elephant Butte Reservoir (Agg/Deg#1792). This model is an available tool to help evaluate operations and maintenance options most likely to result in a stable river channel and minimal future maintenance requirements, thus improving the effectiveness of the river maintenance program. The future hydraulic geometry and morphology projections are valuable for assessment of river operations, maintenance, and restoration activities such as changing Low Flow Conveyance Channel diversions, adding sediment to degrading reaches, bank stabilization or terrace lowering.

Data from two periods, 1972 through 1992 and 1992 through 2002, were available to develop calibration parameters for the predictive model using historical hydrology and cross-section geometry. These two periods were typical of dry and wet hydrologic conditions respectively. The modified GSTAR-1D model reproduced the general shape and magnitude of the cumulative erosion and deposition in the main channel and the total cross-section for both calibration time periods. Additionally, the degradation in the mean bed profile downstream of San Acacia Diversion Dam as well as the aggradation in the mean bed profile near the reservoir was predicted fairly well. The average difference in mean bed elevation between the 1992 measured and the 1972 to 1992 simulation is only 0.26 ft. with a standard deviation of 1.75 ft. The average difference in mean bed elevation between the 2002 measured and the 1992 to 2002 simulation is only 0.94 ft. with a standard deviation of 2.05 ft. Though the calibration model results show trends similar to the historical record, it should be noted that the reach by reach volumes of deposition are somewhat different from the historical volumes of deposition.

The calibrated sediment model was used to predict future sedimentation for a 20-year period using 2002 data as the starting point with three predicted hydrologic regimes: wet, average, and dry. For this study, two maintenance alternatives were considered, one with sediment augmentation and one without. The predicted erosion and deposition for the 20-year period are, in general, greater than historical trends. The predictive model results without sediment augmentation show deposition in the main channel with the dry

hydrology and main channel erosion with the average and wet hydrology just downstream of San Acacia Diversion Dam. The predictive model results reveal that additional channel incision may take place upstream of Agg/Deg#1352 if the future hydrology is relatively wet or has many high peak flows and that the coarsening of bed material may continue. Downstream of Agg/Deg#1352, the model produced similar sediment erosion in the main channel for all three hydrologic scenarios. The main channel appears to be relatively stable downstream from Agg/Deg#1352 with a general trend towards channel incision at the furthest downstream cross sections. The most likely causes of the erosion in the main channel are the large unregulated peak flows present in the predictive hydrology combined with the low reservoir levels and temporary channel geometry. If these large flows occur, the channel capacity could increase throughout the entire river.

It is difficult to predict the effect of sediment augmentation because very few sediment loads at the San Acacia Floodway gage have been measured above 4,000 ft^3/s. If the current loads are unknown it is difficult to predict the effect of incremental change. Using data available for 2002, the 20-year predictive model results for the sediment augmentation plan show that increasing the sand load at San Acacia Diversion Dam has the potential to stop or reverse the erosion occurring in the upper reach. For dry hydrological conditions, no additional sediment may be necessary but for average to wet hydrology, the increase in sand load would have to be large, up to approximately several thousand acre-ft. However, collection of additional sediment data (suspended and bed material) to further define the incoming sediment rating curve, especially at higher discharges, and additional modeling of the upper reach is required to better predict the volume of sediment currently entering the reach. If fine sediment is added to the system, additional floodplain deposition may occur in the downstream portion of the reach, and/or additional deposition will occur in Elephant Butte Reservoir.

The overall bed changes in the predictive models appear to differ from the historical trends due to the magnitude and duration of the unregulated discharges present in the predictive hydrology and the presence of a perched channel system in the lower portion of the study reach. Therefore, additional analysis of the predictive hydrology should be conducted to determine if flow regulation should be included in generating future flows. Additionally, refining the sediment diffusion between the main channel and floodplains to better predict the main channel floodplain interaction in a perched system, and refinement of bed material mixing and armor layer development for Rio Grande conditions should be considered within the GSTAR-1D code for future use.

Table of Contents

ACKNOWLEDGEMENTS ..... **II**

EXECUTIVE SUMMARY ..... **V**

TABLE OF CONTENTS ..... **VII**

LIST OF FIGURES ..... **IX**

LIST OF TABLES ..... **XII**

1 INTRODUCTION **1**

2 BACKGROUND **3**

2.1 HISTORICAL AND CURRENT REACH CONDITIONS 3

2.1.1 Construction and Maintenance Practices *3*

2.1.2 Hydrology *6*

2.1.3 Sediment/Geology *12*

2.1.4 Geomorphology *13*

2.1.4.1 Width 13

2.1.4.2 Slope 17

2.1.4.3 River migration and sinuosity 19

2.1.4.4 Terraces 21

2.2 PROJECT OBJECTIVES 21

2.2.1 Data Collection *22*

2.2.2 Analysis of available data *22*

2.2.3 Sediment model development *22*

2.2.3.1 Customization of GSTAR-1D 22

2.2.3.2 Calibration 23

2.2.4 Future conditions with and without sediment augmentation *24*

3 DATA COLLECTION, ANALYSIS, AND MODEL DEVELOPMENT **25**

3.1 DATA COLLECTION 25

3.1.1 Surface bed material *25*

3.1.2 Cone penetrometer and soil auger data *25*

3.1.3 Arroyo cross-section survey *26*

3.1.4 Agg/Deg photogrammetric data and Field Survey Data *26*

3.2 DATA ANALYSIS AND MODEL INPUT 27

3.2.1 Cross-section Geometry *27*

3.2.2 Channel Capacity and Channel Erosion *32*

3.2.2.1 1972 to 1992 Period 32

3.2.2.2 1992 to 2002 Period 32

3.2.3 Sediment *34*

3.2.3.1 Main channel sediment 34

3.2.3.2 Tributary sediment inflow 37

3.2.4 Hydrology *37*

4 MODEL CALIBRATION 43

4.1 MODEL INPUT 43

4.1.1 Hydrology and Boundary Conditions 43

4.1.2 Cross-section Geometry 44

4.1.3 Sediment 45

4.1.4 Lateral Water and Sediment Inflow 47

4.1.5 Transport Calibration Parameters 48

4.2 SENSITIVITY ANALYSIS 48

4.2.1 Sediment Transport Equation 49

4.2.2 Incoming sediment load 49

4.2.3 Silt/clay transport parameters 50

4.2.4 Time Step 50

4.3 FINAL RESULTS 51

4.3.1 1972-1992 Final Results 51

4.3.2 1992–2002 Final Results 60

5 PREDICTIVE MODELING 69

5.1 NO ACTION OPTION 69

5.1.1 Model input 69

5.1.2 Hydrology and Boundary Conditions 69

5.1.3 Sediment 70

5.1.4 Results 72

5.2 SEDIMENT AUGMENTATION OPTION 85

6 CONCLUSION 87

REFERENCES 89

APPENDIX A - CHRONOLOGY OF SIGNIFICANT RIO GRANDE EVENTS

APPENDIX B – WATER AND SEDIMENT DISCHARGE DATA

APPENDIX C – HISTORICAL CROSS-SECTION PLOTS

APPENDIX D – HISTORICAL PLANFORM PLOTS

APPENDIX E – 1972-1992 CALIBRATION CROSS-SECTION PLOTS

APPENDIX F – 1992-2002 CALIBRATION CROSS-SECTION PLOTS

APPENDIX G – PREDICTED FUTURE CROSS-SECTION PLOTS

List of Figures

Figure 1: Site map of the Middle Rio Grande and the study area.....2
Figure 2: San Acacia floodway average monthly water volume. 7
Figure 3: San Marcial floodway average monthly water volume.....7
Figure 4: San Acacia floodway mean daily discharge.....8
Figure 5: San Acacia floodway cumulative water volume. 8
Figure 6: San Marcial floodway mean daily discharge. 9
Figure 7: San Marcial floodway cumulative water volume.....9
Figure 8: Elephant Butte Reservoir elevation.....10
Figure 9: Site map of major arroyos entering the Rio Grande in the San Acacia reach....11
Figure 10: Discharge and sediment difference between San Acacia and San Marcial.....13
Figure 11: Channel widths - San Acacia Diversion Dam to Arroyo Alamillo (1918 to 2001). 14
Figure 12: Channel widths - Arroyo Alamillo to Arroyo de la Parida (1918 to 2001).....14
Figure 13: Channel widths - Arroyo de la Parida to Arroyo de las Canas (1918 to 2001).15
Figure 14: Channel widths - Arroyo de las Canas to Hwy 380 Bridge (1918 to 2001).....15
Figure 15: Channel widths - Hwy 380 Bridge to Agg/Deg#1584 (1918 to 2001). 16
Figure 16: Channel widths - Agg/Deg#1584 to San Marcial (1918 to 2001).....16
Figure 17: Channel widths - San Marcial to Agg/Deg#1792 (1918 to 2001).....17
Figure 18: Historical mean bed between San Acacia Diversion Dam and Elephant Butte Reservoir. 18
Figure 19: Historical mean bed between San Acacia Diversion Dam and Escondida Bridge.....18
Figure 20: Historical mean bed between San Marcial and Elephant Butte Reservoir.....19
Figure 21: Historical active channel planform change. 20
Figure 22: Example of artificial berm removal.....29
Figure 23: 1992-2002 adjusted floodplain aggradation/degradation volumes. 30
Figure 24: Example of possible error in 1992 floodplain survey data.....31
Figure 25: 1972-1992 adjusted floodplain aggradation/degradation volumes. 31
Figure 26: 1972 – 2002 bankfull discharge comparison.....33
Figure 27: 1972 – 2002 change in bankfull discharge.....34

Figure 28: d_{50} of suspended sediment samples. 35
Figure 29: Average bed material gradation for San Acacia reach. 36
Figure 30: Total sediment load 1972 to 2002. 36
Figure 31: Mean daily discharges for 1972 to 2002. 37
Figure 32: Elephant Butte Reservoir elevations for 1972 to 2002.....38
Figure 33: Historical vs. predictive stochastic total water volume. 39
Figure 34: Generated stochastic mean daily discharge for dry hydrology. 39
Figure 35: Generated stochastic mean daily discharge for average hydrology. 40
Figure 36: Generated stochastic mean daily discharge for wet hydrology. 40
Figure 37: Generated stochastic Elephant Butte Reservoir elevations. 41
Figure 38: Historical vs. generated stochastic mean daily discharges. 41
Figure 39: Distribution of flows for calibration models. 44
Figure 40: Example cross-section with channel limits, levee, ineffective flow, and blocked obstruction designations. 45
Figure 41: Total sediment load with adjusted rating curve.....46
Figure 42: Affects of sediment transport equation on model results. 49
Figure 43: Affects of incoming sediment load on total sediment volume. 50
Figure 44: Change in total volume of sediment 1972-1992. 52
Figure 45: Cumulative total volume of sediment 1972-1992. 52
Figure 46: Change in main channel volume of sediment 1972-1992. 53
Figure 47: Cumulative main channel volume of sediment 1972-1992. 53
Figure 48: Change in floodplain volume of sediment 1972-1992. 54
Figure 49: Cumulative floodplain volume of sediment 1972-1992. 54
Figure 50: 1972-1992 change in mean bed. 55
Figure 51: 1972-1992 mean bed elevation profile. 56
Figure 52: 1972-1992 mean bed elevation difference. 56
Figure 53: Change in bed material size (d_{50}) during model simulation. 57
Figure 54: Plot of cumulative volume change by sediment type (Agg/Deg#1276). 58
Figure 55: 1972-1992 cross-section change at Agg/Deg#1214. 59
Figure 56: 1972-1992 cross-section change at Agg/Deg#1276. 59
Figure 57: 1972-1992 cross-section change at Agg/Deg#1494. 59
Figure 58: 1972-1992 cross-section change at Agg/Deg#1792. 60
Figure 59: Change in total volume of sediment 1992-2002. 61

Figure 60: Cumulative total volume of sediment 1992-2002. 61
Figure 61: Change in main channel volume of sediment 1992-2002 62
Figure 62: Cumulative main channel volume of sediment 1992-2002.....62
Figure 63: Change in floodplain volume of sediment 1992-2002 63
Figure 64: Cumulative floodplain volume of sediment 1992-2002.....63
Figure 65: 1992-2002 change in mean bed. 64
Figure 66: 1992-2002 mean bed elevation profile. 64
Figure 67: 1992-2002 mean bed elevation difference. 65
Figure 68: Change in bed material size (d_{50}) during model simulation. 66
Figure 69: Plot of cumulative volume change by sediment type (Agg/Deg#1276). 66
Figure 70: 1992-2002 cross-section change at Agg/Deg#1214. 67
Figure 71: 1992-2002 cross-section change at Agg/Deg#1276. 67
Figure 72: 1992-2002 cross-section change at Agg/Deg#1501. 68
Figure 73: 1992-2002 cross-section change at Agg/Deg#1792. 68
Figure 74: Distribution of flows for 20-year predictive models. 70
Figure 75: Adjusted total sediment load with capacity limits.....71
Figure 76: Change in total volume of sediment for 20-year projection.....73
Figure 77: Cumulative total volume of sediment for 20-year projection. 73
Figure 78: Change in main channel volume of sediment for 20-year projection. 74
Figure 79: Cumulative main channel volume of sediment for 20-year projection. 74
Figure 80: Change in floodplain volume of sediment for 20-year projection. 75
Figure 81: Cumulative floodplain volume of sediment for 20-year projection. 75
Figure 82: 20-year projected adjusted cumulative channel volume comparison.....76
Figure 83: 20-year projected adjusted cumulative floodplain volume comparison.....76
Figure 84: 20-year projected change in mean bed. 77
Figure 85: 20-year projected mean bed elevation profile (dry hydrology).....77
Figure 86: 20-year projected mean bed elevation profile (average hydrology).....78
Figure 87: 20-year projected mean bed elevation profile (wet hydrology). 78
Figure 88: Change in bed material size (d_{50}) during model simulation. 79
Figure 89: Plot of cumulative volume change by sediment type (Agg/Deg#1276). 80
Figure 90: 20-year projected cross-section change at Agg/Deg#1214. 81
Figure 91: 20-year projected cross-section change at Agg/Deg#1276. 81
Figure 92: 20-year projected cross-section change at Agg/Deg#1501. 81

Figure 93: 20-year projected cross-section change at Agg/Deg#1792. 82
Figure 94:20-year projected wet hydrology prior to end of model high flows.....82
Figure 95: 20-year projected wet hydrology mean bed comparison.....83
Figure 96: 20-year projected wet hydrology cumulative total sediment volume comparison. 83
Figure 97: 20-year projected wet hydrology cumulative channel sediment volume comparison. 84
Figure 98: 20-year projected wet hydrology cumulative floodplain sediment volume comparison. 84
Figure 99: 20-year projected cumulative total sediment augmentation comparison. 85
Figure 100: 20-year projected cumulative channel sediment augmentation comparison..86
Figure 101: 20-year projected cumulative floodplain sediment augmentation comparison.86

List of Tables

Table 1: Selected cross-sections used in sediment model. 28
Table 2: 1972 – 1992 bankfull discharge estimation. 32
Table 3: 1992 – 2002 bankfull discharge estimation. 33
Table 4: Sediment size over time (Makar and Strand, 2003). 35
Table 5: Flow statistics for calibration models. 43
Table 6: Adjusted total sediment load comparison. 46
Table 7: Incoming sediment load data from Modified Einstein calculations. 47
Table 8: Bed material for the San Acacia reach. 47
Table 9: Arroyo flow and sediment statistics. 48
Table 10: Flow statistics for hydrologic traces used in predictive modeling. 69
Table 11: Adjusted incoming sediment load data for predictive model. 71
Table 12: Bed material gradation for predictive models. 72

1 Introduction

The purpose of this project was to develop a comprehensive calibrated sediment transport model of the Middle Rio Grande from San Acacia Diversion Dam to Elephant Butte Reservoir (Figure 1). The Generalized Sediment Transport for Alluvial Rivers - One Dimension (GSTAR-1D) computer program, developed by Reclamation, and customized specifically for the Middle Rio Grande (Yang et al, 2004), was used. The resulting comprehensive sediment model was used to predict future sediment transport trends and will provide a valuable tool to analyze the impacts to channel geometry and sediment size from various future operation and maintenance alternatives.

Successful management of the Middle Rio Grande relies a great deal on predicting changes in channel geometry, sediment transport, and river planform while protecting and maintaining habitat during various operation and maintenance activities. The reduction of sediment supply to the Middle Rio Grande below Cochiti Dam, Isleta Dam, and San Acacia Diversion Dam to a lesser degree, is a factor in the recent trend of channel incision and narrowing. This incision and narrowing in the river (in this report, river and floodway are synomonous and channel is used to refer to the main channel of the river that transports the majority of the flow) causes the channel depth and velocity to increase. In many areas the river is coarsening from a sand bed to a gravel bed. The sediment supply reduction and the channel incision and narrowing generally results in the river planform changing from a wide multi-thread low flow channel to a single-thread channel with increased meandering tendencies.

The overall study reach for the Phase 1 Middle Rio Grande Sediment Model is from San Acacia Diversion Dam (AggDeg#1208) to the beginning of Elephant Butte Reservoir (AggDeg#1792). The study reach is referred to as the San Acacia reach. This report focuses on sediment models for the Middle Rio Grande for two calibration periods from 1972 through 1992 and 1992 through 2002, and future analysis for a twenty year period assumed to run from 2002 through 2022. The model inputs include cross-section geometry from San Acacia Diversion Dam to the lower end of Elephant Butte Reservoir to properly model the reservoir effects on the channel.

The purpose of modeling time periods 1972 through 1992 and 1992 through 2002 was to develop calibration parameters for the predictive model using historical hydrology and cross-section geometry. Following calibration procedures for the study reach, an analysis of future sediment trends on the Middle Rio Grande was performed using a sediment transport model based on 2002 data. The projected aggradation/degradation and streambed characteristics provide information to aid management planning to achieve goals regarding effective water delivery to Elephant Butte Reservoir and improving habitat for the Rio Grande silvery minnow (RGSM) and southwestern willow flycatcher (SWFL). Scenarios for the prediction of future sediment conditions used dry, wet, and average hydrologic regimes.

Figure 1: Site map of the Middle Rio Grande and the study area.

2 Background

The reduced sediment supply on the Middle Rio Grande has contributed significantly to the reduced habitat of the RGSM and SWFL. Past geomorphic studies of the Rio Grande found that the sediment discharge and physical channel features have changed significantly from historical conditions and that with the current sediment supply the river channel will continue to narrow, incise, and move toward a gravel bed channel (Lagasse, 1980; Reclamation, 2003; Makar and Strand, 2003). These morphological changes may reduce the amount of available habitat as well the creation of good habitat for both the RGSM and SWFL in the future. Sediment supply and transport studies are needed to analyze the effects of the current sediment supply on the Middle Rio Grande, and to determine the spatial and temporal change in geometry along the reach. A viable maintenance program is essential to reduce and potentially reverse many of these trends.

The San Acacia Reach, as seen on Figure 1, is approximately 80 miles long extending from San Acacia Diversion Dam to Elephant Butte Reservoir. Engineered structures/features in the study reach consist of the diversion dam, the generally parallel Low Flow Conveyance Channel (LFCC), levees, riverside railroad line, multiple sets of Kellner Jetty Jack lines, and multiple bridge crossings.

2.1 Historical and Current Reach Conditions

2.1.1 Construction and Maintenance Practices

The San Acacia Diversion Dam was originally constructed in 1934 by the Middle Rio Grande Conservancy District, and was later rehabilitated by Reclamation in 1958. The diversion dam currently diverts water into the Socorro Main Canal and the LFCC. It is a concrete gate structure 7.5 feet high and 700 feet long with 29 radial gates. There is the capacity to divert about 300 ft^3/s into the Socorro Main Canal and 2000 ft^3/s into the LFCC. (Reclamation 1982, Project Data Book.) The river channel bed immediately downstream of the dam is lined by boulder-sized sediment and rip-rap placed in the mid-1980s to protect the dam's apron.

The majority of the reach is confined by abandoned river surfaces, levees, and berms. The main levee was originally constructed from the LFCC spoils in the 1950s and is located on the west (right) side of the river. Smaller, unconnected spoil piles that act as local levees/berms are located throughout the reach, mostly on the right bank. These spoils appear to originate from realignment efforts of the floodway during the building of the LFCC (Reclamation, 2003).

The LFCC (which extends from AggDeg#1208 to AggDeg#1792) was constructed by Reclamation in the 1950s to aid delivery of water to Elephant Butte Reservoir. It is a part of the Middle Rio Grande Project as authorized by congress in the Flood Control Acts of 1948 and 1950. The LFCC is a man-made channel located on the west side of the Rio Grande and is designed to convey water from San Acacia Diversion Dam to Elephant Butte Reservoir. The intent of the LFCC was to carry the flows of the Rio Grande in an efficient manner with minimum losses. The design capacity of the LFCC was 2,000 ft^3/s, but in practice, diversions greater than 1,800 ft^3/s have rarely occurred.

The LFCC was completed up to San Acacia Diversion Dam in 1959. During the 1960s to 1970s the entire river flow was carried in the LFCC much of the time; only during periods of high flow in the spring and occasionally during the summer monsoons was there flow in the river. The lower 15 miles of the LFCC were inundated and filled with sediment as the reservoir pool rose in the early 1980s. This prevented maintenance of a suitable outfall into the reservoir and therefore LFCC diversions were stopped in March 1985. Since then, with minor exceptions, the LFCC has carried only drainage and irrigation return flows. The LFCC continues to provide water to the Bosque del Apache National Wildlife Refuge, and provides supplemental water to the Middle Rio Grande Conservancy District, Socorro Division (Gorbach, 1999).

From the mid-1950s to mid-1960 several Kellner Jetty Jacks were installed in the historical floodplain along the levee in order to narrow and straighten the channel and protect the levee from bank erosion and channel avulsions. The Kellner Jetty Jack fields caused sediment deposition, allowing vegetation to grow and banks to form, resulting in a narrower channel that was more efficient in the transport of water and sediment.

Following the drought of the 1950s and prior to 1962 several bends in the Rio Grande were straightened to shorten the length of the river and improve water delivery efficiency to Elephant Butte Reservoir. Additional bend removal activities occurred again from 1972 to 1992. After these large-scale channel modifications were completed, the most common form of channel maintenance in this reach consisted of removal of vegetation debris in the channel and clearing of riparian vegetation to create more conveyance capacity in the Floodway. Beginning in the mid-1980s when maintenance floodway clearing was discontinued, the deposition area has become vegetated with many dense stands of tamarisk, willow, and cottonwood.

The AT&SF Railroad Bridge near the San Marcial gaging station (AggDeg#1701) was originally constructed around 1895 and is located about 8 miles upstream of high water pool of Elephant Butte Reservoir. Before 1920, the railway crossed the river on a steel bridge about a half mile upstream from where the present bridge is located. During a flood in 1920, the river shifted to a new channel, breaching the railway embankment at the site of the present bridge. In 1930 the railroad company raised the tracks nine feet due to sedimentation and in 1943 the railroad company raised the tracks and bridge another 12 feet due to sedimentation occurring during the flood of 1941 and 1942 (Gorbach, 1999). Records going back to before 1900 indicate that there has been a rapid rate of sedimentation occurring over the past century in this area and continuing downstream into Elephant Butte Reservoir. The continued sedimentation has resulted in reduced hydraulic capacity under the bridge and excessive channel filling near the entrance to Elephant Butte Reservoir. The reduced hydraulic capacity under the bridge has become a controlling point for high flow releases from Cochiti Dam. The shifts in the hydrograph from operations as Cochiti Dam have caused significant impacts to the Rio Grande throughout the Middle Rio Grande valley.

During the summer of 1963, a pilot channel with 1,000 ft^3/s capacity and 14,300 feet long was constructed from the end of the LFCC to a point about one mile upstream of the Narrows. Draglines were used to keep the LFCC clear of sediment, and through the late 1960s the pilot channel was reported to be functioning satisfactorily (Reclamation, Middle Rio Grande Project Histories). This reach continues to undergo aggradation due

to several factors. These factors include high sediment loads that aren't fully transported because of the existing flat valley slope, clay deposits that are highly cohesive, and the thick vegetation growth in the floodplain that continues to grow aggressively and trap sediment. These conditions exacerbate the disconnection that can occur between the river and the reservoir pool during times of rapidly declining reservoir storage. Therefore, temporary channels are routinely constructed for maintenance purposes, most recently in 1991, 1996, and 2002.

In 1997 the river again became disconnected, and in the summer of 2000 extensive work started to reconnect the river to the reservoir. By the spring of 2002, a channel with a width of at least 50 feet had been constructed for 7 miles, and the LFCC outfall was connected to the reservoir through this channel (Collins, 2003). During 2003, the reservoir pool had dropped below the Narrows (EB#51), allowing for much of the temporary channel to dry out and providing for easier excavation than when it was wet and boggy. By the spring of 2003, an average width along the channel of 180 feet was completed (Smith, 2003).

In February of 2003, maintenance strategies were further expanded in the Biological Assessment of Bureau of Reclamation's Water and River Maintenance Operations, Army Corps of Engineers' Flood Control Operation, and Related Non-Federal Actions on the Middle Rio Grande, New Mexico, March 1, 2003 – February 28, 2013 (BA). The BA emphasized that geomorphic analysis and investigations are performed prior to implementation of river maintenance activities to identify the underlying geomorphic causes of problems and to project future river conditions using available qualitative and quantitative methods. Activities were categorized by their primary objective in the BA, the categories included: river maintenance activities, sediment removal, vegetation management, levee maintenance, and access and construction requirements. The river maintenance techniques itemized in the BA include traditional techniques as well as recent advances, many are considered bioengineering techniques. The list includes:

- Terrace and overbank lowering (re-establish floodplain hydrologic connectivity)
- channel widening/bank destabilization
- woody debris snags and boulder placements
- high flow side channels
- removal of lateral confinement
- vegetation planting
- gradient restoration facilities (GRFs)
- oxbow re-establishment
- non-native vegetation clearing and floodplain expansion
- channel realignment/ channel avulsions/ pilot channel work
- river bar/ island maintenance
- jetty/ snag removal
- toe revetment plantings
- native material bank stabilization – rock and/or log spurs
- revetments
- curve shaping
- stabilized soil, manufactured revetment units, and cellular confinement systems
- reasonable alternative techniques (new or future methods not identified above)

Environmental constraints to maintain or improve habitat for the two listed endangered species, the RGSM and the SWFL, often conflict and eliminate consideration of many historical, often more economical, maintenance practices. Revised river maintenance techniques in the BA will have more desirable effects on both the river geomorphology and the terrestrial and aquatic environment than historical techniques. A time line of maintenance along the Rio Grande is provided in Appendix A (Makar and Strand, 2003).

2.1.2 Hydrology

Precipitation in the Rio Grande watershed comes in two forms: snow and rain. Although snowfall occurs in the area of the study reach, it is short-lived and does not usually produce large flow events in the channel whereas snowfall in the headwaters provides water for spring runoff. Local rainfall from thunderstorms produce short-lived sporadic flow events in the Rio Grande, and may occur throughout the year but most often in July, August, and September (Reclamation, 2003).

There are two sites along the San Acacia Reach that have stream flow gages, both are operated and maintained by the U.S. Geological Service. River discharge and suspended sediment loads are measured at two locations at each site; a river gage and a LFCC gage. Only the floodway gages are used because this study does not include modeling of the LFCC. The Rio Grande Floodway at San Acacia gage (08354900) provides stream discharge records back to 1958 (Figure 2 - Figure 4), and suspended sediment discharge data back to 1960. The Rio Grande Floodway at San Marcial gage (08358400) provides stream discharge records back to 1949 (Figure 3 - Figure 6), and suspended sediment discharge data back to 1959. Elephant Butte Reservoir, located at the end of the project reach, provides flood control and water storage for irrigation. The elevation of the reservoir pool (Figure 8) affects the aggradation/degradation that occurs in the lower section of this reach. When the reservoir is full, many of these cross-sections are inundated and backwater effects from the reservoir progress farther upstream.

The flow in the Rio Grande varies from year to year depending on weather, operation of reservoirs and diversions. There is a typical pattern through the year of relatively constant low flows from November to February and an increase in flow from snowmelt generally begins in March, continues through June, with the peak often in May (Figure 2 and Figure 3). Diversion and flood control activities occur during this period.

Figure 4 through Figure 7 shows the variation in discharge over time. The data shows the channel experienced a fairly dry hydrology until the early 1980s followed by a generally wetter period that lasted until the late-1990’s. From the late-1990s to the present, the hydrology has continued to decrease and remain fairly dry. Note the effect of the LFCC diversions on the cumulative water volume at the San Acacia and San Marcial Floodway gages prior to the 1980’s. Flow was diverted from the floodway to the LFCC in order to provide an efficient method of water delivery to Elephant Butte Reservoir. As a result, the cumulative water volume plotted in Figure 5 and Figure 6 remains fairly constant until the early 1980’s. At this time there were no diversions made to the LFCC because the downstream outfall of the LFCC was no longer maintained. Therefore, all flows were transported in the floodway rather than the LFCC resulting in the increase in the cumulative water volume plotted in Figure 5 and Figure 6.

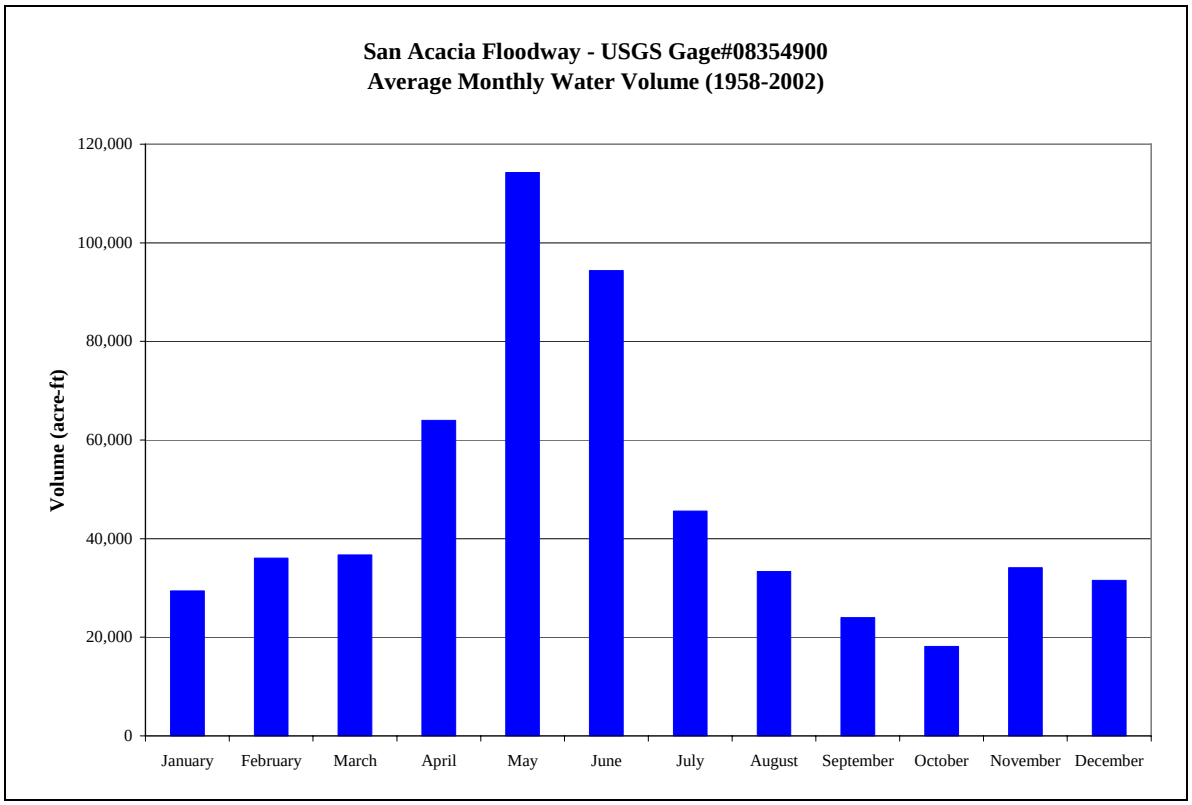

Figure 2: San Acacia floodway average monthly water volume.

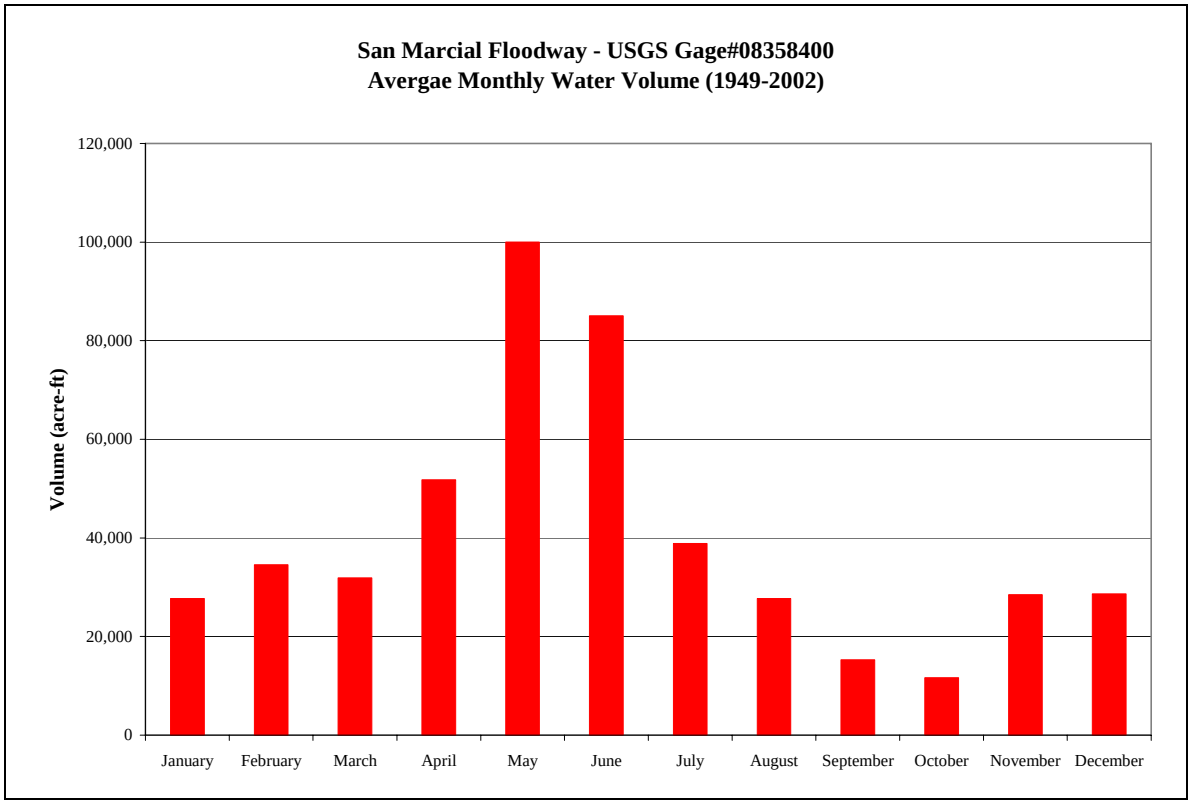

Figure 3: San Marcial floodway average monthly water volume.

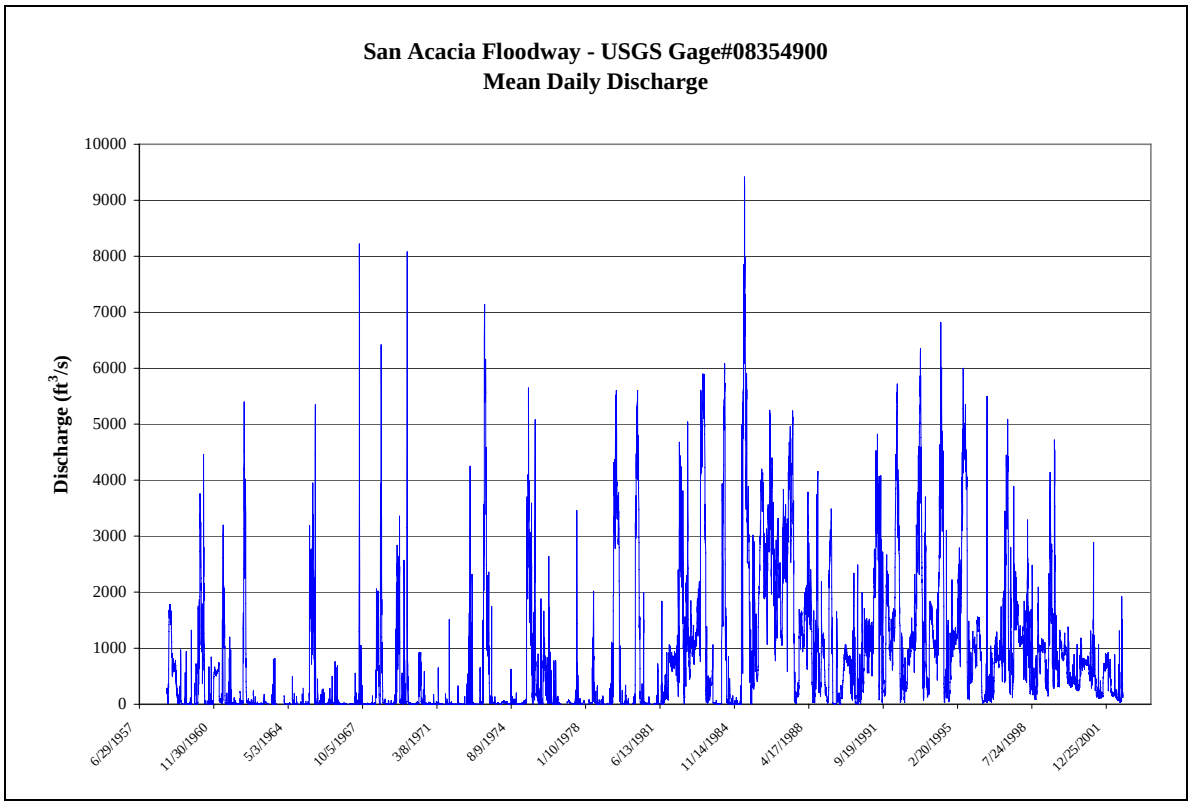

Figure 4: San Acacia floodway mean daily discharge.

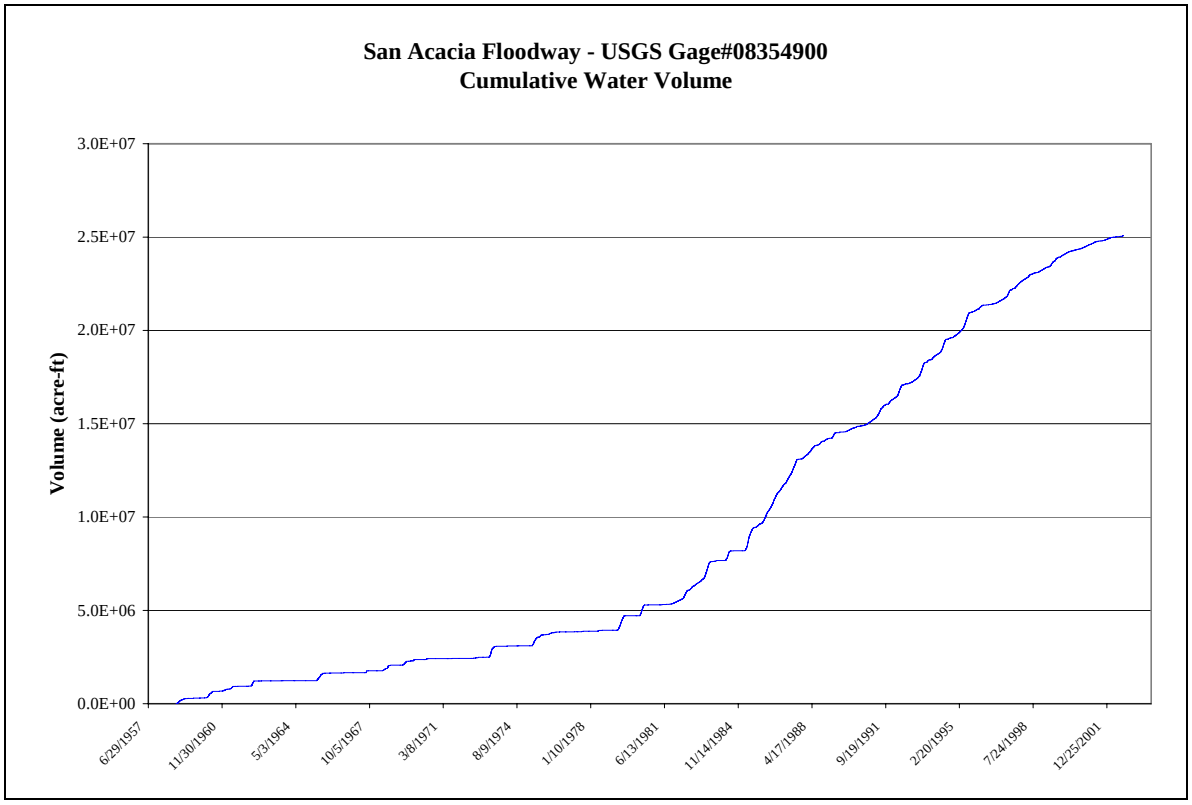

Figure 5: San Acacia floodway cumulative water volume.

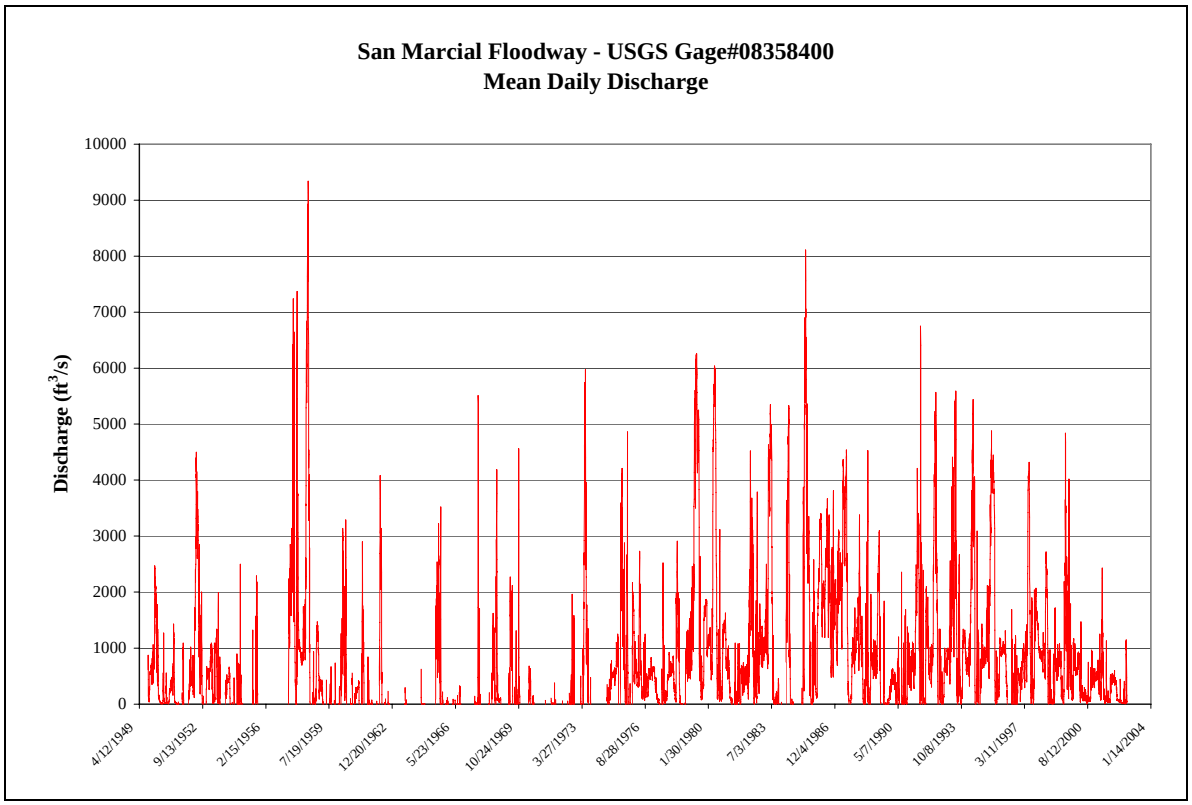

Figure 6: San Marcial floodway mean daily discharge.

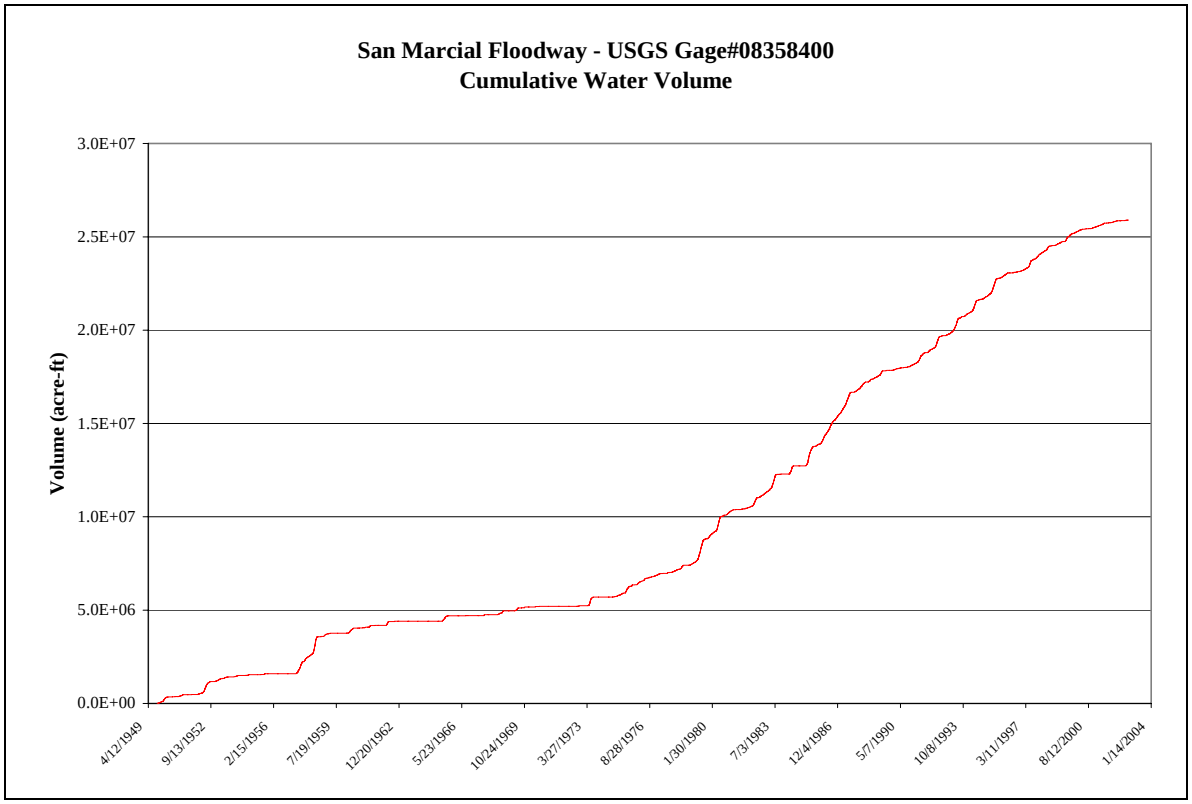

Figure 7: San Marcial floodway cumulative water volume.

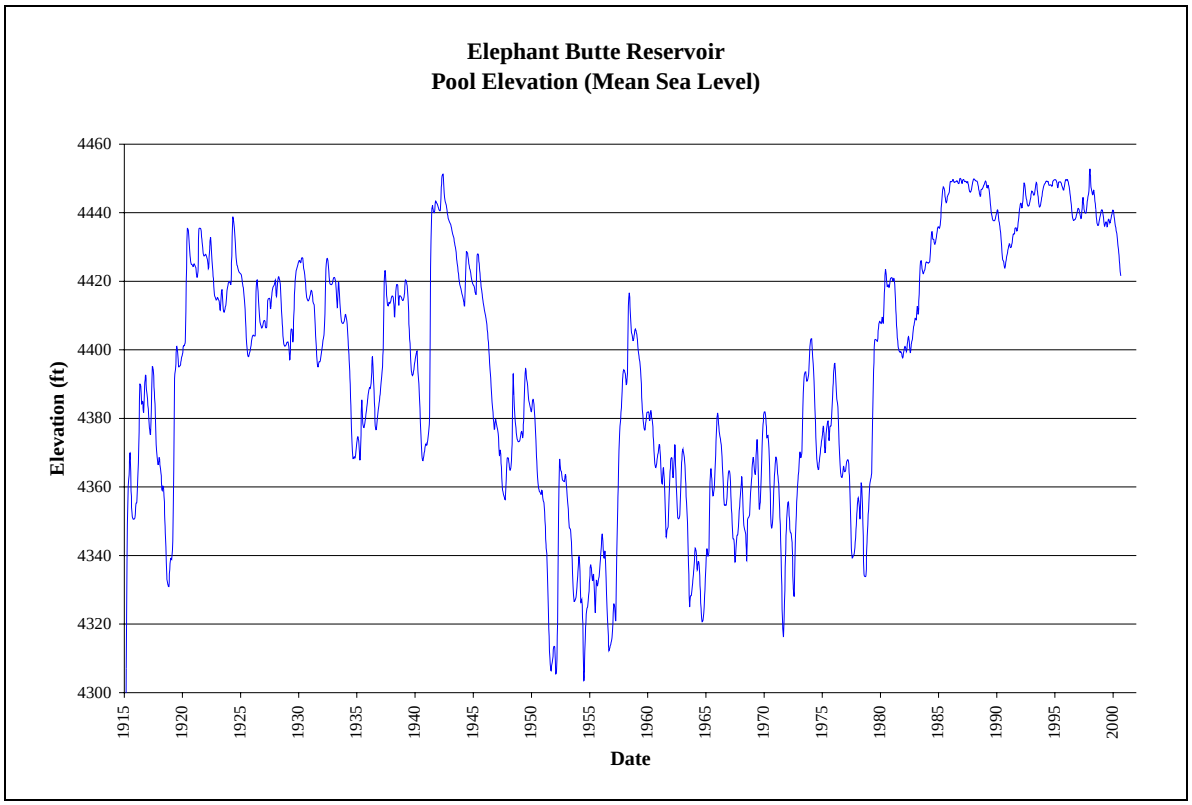

Figure 8: Elephant Butte Reservoir elevation.

There are several ephemeral ungaged tributaries in the San Acacia Reach (Figure 9). Tributaries draining to the Rio Grande on the east side of the river that were included in the model consist of Arroyo de Alamillo (AggDeg#1246), Arroyo de la Parida (AggDeg#1312), and Arroyo de las Canas (AggDeg#1398). Runoff from the west of the Rio Grande is primarily intercepted by the Middle Rio Grande Conservancy District's canals and drains, and the LFCC except for two points of direct connection to the Rio Grande at the North Socorro Diversion Channel (NSDC) (AggDeg#1330), and Brown Arroyo (AggDeg#1409).

The compilation of measured Rio Grande water discharge and suspended sediment loads for the gaging stations is presented in Appendix B. The source of these data was from Makar and Strand (2003); the data was expanded to include 1996 to 2002. The sources of these data were the records compiled by the International Boundary and Water Commission and the U.S. Geological Survey (USGS) and reported by the latter agency in its Water Supply Papers and online database.

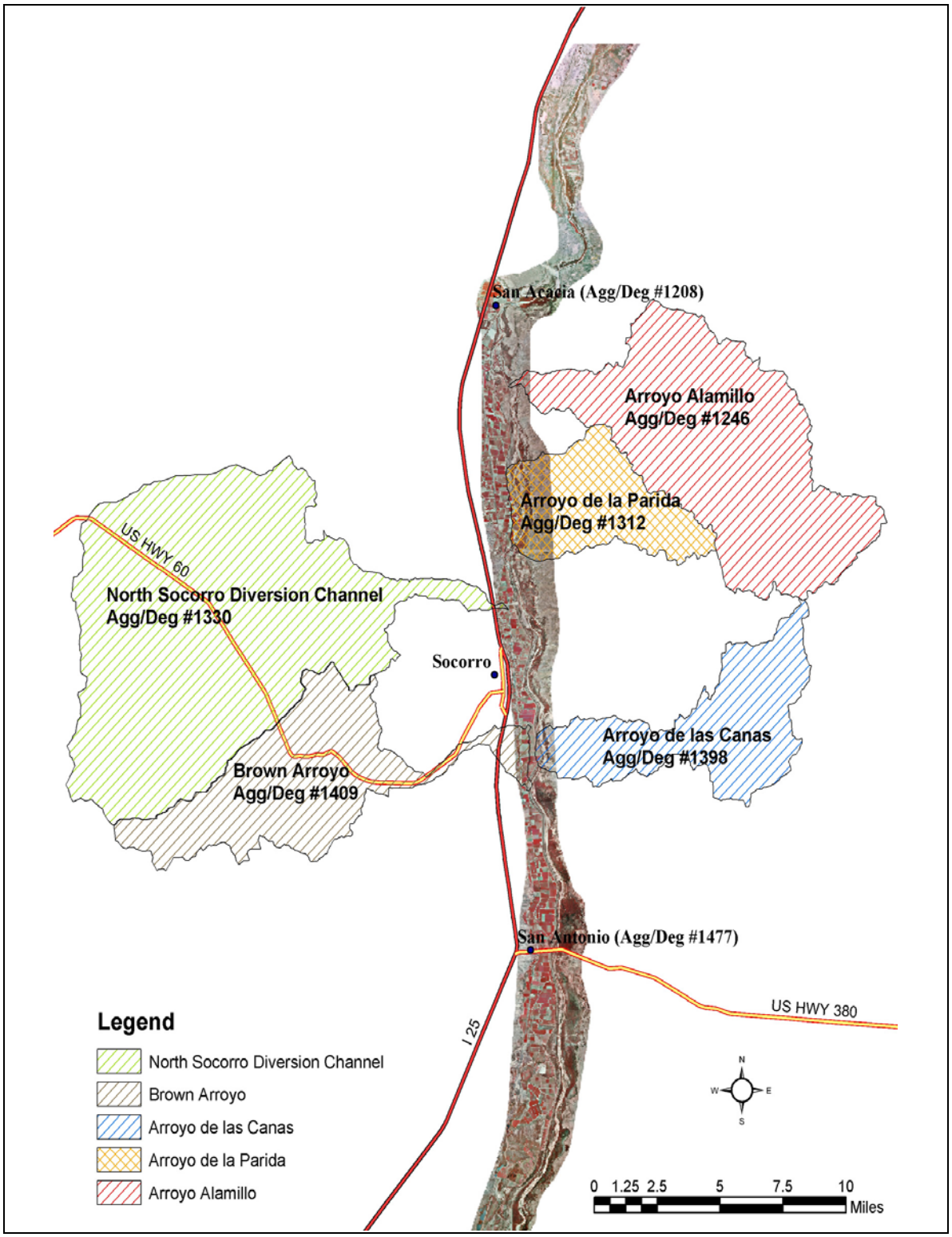

Figure 9: Site map of major arroyos entering the Rio Grande in the San Acacia reach.

2.1.3 Sediment/Geology

Suspended sediment discharge data in the San Acacia reach are available from the San Acacia and San Marcial USGS gaging stations as listed above. The Rio Grande Floodway at San Acacia (08354900) provides suspended sediment discharge data back to 1960. The Rio Grande Floodway at San Marcial (08358400) provides suspended sediment discharge data back to 1959. Bed material data have been collected periodically at the USGS San Acacia gaging station from 1966 to 2002 and along Reclamation's San Acacia and Socorro range lines from 1995-1999. These data are used here for two purposes: to estimate the change in particle size distribution on the channel bed over time, and to estimate the sand load from upstream sources.

The suspended sediment and bed material samples are the basis for computing total sediment loads (i.e. the sum of the measured suspended load, the suspended sediment moving below the sampler nozzle in the unmeasured zone, and the sediment moving as bedload) in the river. The method of total load computation is the Modified Einstein Procedure (Colby and Hembree, 1955) as adapted by Reclamation. This method employs measured suspended sediment concentrations, bed material particle size distribution, and measured hydraulic parameters to compute total sediment load. Reclamation prepared a document, "Step Method for Computing Total Sediment Load by the Modified Einstein Procedure" in 1955 which documents Reclamation's procedure. This procedure has subsequently been computerized (Reclamation, 1969; Holmquist-Johnson and Raff, 2004).

Beginning with data from 1959, the total sediment loads of the Floodway at San Acacia and San Marcial have been calculated and the difference in total sediment load at each site tracked over time. Figure 10 is a plot of the difference in total sediment load and discharge of the Floodway at San Acacia and at San Marcial from 1959 to 2001, i.e. San Acacia data minus San Marcial data (Makar and Strand, 2003). Therefore, a positive number signifies deposition in the river channel between the two gages. From 1959 to 1991 there was a general aggrading trend resulting in the deposition of ~150 million tons of sediment in that reach of the Rio Grande. In 1991 there is a dramatic shift in the trend line. This indicates that suddenly the process shifted from aggradation to degradation and /or there was an increase in sediment contribution from the tributaries in this reach. Up to 28 million tons of deposited material may have been transported downstream of San Marcial in the last ten years. The majority of the aggradation has occurred downstream of San Antonio, whereas the sediment has been removed near the upper end of the reach downstream of San Acacia Diversion Dam.

The degradation and channel incision taking place downstream from San Acacia Diversion Dam has resulted in a coarsening of the bed material and an increase in the size of suspended particles reaching San Marcial. This, in turn, has led to a change in the suspended to total load relationships (Makar and Strand, 2003).

The sediment contributed by arroyos and erosion of the channel bed/banks dominates the current local supply of sediment. Four medium-sized arroyos and a diversion canal currently enter into the Rio Grande in this study reach: Arroyo Alamillo, Parida, Canas, Brown, and the North Socorro Diversion Canal. These channels transport mainly silt, sand, and gravel-sized particles to the Rio Grande. These tributaries and relic sediment deposits in the channel bed/banks are especially important as local sources of gravel.

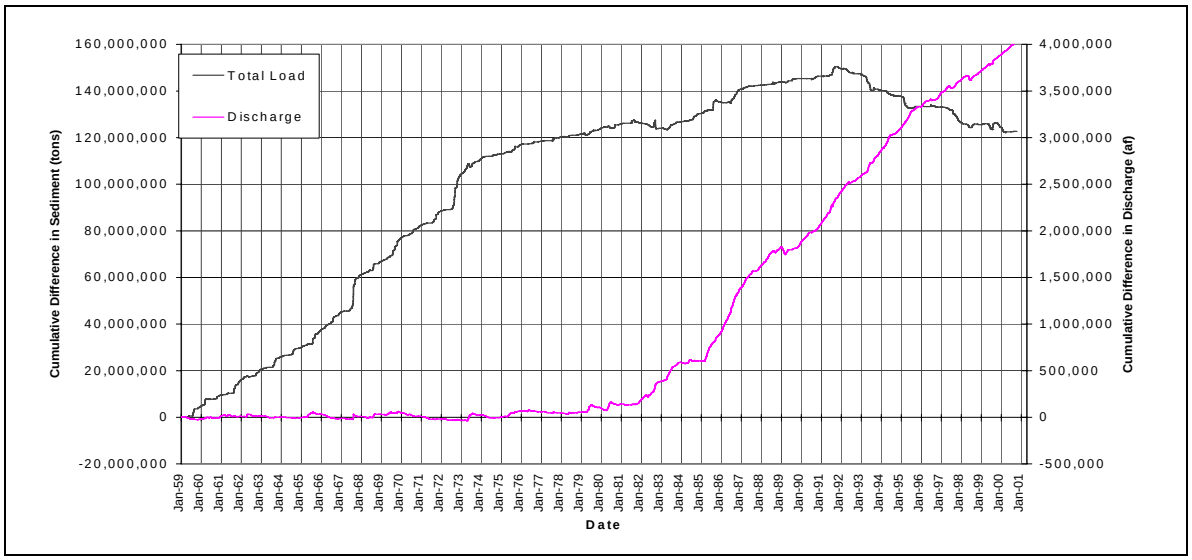

Figure 10: Discharge and sediment difference between San Acacia and San Marcial.

2.1.4 Geomorphology

A series of reservoirs were built upstream from this study site from the 1950s through the 1970s. These reservoirs trap sediment and store water. As a result, the annual volume of sediment being transported at San Acacia has decreased and the flow pattern has changed. Data show the bed elevation has decreased over five feet in several locations downstream from San Acacia Diversion Dam since 1972. On the other hand, the downstream portion of the reach has experienced long term aggradation, in part because of the existence of the Elephant Butte Dam and Reservoir. Cross-sections were examined by Makar and Bauer (2003) to determine rates of change in channel parameters such as width, depth, active channel area, velocity, and sinuosity using both the location of riparian vegetation on historical aerial photography, photogrammetric cross-section data, and field-measured cross-section surveys. The variation in cross-section geometry over time (1962, 1972, 1992, and 2002) can be seen in the historical cross-section plots provided in Appendix C.

2.1.4.1 Width

Historical channel widths between San Acacia Diversion Dam and Elephant Butte Reservoir were much wider than present day widths. Figure 11 through Figure 17 (Makar and Bauer, 2003) shows the maximum, 75th percentile, mean, 25th percentile, and minimum channel widths for subreaches between San Acacia Diversion Dam and Elephant Butte Reservoir. Mean channel width decreased from over 2,000 feet in 1918 to 200 feet in 2001 (Makar and Bauer, 2003).

Channel narrowing is often accompanied by channel incision and terrace formation. For a given flow and roughness, a narrower channel will have higher depths and velocities than a wide channel. Data show that the channel in the upstream portion of the study reach (Agg/Deg#1208-1477) is narrower (Makar and Bauer, 2003) and deeper (Reclamation, 2003) now than in 1962. For most flows, there is less overbank flooding and main channel velocities are higher. Conversely, in the lower portion of the study reach there is more overbank flooding and main channel aggradation is occurring as a result of lower channel capacities, more overbank flows, and backwater effects from the reservoir.

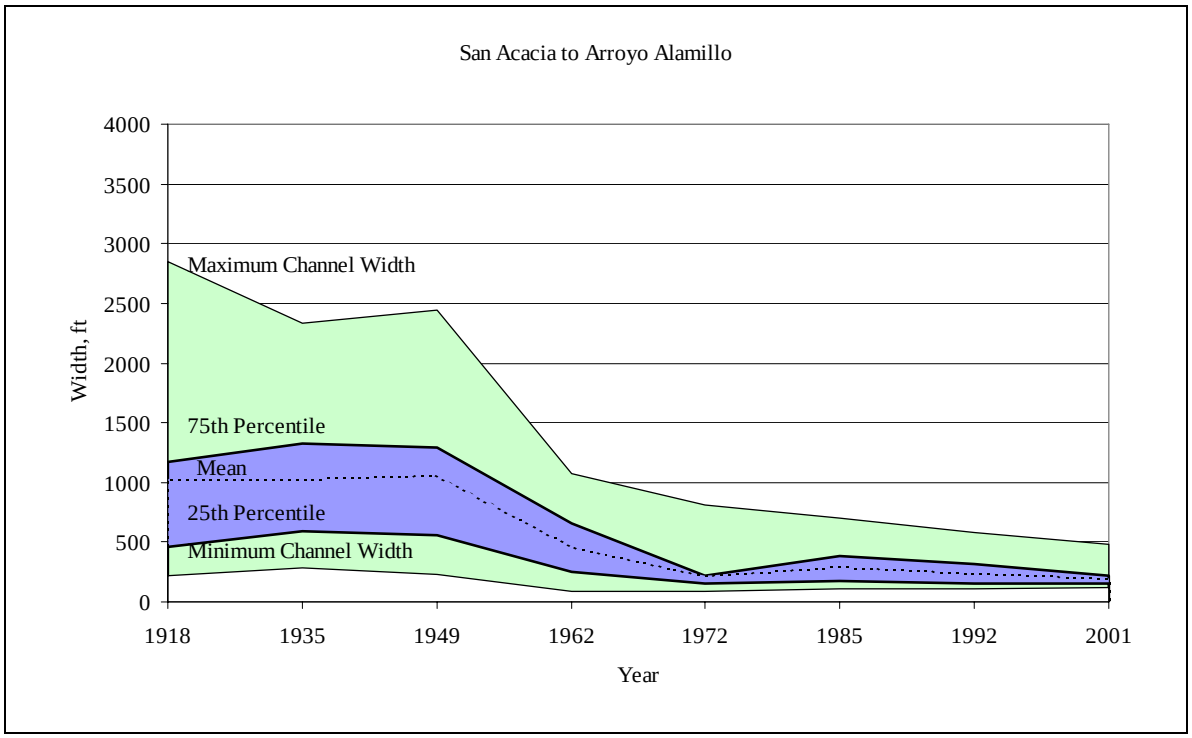

Figure 11: Channel widths - San Acacia Diversion Dam to Arroyo Alamillo (1918 to 2001).

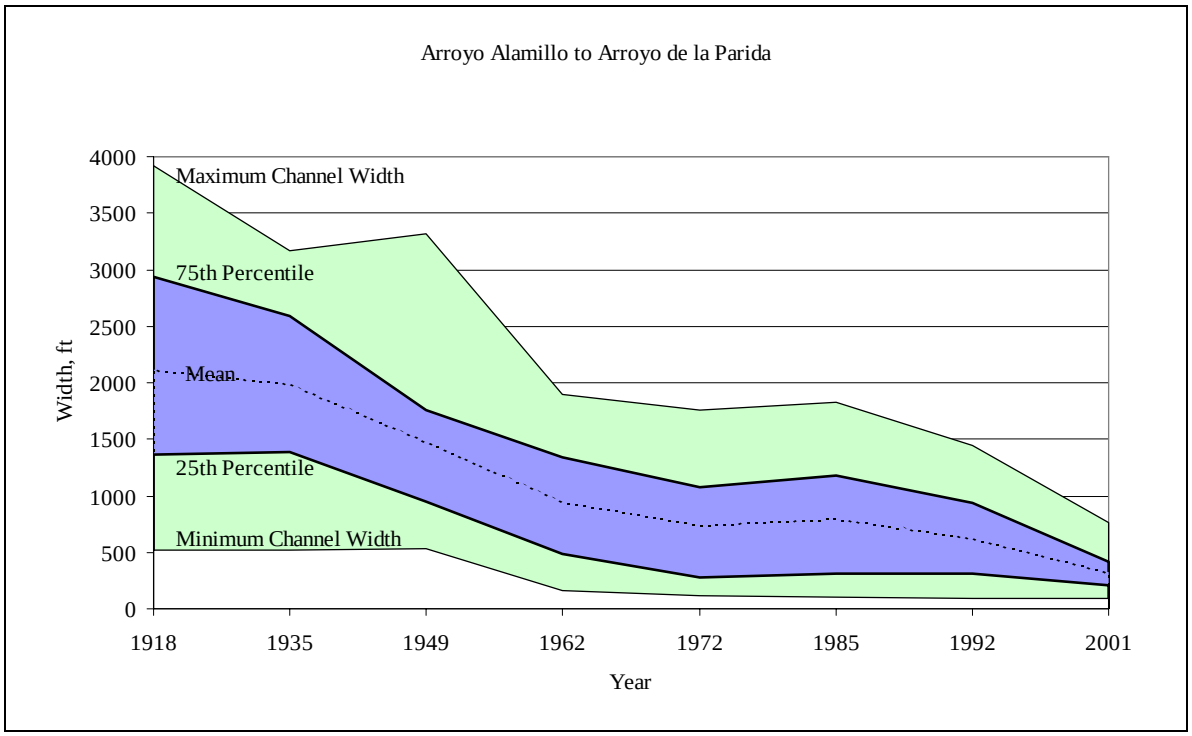

Figure 12: Channel widths - Arroyo Alamillo to Arroyo de la Parida (1918 to 2001).

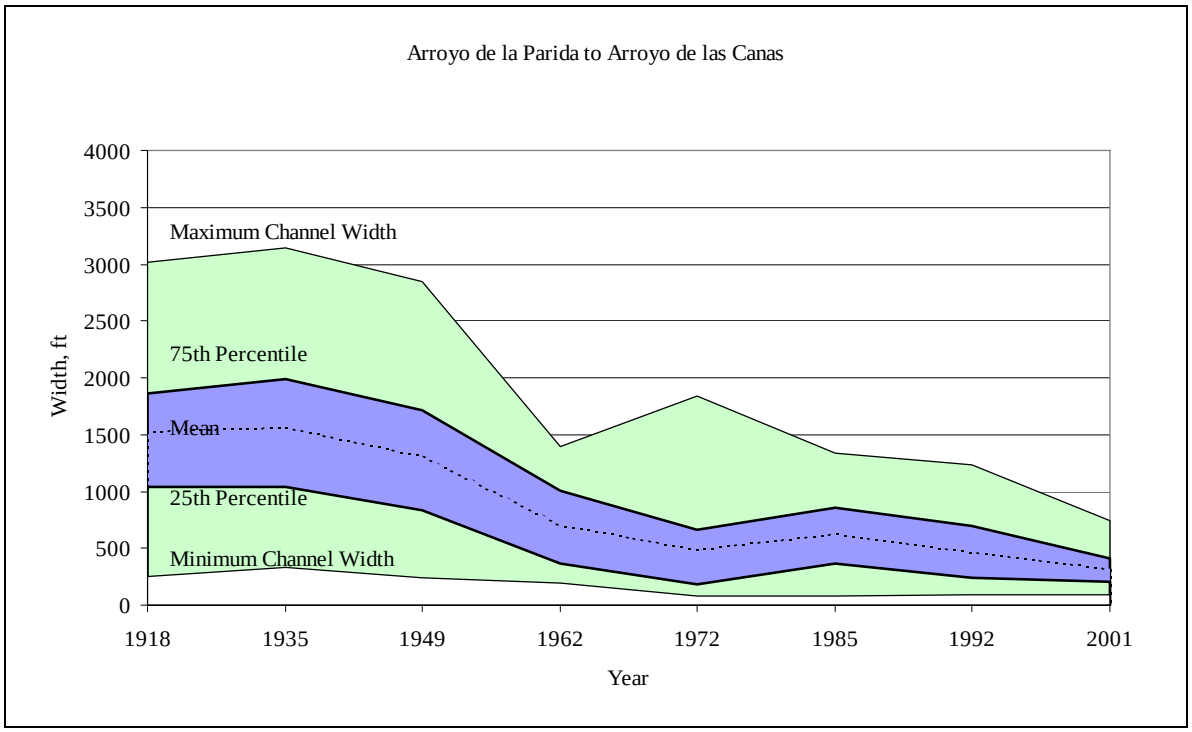

Figure 13: Channel widths - Arroyo de la Parida to Arroyo de las Canas (1918 to 2001).

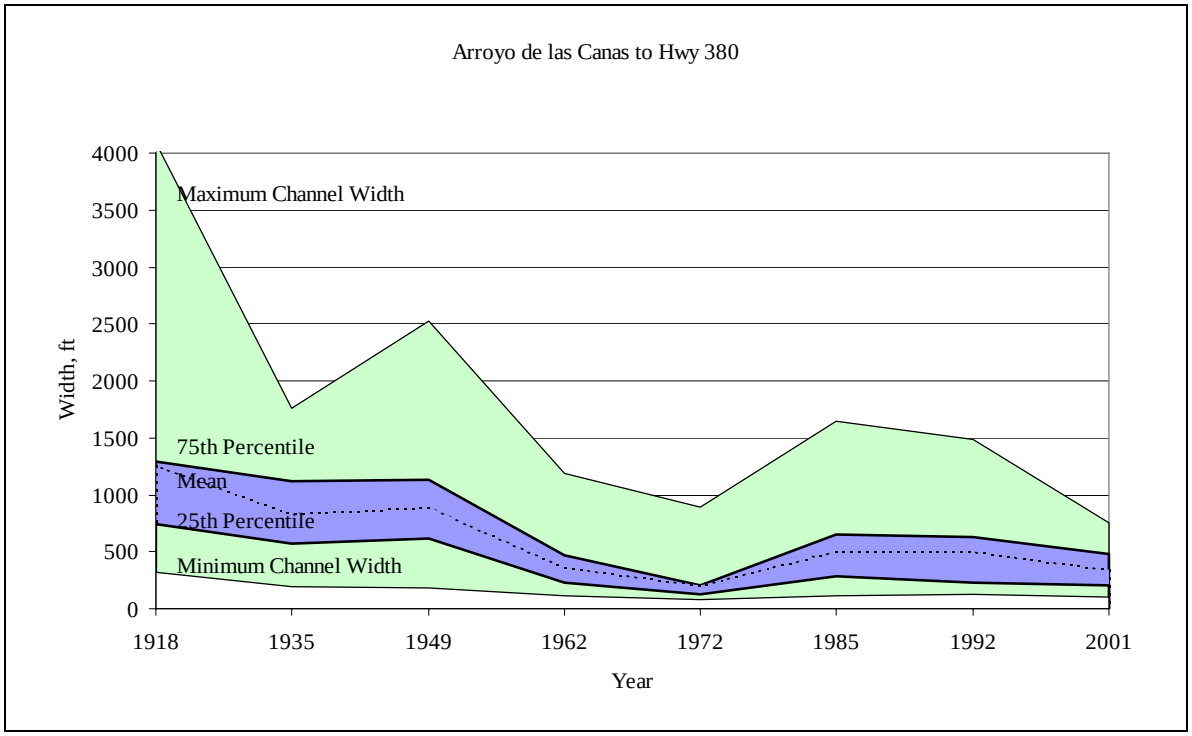

Figure 14: Channel widths - Arroyo de las Canas to Hwy 380 Bridge (1918 to 2001).

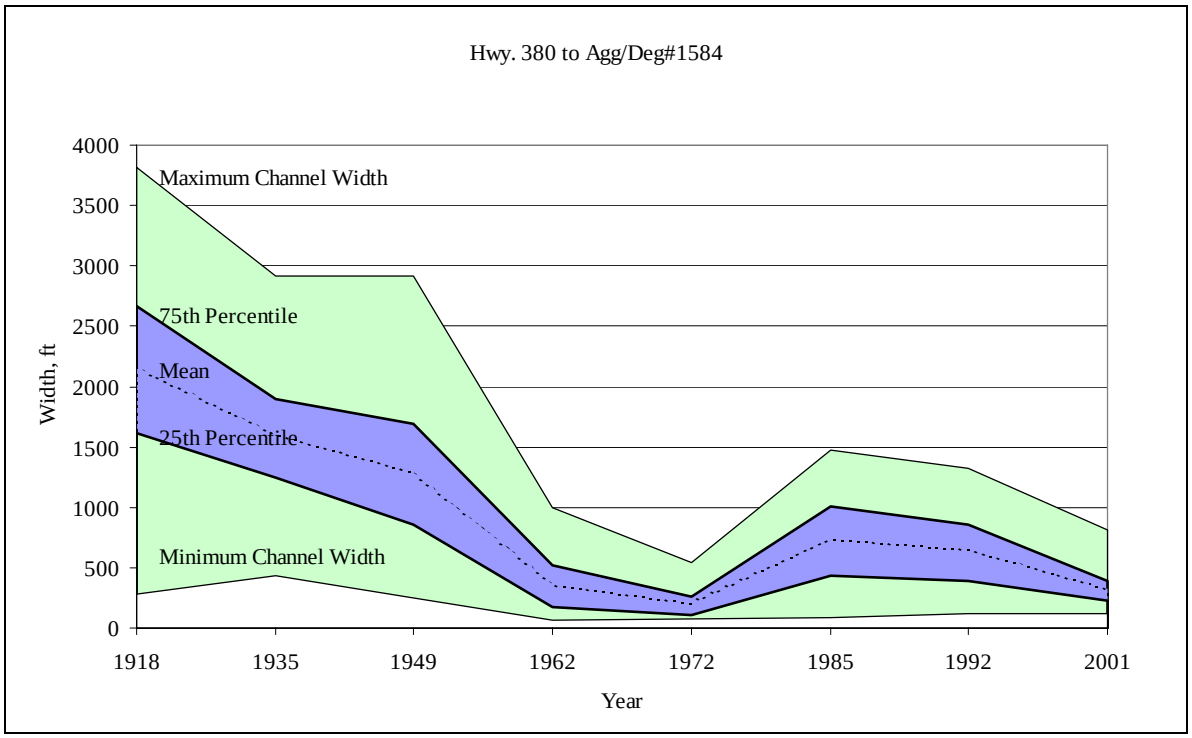

Figure 15: Channel widths - Hwy 380 Bridge to Agg/Deg#1584 (1918 to 2001).

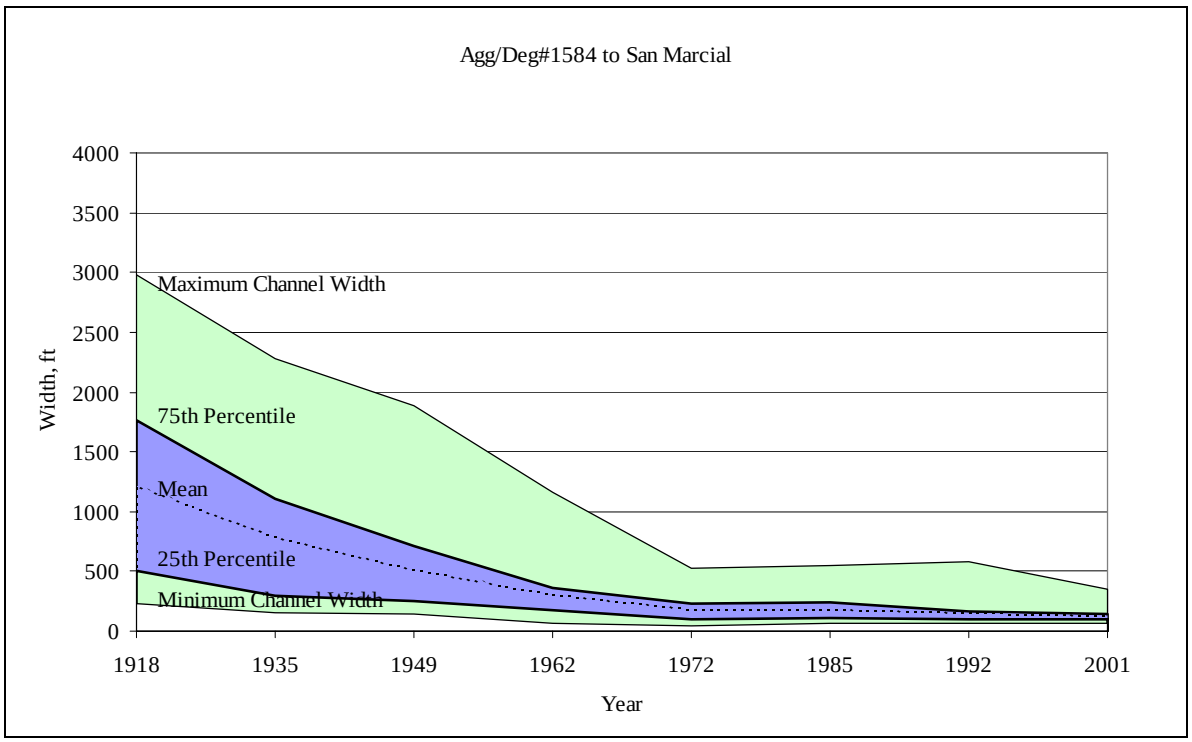

Figure 16: Channel widths - Agg/Deg#1584 to San Marcial (1918 to 2001).

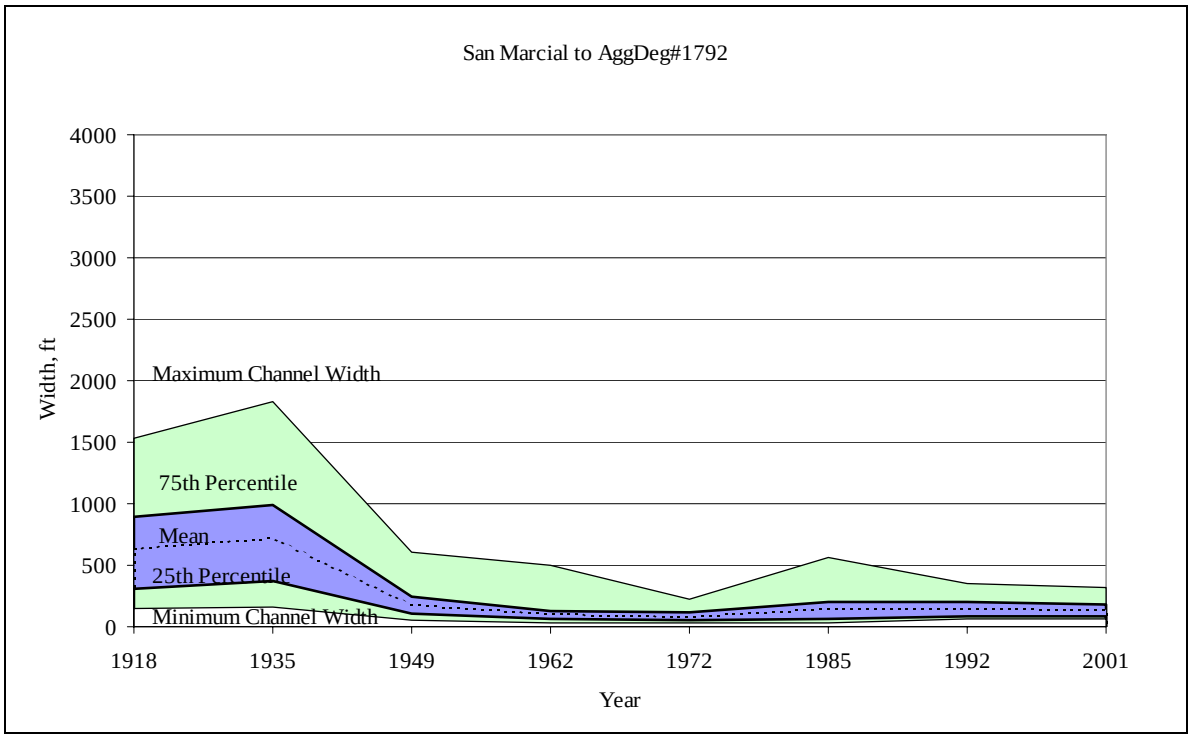

Figure 17: Channel widths - San Marcial to Agg/Deg#1792 (1918 to 2001).

2.1.4.2 Slope

The overall channel slope in the San Acacia reach has decreased as a result of channel narrowing and degradation in the reach downstream from San Acacia Diversion Dam and aggradation in the reach upstream of Elephant Butte Reservoir (Sailer and Young, 2002). Figure 18 shows the progression of channel aggradation/degradation in the San Acacia reach. Mean bed elevations collected from several sources (Soil Conservation Service, U.S. Army Corps of Engineers, Bureau of Reclamation Agg/Deg study, and Tetra Tech field data collection for Reclamation) steadily decrease downstream from San Acacia Diversion Dam and steadily increase upstream from Elephant Butte Reservoir between 1936 and 1962. Beginning in 1972, the rate of channel incision starts to increase and then progresses further downstream from San Acacia Diversion Dam (Figure 19). Conversely, the rate of channel aggradation is continuing to increase upstream of Elephant Butte Reservoir (Figure 20).

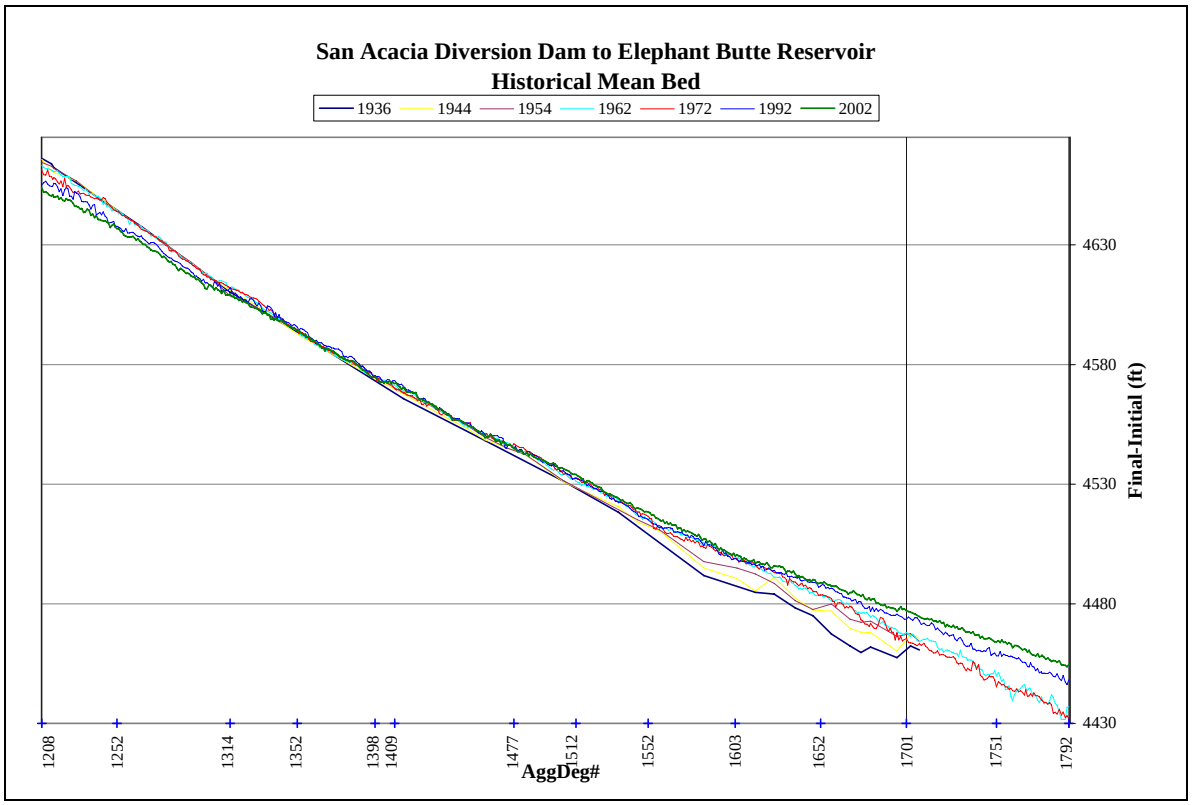

Figure 18: Historical mean bed between San Acacia Diversion Dam and Elephant Butte Reservoir.

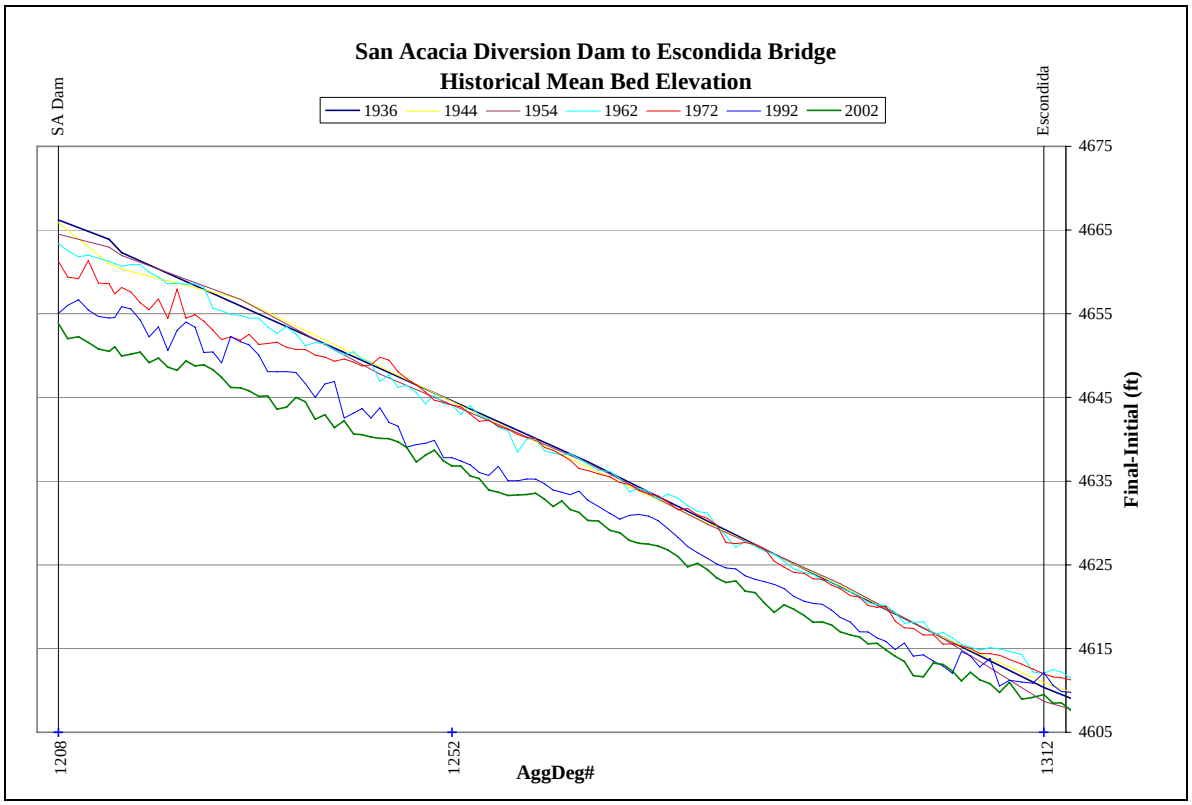

Figure 19: Historical mean bed between San Acacia Diversion Dam and Escondida Bridge.

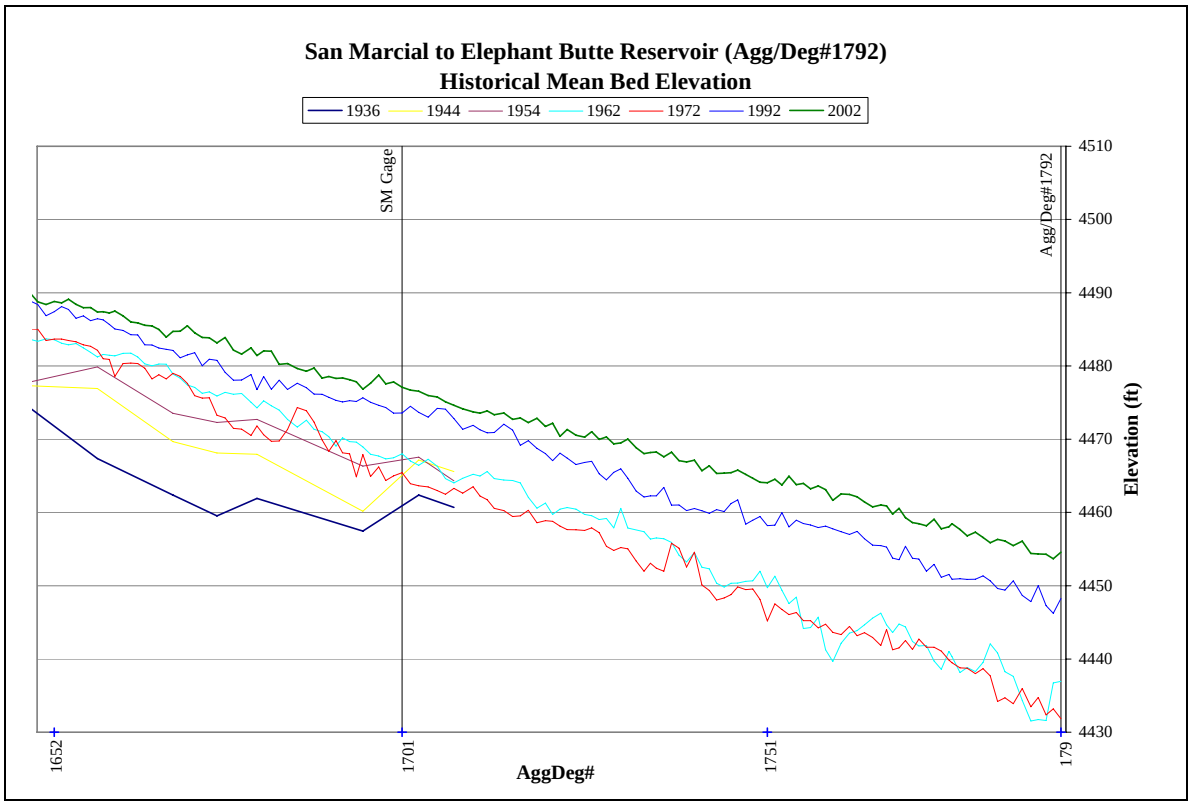

Figure 20: Historical mean bed between San Marcial and Elephant Butte Reservoir.

2.1.4.3 River migration and sinuosity

The long-term series of maps and aerial photographs digitized into the GIS database (Oliver, 2004) allowed comparison of channel location, sinuosity, and width over time. Specific features of interest included change in the active river channel, vegetated islands, and the thalweg of the river. The active river channel is defined as that portion of the river corridor that the Rio Grande is actively working and changing. It is usually free of vegetation depending on the magnitude of the flows.

Figure 21 illustrates active channel movement over time back and forth across the valley. The varying degree of change in channel location can be seen as well as the general narrowing of the active channel. A series of aerial photographs showing historical planform change from San Acacia Diversion Dam to Elephant Butte is provided in Appendix D.

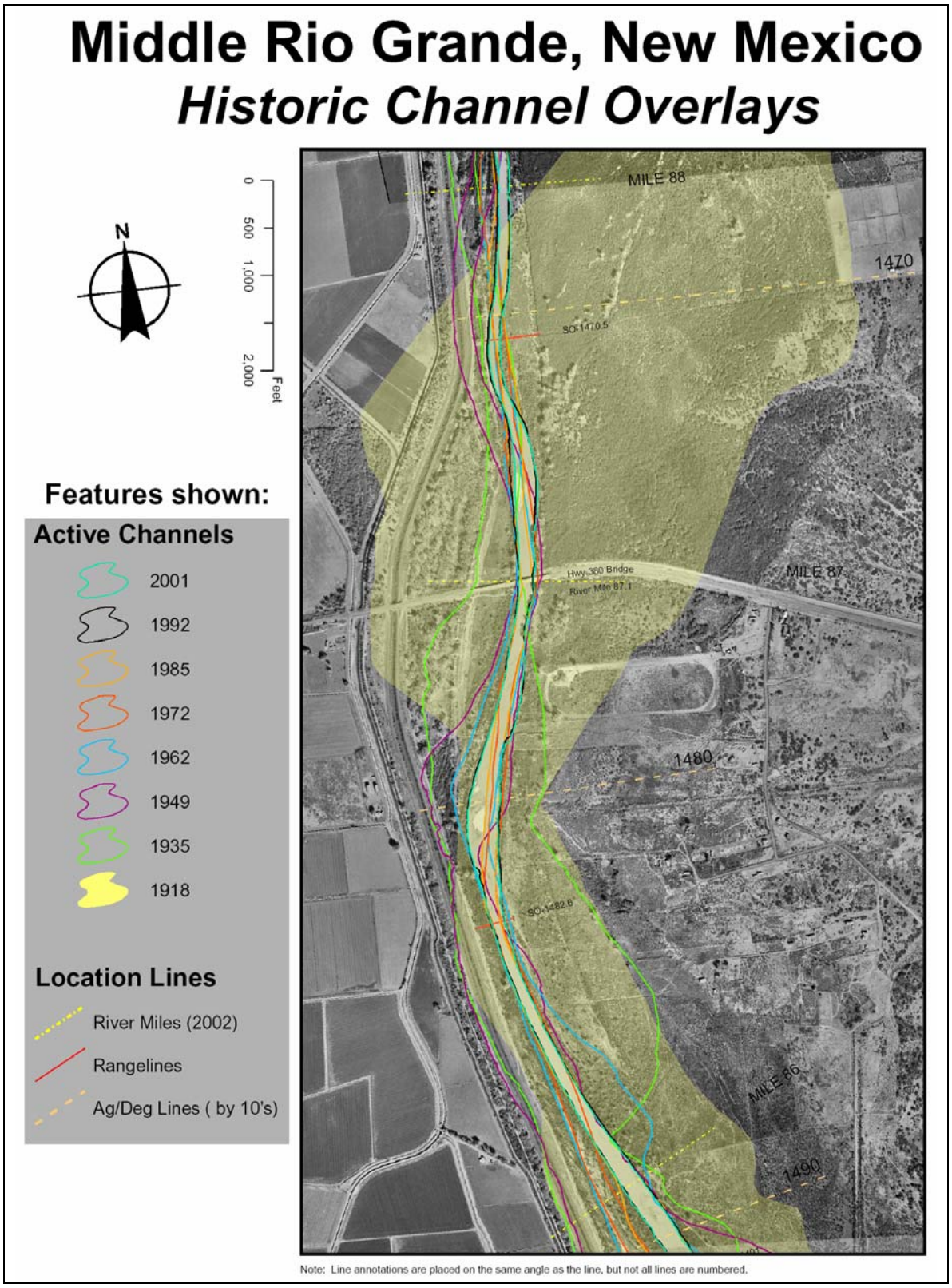

Figure 21: Historical active channel planform change.

2.1.4.4 Terraces

The river between San Acacia Diversion Dam and Escondida is generally incised. Six fairly distinct abandoned alluvial surfaces/terraces have been identified in that reach. These abandoned alluvial surfaces or terraces are indicative of incised reaches and can become disconnected from the river. Two of the identified terraces pre-date 1918 maps: a 30-foot terrace near Arroyo Alamillo is likely the oldest surface mapped and contains silts, sands and gravel; and the 12 to 15-foot terrace found predominantly near the diversion dam is composed of both channel and floodplain type sediments. A 10-foot high terrace, abandoned by the active channel by 1935, contains distinct layers of sand, silt, and clay that often form vertical banks. The 8-foot terrace is the most extensive terrace and composed of mostly silty-sands to gravelly-sands. By 1935 much of this surface was above the channel, it was completely abandoned by 1949. The 4 to 6-foot terrace has more sand and gravel than the 8-foot and is less cohesive. It was the active channel in 1972 and abandoned by 1985. The most recent terrace is approximately 3 feet high and was the active channel in 1985 and abandoned by 1992. It is composed of non-cohesive sand and gravel (Reclamation, 2003).

From Escondida to Elephant Butte Reservoir, the main channel of the Rio Grande has occupied most of the five historical terraces/surfaces at some time during the period from 1918 to present. The highest surface found in this reach is in the upstream 6 to 7 miles of the reach. This 8 to 10-foot high terrace/surface was abandoned by 1949. Two different surfaces were identified that were no longer river channel by 1962, a 4 to 6-foot surface and a 3 to 4-foot surface. The higher surface is also a short section in the upstream portion of the reach. The 3 to 4-foot surface is the most commonly found surface in this reach followed by the 2 to 3-foot surface which was abandoned by 1985. As the active channel has continued to narrow, a very low floodplain surface of 1 to 2-feet appears at various locations from Arroyo de las Canas downstream. Terraces/surfaces in this reach are generally composed of silt loam or sandy loam units underlain by interbedded silt and sand. Gravelly deposits are found at the base of many well logs from the reach and are dominant in the subsurface of the current floodplain soils. Clay-rich beds are prevalent near the surface in the Bosque del Apache and in the downstream reach to Elephant Butte (Klawon and Makar, 2003).

Although some of the terraces in the upper and lower reaches are similar in the age of active channel abandonment, they do not necessarily represent the same geomorphic surface. This is because the channel in the upstream reach is degrading and many of the mapped units are not inundated by Rio Grande discharges (Reclamation, 2003), while much of the channels in the lower part of the study reach are undergoing aggradation. Although the terraces in the lower reach have been abandoned by the active channel, many terraces continue to be inundated by moderate to high flows. This is generally not the case in the reach between San Acacia Diversion Dam and Escondida (Reclamation, 2003).

2.2 Project Objectives

The overall purpose of this project was to analyze available data, gather additional data (bed material data, arroyo surveys, and cone penetrometer data), and to set up and calibrate a sediment model to assist in determining future spatial and temporal changes in cross-section geometry, bed slope, and sediment size along the reach. Additionally, the

predictive model was used to investigate the effects of a sediment augmentation plan to assist in channel stabilization along the reach.

2.2.1 Data Collection

Cross-sections (transects) and surface sediment samples of the San Acacia, Socorro, and Elephant Butte survey lines were collected and analyzed to determine input parameters for GSTAR-1D. The historical data that Reclamation had previously collected at these sites was used in model calibration. Existing bed material data were not sufficient to provide input to the predictive model. Therefore, additional subsurface sediment sampling, arroyo surveys, and cone penetrometer analysis were completed to help understand the stratigraphy of the subsurface riverbed and determine if the clay and gravel layers would significantly impact degradation rates. As the Rio Grande continues to evolve there will be a need to continue bed material sampling in support of maintenance efforts.

2.2.2 Analysis of available data

Data available for use in the model consisted of suspended sediment data, bed material samples, cross-section surveys, flow hydrology, reservoir elevations, lateral sediment inputs, and aerial photography.

USGS gages at San Acacia and San Marcial were used to generate inflow sediment rating curves, bed gradations, and flow hydrology. Data at Elephant Butte Reservoir were used to determine reservoir pool elevations for the downstream boundary condition. Aerial photography from 1972, 1992, and 2002 were used to generate cross-section geometry, calculate depositional/erosional changes, and identify bank locations, levee locations, ineffective flows, and changes in channel and overbank roughness. Elephant Butte Reservoir surveys were used to provide additional cross-section data downstream of Agg/Deg#1792.

2.2.3 Sediment model development

Input files were prepared for the predictive model and the calibration models that include the initial channel cross-section geometry, bed material size, hydrograph, inflow of sediment, and channel roughness. The calibration models were run and calibrated to match the change in cross-section geometry and volume of sediment removed/deposited from the channel and overbanks. Sediment modeling for the Rio Grande usually requires significant model adjustment to perform the calibration. This has included adjusting the GSTAR-1D computer code to change the hydraulic and sediment transport conditions to match those found on the Rio Grande.

2.2.3.1 Customization of GSTAR-1D

GSTAR-1D, Generalized Sediment Transport for Alluvial Rivers – One Dimension, is a hydraulic and sediment transport numerical model developed to simulate flows in rivers and channels with or without movable boundaries. GSTARS-1D is able to compute water surface profiles in single channels, simple channel networks, and complex channel networks. Other capabilities include: both steady and unsteady flow models, many sediment transport equations, floodplain simulation, and computation of width changes using minimization theory. Lateral inflows can be simulated along with internal boundary

conditions, such as time-stage tables, rating curves, weirs, bridges, and radial gates. EPA (Environmental Protection Agency) and Reclamation are funding partners in the development of the GSTAR-1D model.

Efforts were made to customize the GSTAR-1D model to better simulate the sediment transport in the Middle Rio Grande. The customization efforts to date are as follows:

- To better represent the complex cross-section geometry in the Rio Grande, the following features were added to the model: ineffective flow, permanent ineffective flow, blocked obstructions, and levees.
- Bed elevation limitations were provided to limit the erosion and deposition at certain cross-sections.
- The model was modified to use different floodplain options to treat the floodplain sediment transport separately from the main channel. These include floodplain option 1 to simulate the main channel and floodplains in different sub-channels and to calculate the flow and sediment exchanges between the main channel and floodplains, and floodplain option 2 to simulate the sediment transport capacity based on the flow discharge only in the main channel. The floodplain options are currently under development to find the optimum way to simulate the different erosion and deposition processes in the main channel and the floodplains of the Rio Grande.
- GSTAR-1D outputs the simulated channel geometry files in HEC-RAS format at user-specified time steps, allowing users to compare the channel geometry with the existing HEC-RAS interface.
- GSTAR-1D outputs the sediment erosion and deposition in the main channel, floodplains, and the total channel for better comparison with the field data.
- Cohesive sediment transport parameters are input at user-specified locations and then extrapolated to the whole reach. This change enables more accurate simulation of the near-freshly-deposited sediment upstream and the near-consolidated sediment in the reservoir.
- A separate program was written to transfer the HEC-RAS input geometry file into the GSTAR-1D geometry format to facilitate the use of the Rio Grande geometry data originally generated with HEC-RAS.

2.2.3.2 Calibration

Historical (1962, 1972, 1992) and current (2002) cross-section data comparisons were used to determine aggradation/degradation trends along the study reach. Computing the volume change between cross-sections and then generating a cumulative sediment volume plot allowed for a comparison of the model results. Comparison of the model results with the calculated sediment volumes provided a method for calibrating the sediment model in order to produce similar results to the measured data. In addition to the sediment volume change, changes in bed material, slope, and mean bed elevations were also used in calibrating the model. The model was calibrated for two time periods, 1972-1992 and 1992-2002. Calibration over these two time periods provided verification that the model could be used consistently for two different hydrologic time periods (dry and average) and provided calibration parameters for the future predictive models.

2.2.4 Future conditions with and without sediment augmentation

Modeling included analysis of both a condition with and a condition without sediment augmentation. Future model inflows were estimated using generated stochastic hydrology and reservoir elevations (Lane, 2004), which represented sequences of below average (dry), average, and above average (wet) hydrologic conditions. The 2002 cross-section data and the most recently collected bed material data were also used as input to the predictive model.

For each of the stochastic hydrology flow regimes, dry, average, and wet, the model was used to estimate channel conditions for a future projected 20 year period (2002 to 2022). Output from the model includes the average river bed elevation (slope), cross-section geometry, and bed material size.

3 Data Collection, Analysis, and Model Development

3.1 Data Collection

There was a significant amount of data collection for this project. Data was collected to verify model results and provide model input. Data collection included bed material sampling, subsurface drilling and dynamic cone penetrometer (DCP) measurements, cross-section surveys on several tributaries, field surveys conducted in 2001, and aerial photography collected in 2002.

3.1.1 Surface bed material

Samples were mostly collected as part of the DCP data collection. Other samples were collected during the arroyo surveys while others were collected on a specific bed material data collection trip. In 2003 bed material samples were collected from the Rio Grande between the Rio Salado and San Acacia Diversion Dam, Cochiti Pueblo, and near the Alameda Bridge and Calabacillas Arroyo. Additional bed material samples were collected in 2003 from Peralta Canyon, Calabacillas Arroyo, Abo Arroyo, Salas Arroyo, Los Alamos Arroyo, Rio Salado, Arroyo Alamillo, Arroyo de la Parida, and Arroyo de las Canas during arroyo surveys.

Additional bed material samples for the predictive model were collected on two separate trips to the Rio Grande in July and August 2004. Between the two trips the area between Angostura Diversion Dam and Silver Canyon in Elephant Butte Reservoir were covered (Bauer, 2004a). In addition to bed samples in the main floodway, bed material samples were also taken at each of the five major arroyos. The larger arroyos, e.g. Arroyo de las Canas, have historically supplied a significant amount of larger-sized sediment to the Rio Grande. The surface samples generally represent the coarsest sediment found at a cross-section. Most of the surface samples were collected from riffles or gravel patches. In many cases the gravel was only found in isolated areas and does not cover the entire cross-section. Sand samples representative of the sand portion of the cross-section were also collected. Additional information on the bed material data collection can be found in the Middle Rio Grande Sediment and Substrate Data Collection report (Bauer and Hilldale, 2004).

3.1.2 Cone penetrometer and soil auger data

Cone penetrometer and soil auger data was collected during numerous trips to the Rio Grande between 2001 and 2004 to determine the stratigraphy of the subsurface riverbed. Samples were primarily collected in the overbank area but several were collected from the margin of the active channel. The primary objective of the drilling was to identify distinct layers of sand, gravel and clay below the riverbed. The stratigraphy of the riverbed provides detailed information on the thickness of bed material layers present in the Rio Grande. The location and thickness of these bed layers is used in the sediment model to limit the amount of erosion that might occur as a result of a gravel/armor layer as well as the location and depth of the consolidated fat clay material encountered throughout the San Acacia reach.

From July 2002 to August 2004, additional subsurface measurements were collected with a DCP. The initial DCP work coincided with the drilling sites so a side-by-side

comparison could be made between the two methods. Comparison of the results resulted in a general range of DCP blow counts that are used to identify the substrate as silt and clay, sand, or gravel. DCP data are not detailed enough to identify specific grain sizes in the substrate, but they can provide information on substrate that could limit degradation in the model. DCP testing ranged from just downstream of Cochiti Dam to the temporary channel into Elephant Butte Reservoir. Unlike the drilling, samples were not limited to the overbank areas. DCP data were often collected from bars and islands in the active channel. Additional information on the data collection and results of the DCP analysis can be found in the Middle Rio Grande Sediment and Substrate Data Collection report (Bauer and Hilldale, 2004).

3.1.3 Arroyo cross-section survey

In September 2003 nine arroyos along the Rio Grande were surveyed between Cochiti Dam and Socorro as part of an effort to estimate sediment loads from ephemeral tributaries to the Rio Grande. The surveyed arroyos were Peralta Canyon, Calabacillas Arroyo, Abo Arroyo, Salas Arroyo, Los Alamos Arroyo, Rio Salado, Arroyo Alamillo, Arroyo de la Parida, and Arroyo de las Canas. At each arroyo, up to nine cross-sections were surveyed upstream from the mouth of the arroyo using survey grade GPS. The data were processed and imported into Arc Map where surface representations of the arroyos were created. Cross-sections were exported from Arc Map into HEC-RAS using the HEC-GeoRAS extension for Arc Map. Once the cross-sections were imported to HEC-RAS, a step backwater model was created for each arroyo.

Sediment loads from the arroyos were estimated by first computing a sediment transport rating curve near the mouth of each arroyo (Bauer, 2004b). Total load was estimated by using the Engelund-Hansen (1972) equation for sediment less than 2 mm and the Meyer-Peter and Muller (1948) equation for sediment larger than 2 mm. Once the rating curves were created, they were applied to hydrographs created for the 2, 5, 10, and 25 rainfall events on each tributary (Bullard, 2004). A weighting scheme based on ten two-year events, four five-year events, two ten-year events, and one twenty-five-year event during a twenty-year span was created to develop average mean daily flow and sediment input values. The events were assumed to take place once a year between July and September and were timed so that the flow in the Rio Grande was greater than the minimum flow set in the model. Additional information on the data collection and results can be found in Middle Rio Grande Sediment and Substrate Data Collection report (Bauer and Hilldale, 2004).

3.1.4 Agg/Deg photogrammetric data and Field Survey Data

Channel geometry data consisted of aerial cross-sections surveyed in 1972, 1992, 2001, and 2002. The Albuquerque Area Office River Analysis Group contracted with Pacific Western Technologies, Albuquerque, NM, to obtain aerial photography imagery and to develop photogrammetric cross-sections at each of the established Agg/Deg lines. The aerial photography does not include the underwater portion of the channel, only the water surface. The geometry below the water surface was constructed by calculating the rectangular channel that would convey the measured flow rate at the observed water surface elevation. Field Survey data were used to compare the configuration of the actual underwater portions to the constructed underwater portion.

Survey data from 2001 was initially used to compare the calibration models and set up the future scenarios but a series of delays allowed for the 2002 data to be available. Use of the 2002 data enabled a more consistent comparison between the two calibration periods and interpretation of the future scenarios because all of the geometry and aggradation/degradation volume data are from a similar source (aerial photography) and at the same locations. The data collection for 2002 was performed between January 22 and February 1, 2002 when obstruction from foliage and flow in the channel would be minimized. River maintenance funds were used for this data collection effort, the subsequent validation of the supplied data, and incorporation of the channel underwater prism (aerial photography only supplies the water surface). The data collection contract specified a vertical accuracy of +/- 0.5 feet for 90-percent of the data points and +/- 1.0 for 100-percent of the data points, and a horizontal accuracy within the 1:4800 National Map Accuracy Standards of +/-1.0 feet of the true location. The data was supplied in both NAD27 and NAD83 formats. The NAD27 format was used in this analysis because of the previous work performed using earlier data sets in that format. The final, validated cross-section data from the 2002 aerial photography were received in March of 2004. These data were used to evaluate the 1992 to 2002 period calibration results and were the basis for future projection simulations.

3.2 Data Analysis and Model Input

3.2.1 Cross-section Geometry

The channel geometry data for the reach consisted of aerial cross-sections surveyed in 1972, 1992, and 2002. Additionally, Elephant Butte Reservoir surveys from 1969 (Lara, 1972), 1980 (Lara, 1983), 1988 (Orvis, 1989), and 1999 (Collins and Ferrari, 2000) were also used to provide additional data for cross-sections in the reservoir. The reservoir data was collected as part of reservoir surveys for monitoring the storage capacity of Elephant Butte Reservoir. In addition to providing cross-section data for model input, the aerial photographic cross-sections were used to calculate volumes of aggradation/degradation between successive surveys. The cross-sections surveyed in 1972, 1992, and 2002 were at identical locations so the difference in cross-section geometry between these sets of data provided the aggradation/degradation volume between successive cross-sections in the modeling reach. These volumes were used as one of the yardsticks for calibration of the model. Mean bed elevation, water surface width, and thalweg elevation were also used as yardsticks for calibrating the model.

GSTAR-1D is a one-dimensional model so it is not necessary to include closely spaced cross-sections. This would add significantly to model run times without necessarily improving the results. For one-dimensional modeling it is necessary to properly represent the general characteristics of the river, paying particular attention to locations where geometric properties change (e.g. width, slope). The San Acacia reach was represented with 226 cross-sections (Table 1) out of the total available Agg/Deg cross-sections of 754. Cross-sections were chosen at an average spacing of ~1,600 feet with 2,700 feet being the maximum. To the extent possible, cross-sections that have been historically field surveyed were chosen for current and future verification.

Table 1: Selected cross-sections used in sediment model.

Agg/Deg #		Agg/Deg #		Agg/Deg #		Agg/Deg #		Agg/Deg #
1208		1352		1494		1649		3032*
1211		1354		1497		1652		3033*
1214		1358		1499		1654		3035*
1216		1362		1501		1657		3036*
1219		1365		1504		1661		3037*
1221		1369		1507		1664		3038*
1224		1373		1510		1668		3039*
1226		1376		1514		1671		3040*
1229		1380		1517		1674		3041*
1232		1383		1520		1677		3042*
1236		1386		1523		1681		3043*
1239		1389		1526		1685		3044*
1242		1393		1529		1689		3045*
1246		1395		1532		1693		3047*
1248		1396		1535		1697		3048*
1252		1398		1539		1701		3049*
1256		1401		1542		1704		3050*
1259		1404		1545		1707		3051*
1263		1407		1549		1710		3052*
1266		1409		1552		1715		3053*
1269		1411		1556		1719		3054*
1271		1414		1559		1723		3055*
1273		1418		1562		1727		3056*
1276		1421		1566		1731		3057*
1279		1424		1570		1735		3058*
1283		1428		1574		1739		3059*
1287		1432		1577		1743		3060*
1291		1436		1581		1747		3061*
1294		1440		1584		1751		3062*
1297		1444		1587		1755		3063*
1299		1447		1591		1759		3065*
1301		1449		1595		1762		3066*
1304		1450		1599		1765		3067*
1308		1452		1603		1769		3068*
1312		1454		1607		1773		3069*
1316		1455		1611		1777		3070*
1320		1459		1615		1780		3071*
1324		1462		1618		1783		3072*
1327		1464		1622		1787		3073*
1330		1468		1625		1792		3074*
1333		1472		1628		3025*		
1336		1477		1632		3026*		
1339		1480		1635		3027*		
1342		1482		1638		3028*		
1345		1486		1641		3029*		
1349		1490		1645		3030*		

**Correspond to EB Lines (3025=EB25)*

After the cross-sections were selected they were filtered to remove redundant and erroneous points. HEC-RAS cannot accept more than 500 points per cross-section, making this a necessary step. Reducing the number of points in the cross-section also improves model run time. The redundant points were removed using an excel macro (RAS XsPoint Filter_03-11-2004.xls, developed by Holmquist-Johnson 2004) that allows the user to enter horizontal and vertical tolerances as well as main channel and floodplain limits to use in filtering the points. The overall width of the floodplains is much greater than the main channel width and the elevation change along the floodplain is minimal compared to that of the main channel, therefore only the floodplain points were filtered.

The main channel limits were chosen based on the vegetated bank line and the geometry of the cross-section. In some cases, the locations of the main channel limits were adjusted to create a gradual transition of channel width for successive cross-sections to help ensure numerical stability. Roughness in the model is represented with Manning *n*. Based on previous calibrations to hydraulic data (Samad et al, 1996), the Manning roughness coefficients were set to 0.02 for the main channel, and 0.1 for the floodplains.

Some cross-sections contained artificial berms created during channel maintenance between surveys which prevented proper calculation of aggradation/degradation between cross-sections. In these cases the berms were removed from the cross-section data. Figure 22 shows two examples of artificial berms removed in 1972, the filtered cross-section points, and how the geometry compares with survey data in 1992.

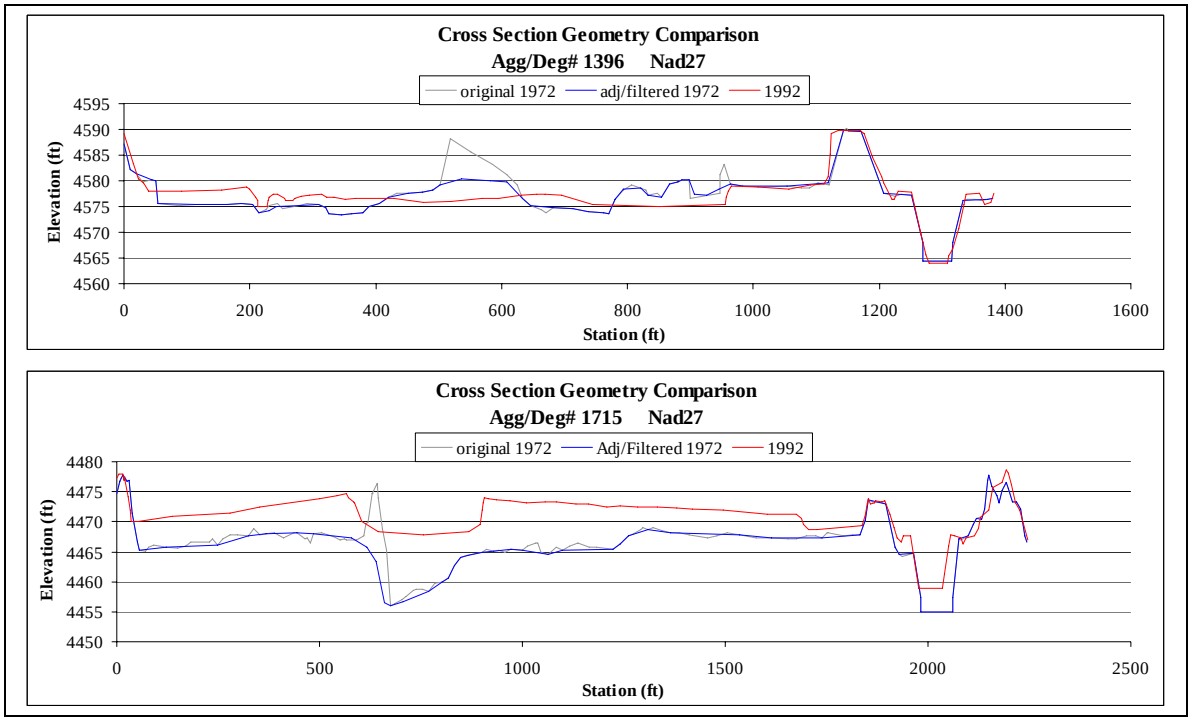

Figure 22: Example of artificial berm removal.

Comparisons between the 1972, 1992, and 2002 geometry showed that some cross-sections exhibited possible errors in the definition of the floodplain elevations. When comparing the floodplain aggradation/degradation volumes between 1992 and 2002 (Figure 23), the floodplains were shown to continually degrade from San Acacia Diversion Dam to ~Agg/Deg#1501. Through personal communication with Reclamation

staff, it was discussed that this is most likely not the case along this reach of the river (Bauer, Makar and Young, private communication, 2004). Figure 24 shows two examples of floodplain degradation from 1992 to 2002. Note that the 2002 and 1972 floodplains show similar elevations while the 1992 data are higher. One possible cause for the discrepancy could be a result of how the photogrammetric data were processed in the overbanks. If the density and height of the floodplain vegetation are underestimated, then the digitized floodplain elevation would be higher than the actual floodplain. Overestimation of the floodplain elevation in the 1992 data would result in excess aggradation in the 1972 - 1992 aggradation/degradation volume calculations and excess degradation in the 1992 - 2002 volume calculations for those cross-sections. For this study, the aggradation/degradation volumes were adjusted such that for the 1992 to 2002 volume calculations, anytime the floodplain calculations showed erosion, the volume of floodplain aggradation/degradation at that cross-section was set to zero. This adjustment was then subtracted from the 1972 to 1992 aggradation/degradation floodplain volumes to account for the possible overestimation of floodplain deposition due to the errors in the 1992 aerial survey data (Figure 25). Due to the limited availability of field survey data that includes floodplain definitions, it is difficult to quantify the error that is associated with the aerial survey data. Therefore, adjusting the aggradation/degradation volumes provides an envelope of aggradation/degradation volumes for comparing model results.

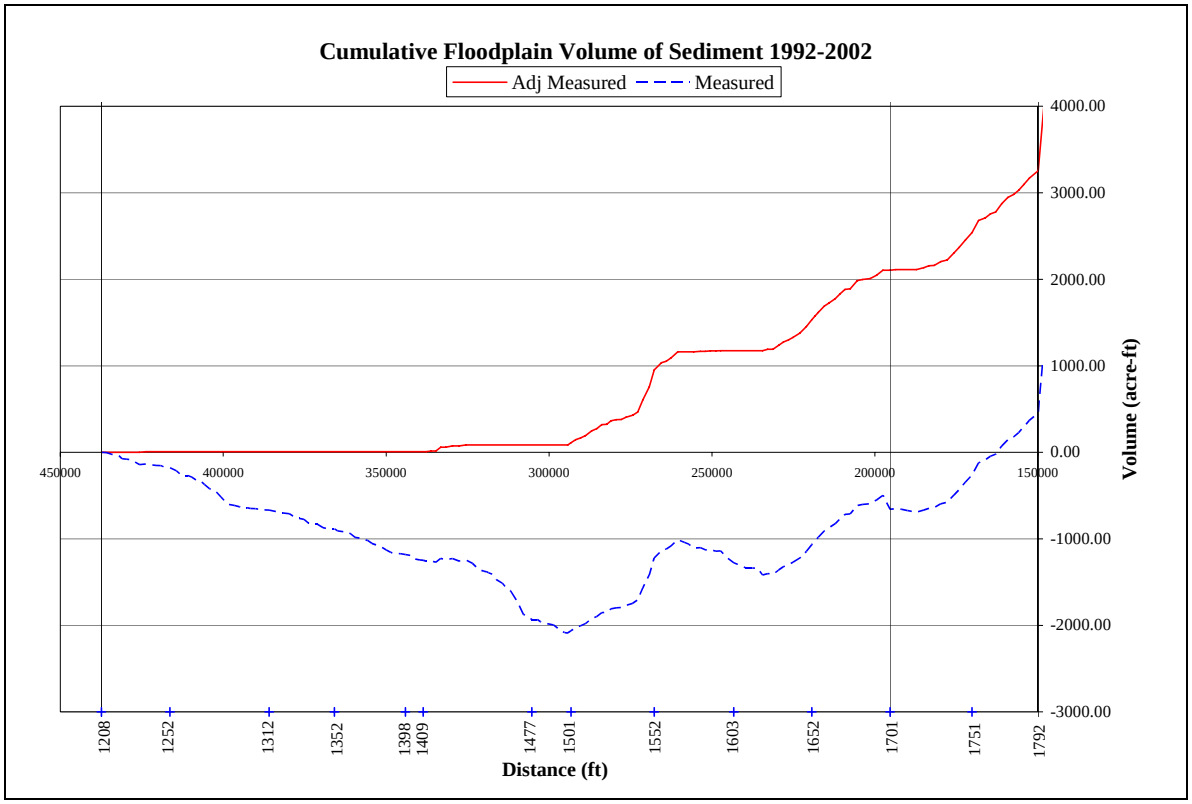

Figure 23: 1992-2002 adjusted floodplain aggradation/degradation volumes.

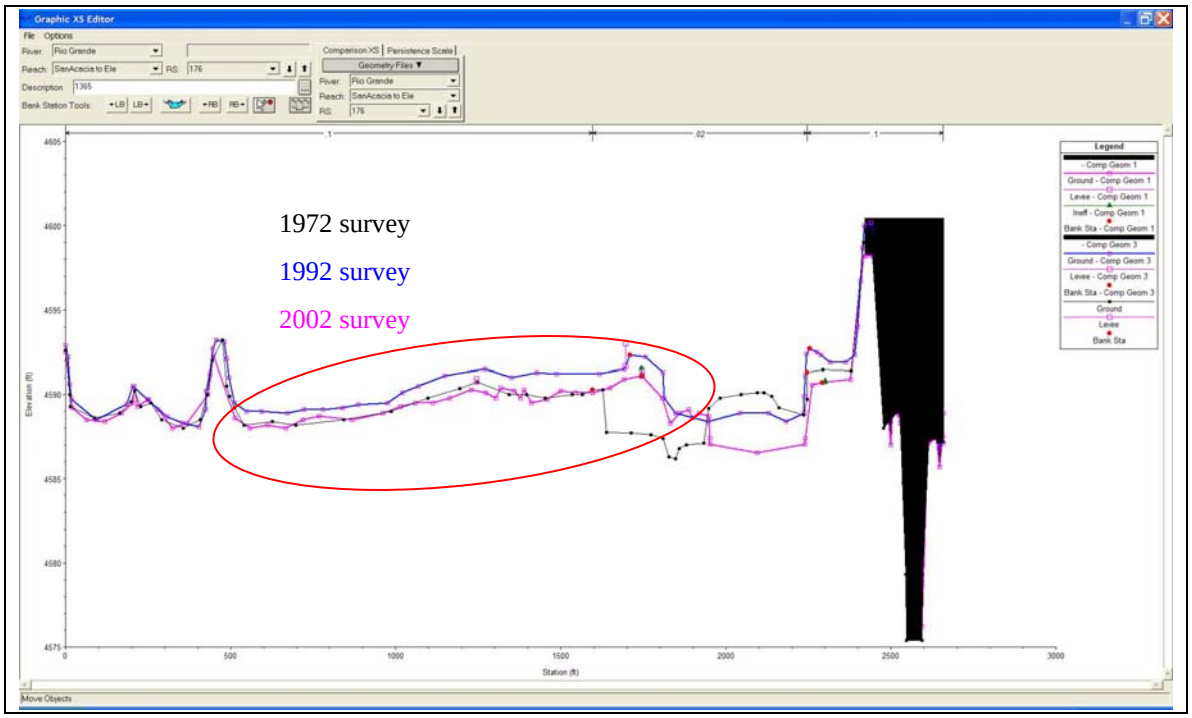

Figure 24: Example of possible error in 1992 floodplain survey data.

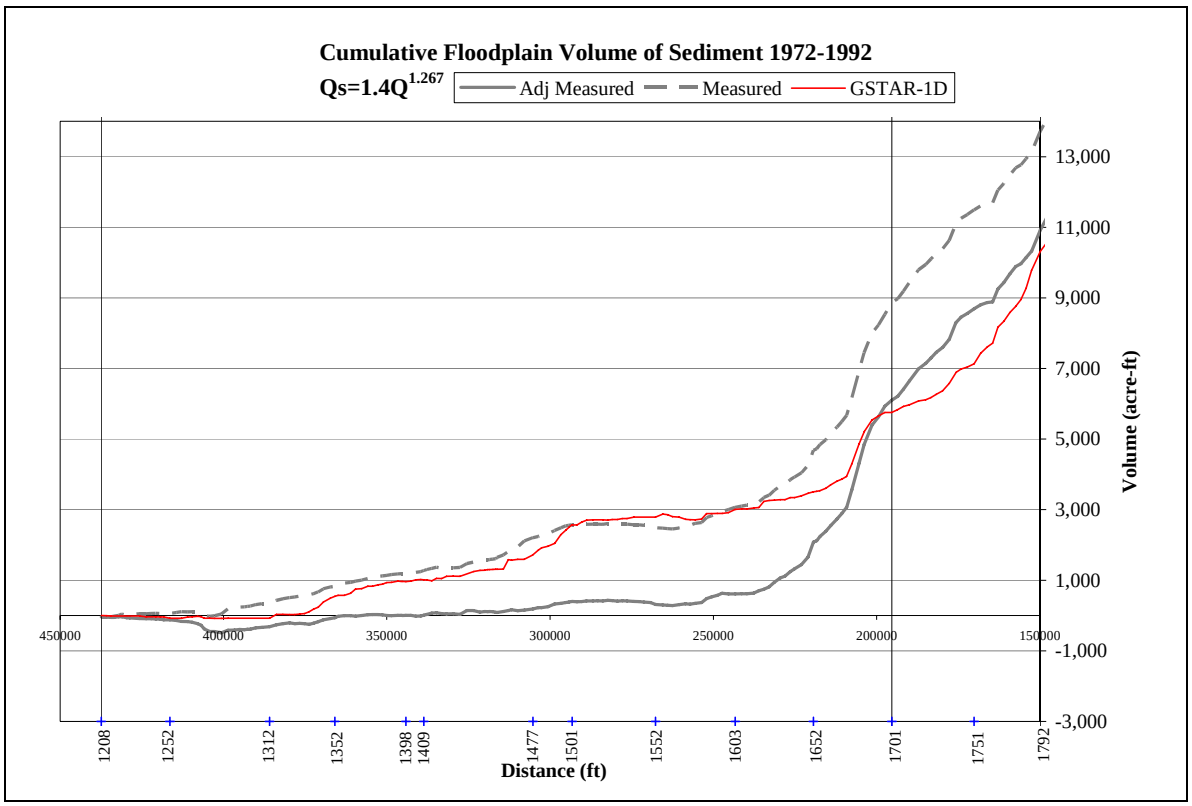

Figure 25: 1972-1992 adjusted floodplain aggradation/degradation volumes.

3.2.2 Channel Capacity and Channel Erosion

The channel capacity was estimated for 1972, 1992, and 2002 using HEC-RAS 3.1 (Table 2 and Table 3). Flows ranging from 1,000 to 20,000 ft^3/s in increments of 1,000 ft^3/s were simulated in the San Acacia reach. The flow corresponding to the water surface just below the bank height was chosen as the bankfull discharge. The bankfull discharge was estimated for every other cross-section throughout the reach and then averaged for specific subreaches. Because this procedure is approximate and does not account for scour that would be experienced at higher discharges, differences in the bankfull discharge less than 1,000 ft^3/s are not considered significant.

3.2.2.1 1972 to 1992 Period

The bankfull discharge can be related to the erosion or deposition occurring in the main channel (Figure 26 and Figure 27). In addition, the bankfull discharge is related to the discharge at which floodplain deposition may start to occur. If the bankfull discharge is increased, floodplain deposition will likely decrease. Conversely, if the bankfull discharge is decreased, floodplain deposition will likely increase.

The bankfull flow from 1972 to 1992 increased in the reach from San Acacia Diversion Dam to approximately Agg/Deg#1365. This reach also experienced significant erosion in the main channel during this time period. The reach from Agg/Deg#1365 to Agg/Deg#1507 maintained a relatively stable bankfull flow from 1972 to 1992. The main channel in this reach also remained relatively stable. In the reach from Agg/Deg#1507 to Agg/Deg#1552 there was a large reduction in bankfull flow from 1972 to 1992 as the channel changed from narrow and deep, to wide and shallow. In the reach from Agg/Deg#1552 to Agg/Deg#1600 there was an increase in channel capacity, but it is largely due to the increase between two cross-sections, Agg/Deg#1577 and Agg/Deg#1584, where the channel was artificially manipulated (pilot channel construction) near Tiffanny Junction as a result of a sediment plug in 1991. Downstream of Agg/Deg#1700, the bankfull discharge decreased from 1972 to 1992 as a result of deposition from backwater effects of a rising reservoir pool.

Table 2: 1972 – 1992 bankfull discharge estimation.

Rangelines	**Bankfull Flow (cfs)**		
Agg/Deg#	**1972**	**1992**	**Comments**
1208 – 1365	14,300	15,700	Increased due to channel erosion
1365 – 1507	6,400	5,900	Stable
1507 – 1552	5,400	3,900	Decreased as channel adjusted after maintenance activities
1552 – 1600	4,100	5,700	Increase due to channel manipulation
1600 – 1700	3,700	3,900	Stable
1700 – 1792	6,800	4,400	Deposition due to influence of reservoir pool and decrease in slope. Channel is becoming perched along this reach

3.2.2.2 1992 to 2002 Period

Figure 26 and Figure 27 show that the bankfull capacity increased between 1992 and 2002 in the reach from Agg/Deg#1208 to Agg/Deg#1372. The lower end of the erosion reach extended further downstream as compared to the 1972 to 1992 periods. The stable reach lengthened, extending from Agg/Deg#1372 - Agg/Deg#1552. From Agg/Deg#1552 to Agg/Deg#1600, the channel adjusted to the channel manipulation performed prior to

1992 (sediment plug near Tiffany Junction in 1991 resulted in temporary channel construction in the area). The reach from Agg/Deg#1600 – Agg/Deg#1674 was stable between 1992 and 2002. From Agg/Deg#1674 to the reservoir, the channel capacity decreased. Agg/Deg#1674 is approximately 3 miles upstream of Agg/Deg#1700, which was the upper extend of the depositional reach from 1972 to 1992.

Table 3: 1992 – 2002 bankfull discharge estimation.

Rangelines	**Bankfull Flow (cfs)**		
Agg/Deg#	**1992**	**2002**	**Comments**
1208 - 1372	12,800	14,000	Increased due to channel erosion
1372 - 1552	5,400	5,100	Stable
1552 - 1600	5,700	2,900	Decreased as channel adjusted after maintenance activities
1600 - 1674	3,600	4,000	Stable
1674 - 1792	4,400	2,400	Deposition due to influence of reservoir pool and decrease in slope. Channel continues to be perched in this reach

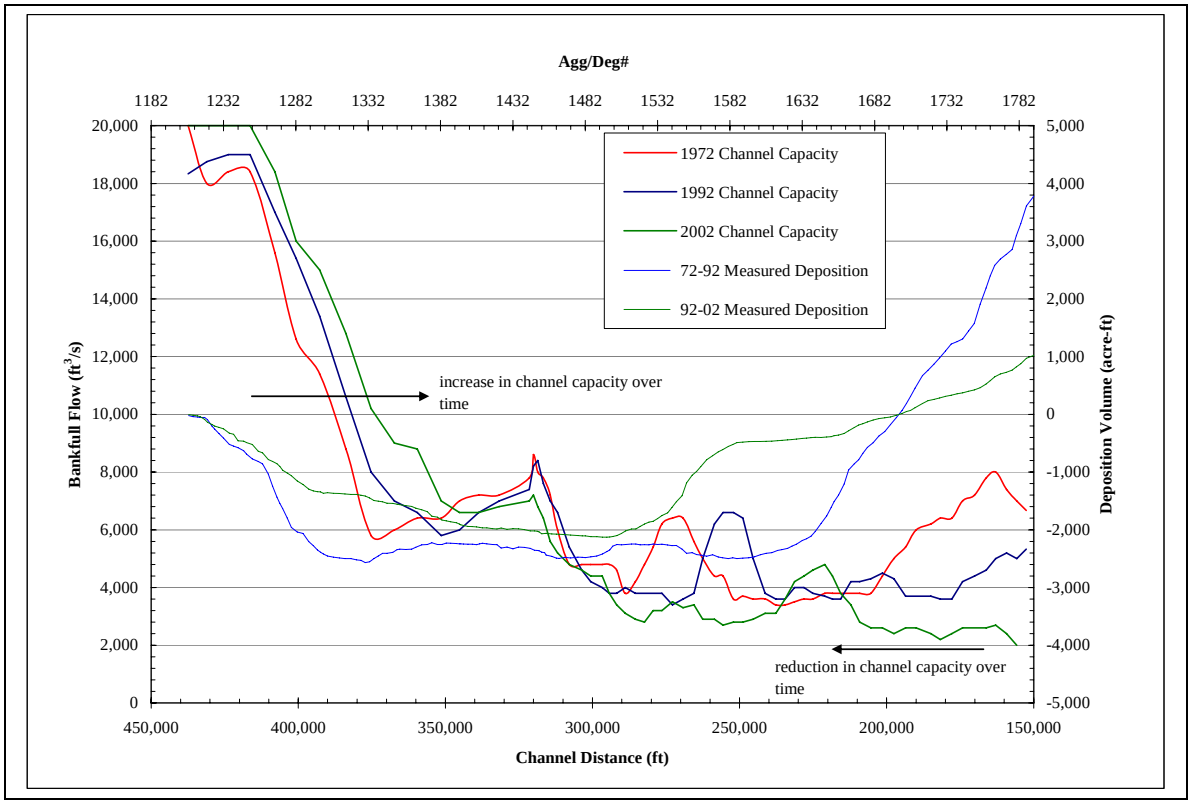

Figure 26: 1972 – 2002 bankfull discharge comparison.

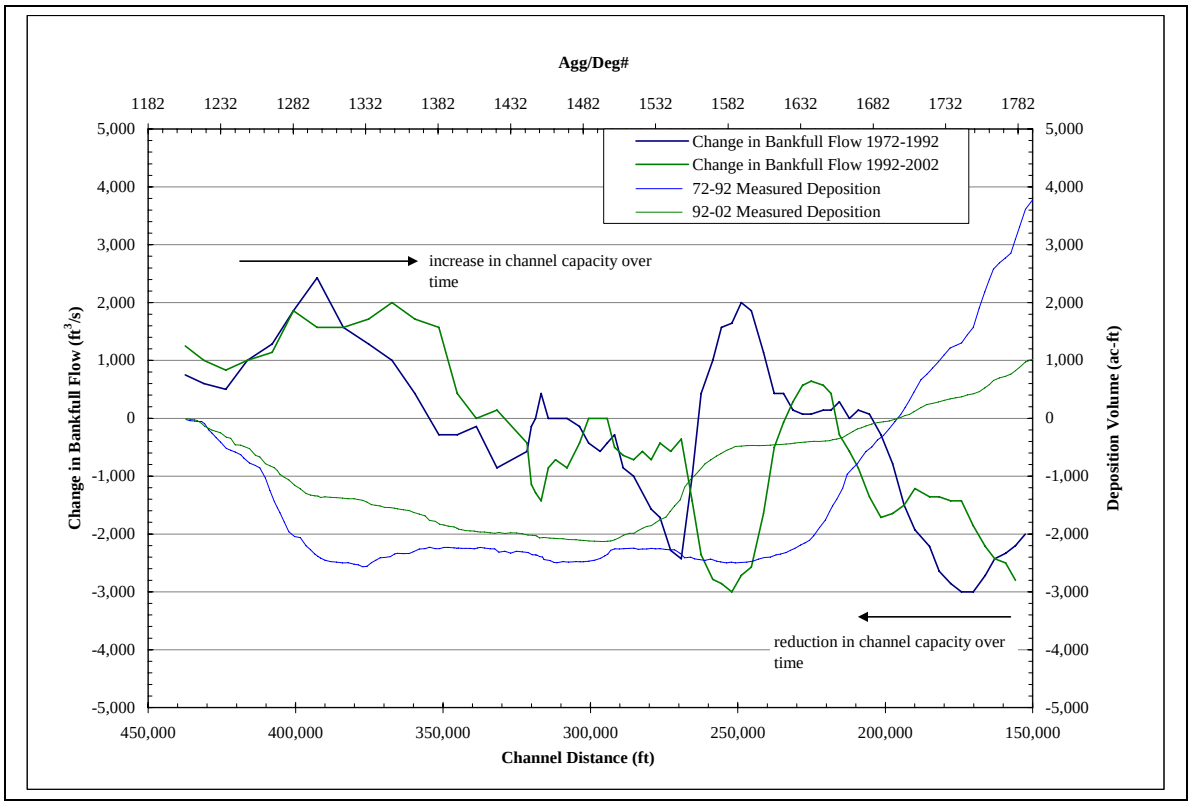

Figure 27: 1972 – 2002 change in bankfull discharge.

3.2.3 Sediment

The sediment data consists of bed-material data, a total load rating curve, and erosion and deposition parameters of cohesive sediments. The bed-material data were obtained from analyzing bed-material samples collected from the river bed. The total load rating curve was determined from Modified Einstein calculations using the BORAMEP (Holmquist-Johnson and Raff, 2004) program, and measured suspended load and bed material data from the USGS floodway gage just below San Acacia Diversion Dam. Sediment size distributions for various discharges were also determined by analyzing gage data. The transport and deposition characteristics of cohesive sediments were based on laboratory results from Vermeyen (1995).

3.2.3.1 Main channel sediment

By their nature, the distributions of particles for both suspended sediment and bed material have a great deal of variability from sample to sample. The source of sediment inflow to the main channel, the change in hydraulic parameters as discharge varies, and the change in sediment concentrations from the rising to falling limb of hydrographs all contribute to this variability. Additionally, each type of large flow event, spring runoff and summer thunderstorm runoff, produce distinct sediment supplies: spring runoff carries a relatively low amount of sediment, while the thunderstorm/arroyo-fed summer events are rich in sediment. Both suspended sediment and bed material particle size changes were examined and the index size d_{50} was calculated for each sample.

Table 4 shows trends in the d_{50} of suspended sediment samples collected from the floodway gages at San Acacia and San Marcial over time (Makar and Strand, 2003). The d_{50} of sediment transported at both gages increased slightly over time. The data indicate

that both suspended sediment and bed material have always been coarser at San Acacia than at San Marcial. They also show a trend at both sites for the sediment to have become coarser over time, particularly in recent years at San Acacia (Figure 28). Sediment samples from the San Acacia and San Marcial gages were used to determine the bed material gain size distributions presented in Figure 29.

Sediment input for the model consisted of 10 grain sizes ranging from clay to coarse gravel. The total sediment load for each time period was determined by using a sediment rating curve with the parameters obtained from the regression of the total load data for each time period (Figure 30). In addition, the fraction of the load within each size class was determined from the results of the total load calculations for each size class. Specific values used for each model are described in the next section under model input. Note that the total load at San Acacia is decreasing over time.

Table 4: Sediment size over time (Makar and Strand, 2003).

Location	Year	Suspended d_{50} (mm)	Bed d_{50} (mm)	Bed d_{84} (mm)
San Acacia	1946	0.026		
	1987	0.056	0.19	1.35
	2000	0.065	0.35	4.04
San Marcial	1946	0.015		
	1987	0.039	0.15	0.22
	2000	0.046	0.21	0.34

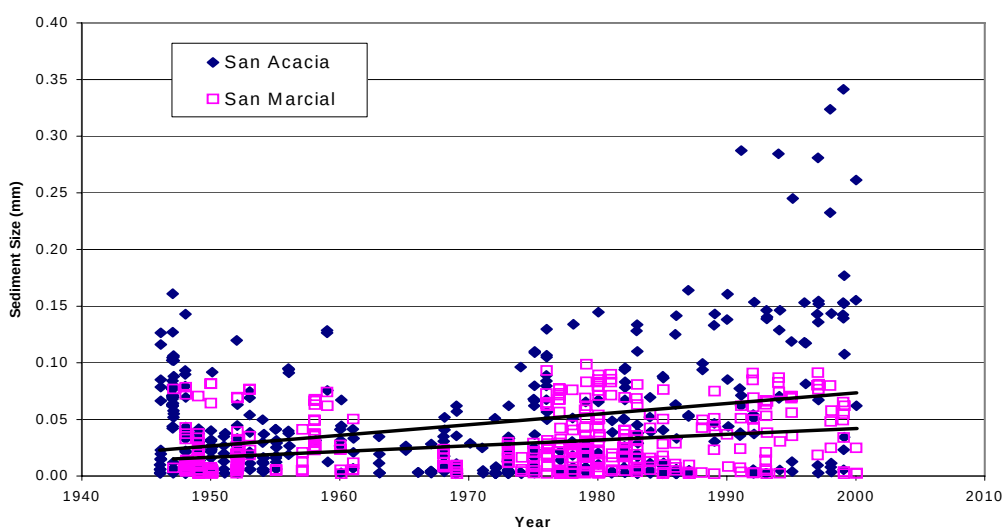

Figure 28: d_{50} of suspended sediment samples.

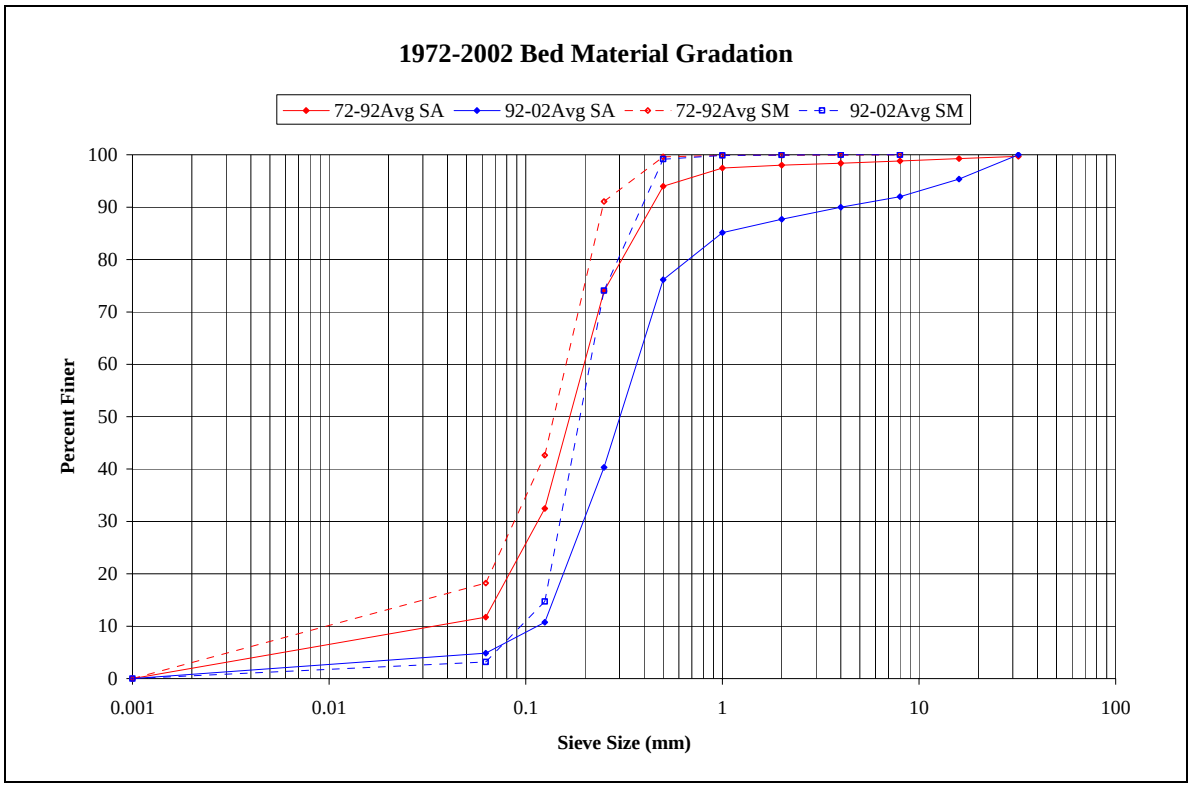

Figure 29: Average bed material gradation for San Acacia reach.

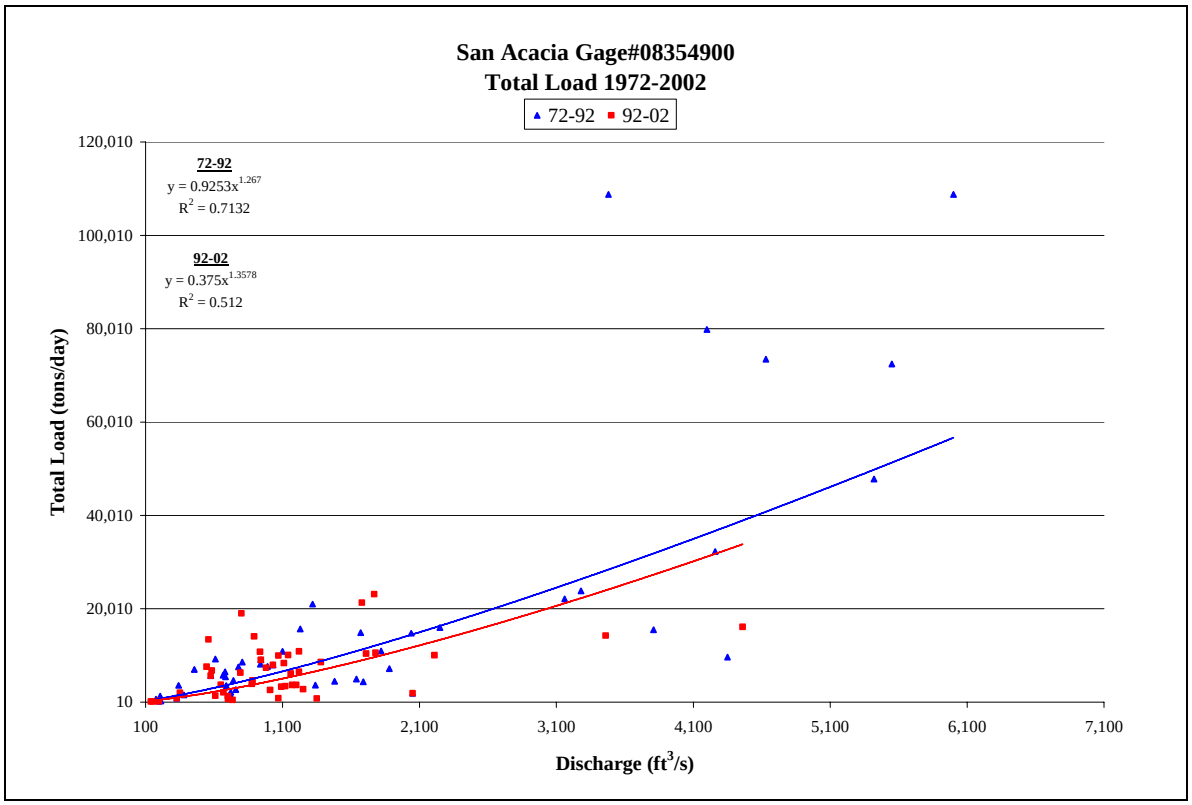

Figure 30: Total sediment load 1972 to 2002.

3.2.3.2 Tributary sediment inflow

There are several ungaged tributaries in the San Acacia reach. A total of five tributaries were considered for this study. Tributaries draining to the Rio Grande on the east side of the river that were included in the model consist of Arroyo Alamillo, Arroyo de la Parida, and Arroyo de las Canas. Runoff from the west of the Rio Grande is primarily intercepted by the Middle Rio Grande Conservancy District's canals and drains, and the Low Flow Conveyance Channel except for two points of direct connection to the Rio Grande at the North Socorro Diversion Channel, and Brown Arroyo. None of these tributaries are gaged; therefore, surface bed-material samples were taken to determine the bed material gradations and sub-basin delineations (Figure 9) were made to estimate the amount of water and sediment being transported into the Rio Grande (Daraio, 2003; Bauer and Hilldale, 2004).

3.2.4 Hydrology

The hydrology data used in the calibration models consisted of daily flows and monthly reservoir elevations of Elephant Butte Reservoir. The monthly reservoir elevations were used as the downstream boundary condition for the model. The daily flows of the Rio Grande Floodway at San Acacia were obtained from the records of surface water flows published by the U.S. Geological Survey. Figure 31 shows the mean daily flows for the period of each model calibration (1972 to 1992 and 1992 to 2002) and a plot of reservoir elevations is provided in Figure 32. Note that the scale of the y-axis is set to match that needed for the stochastic hydrology used in the predictive models.

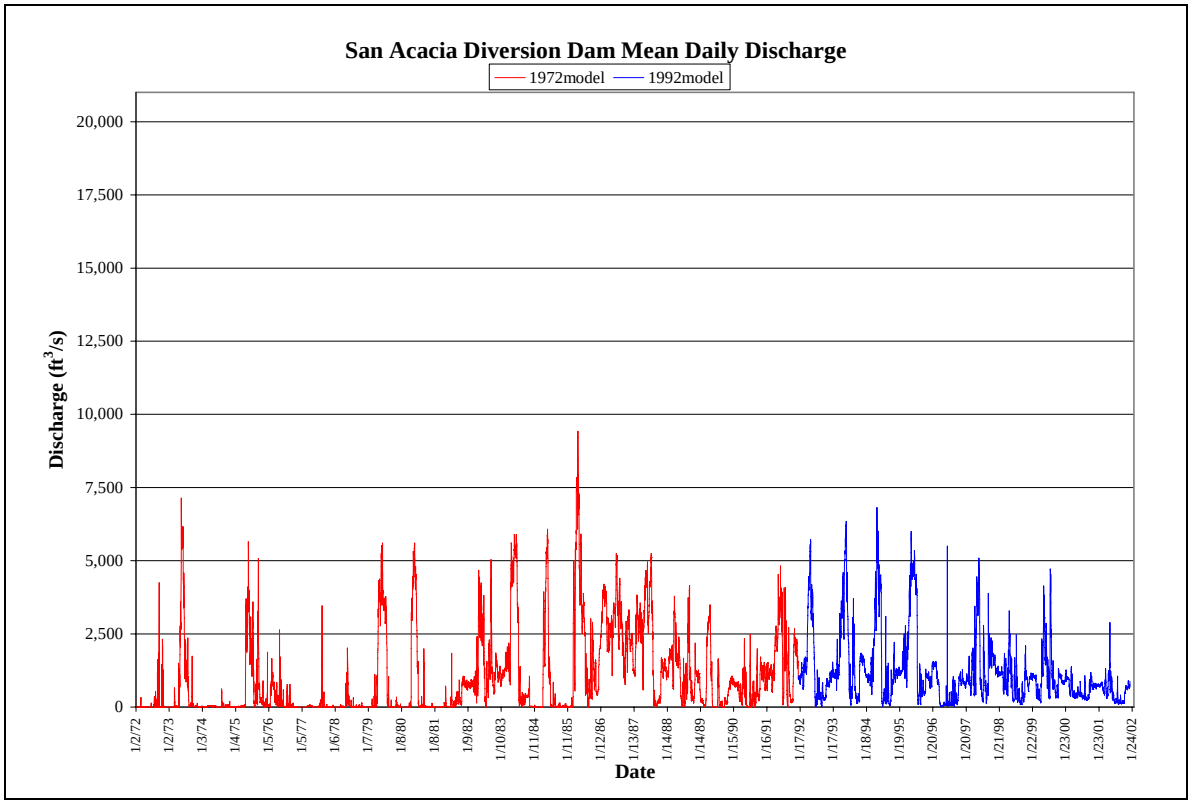

Figure 31: Mean daily discharges for 1972 to 2002.

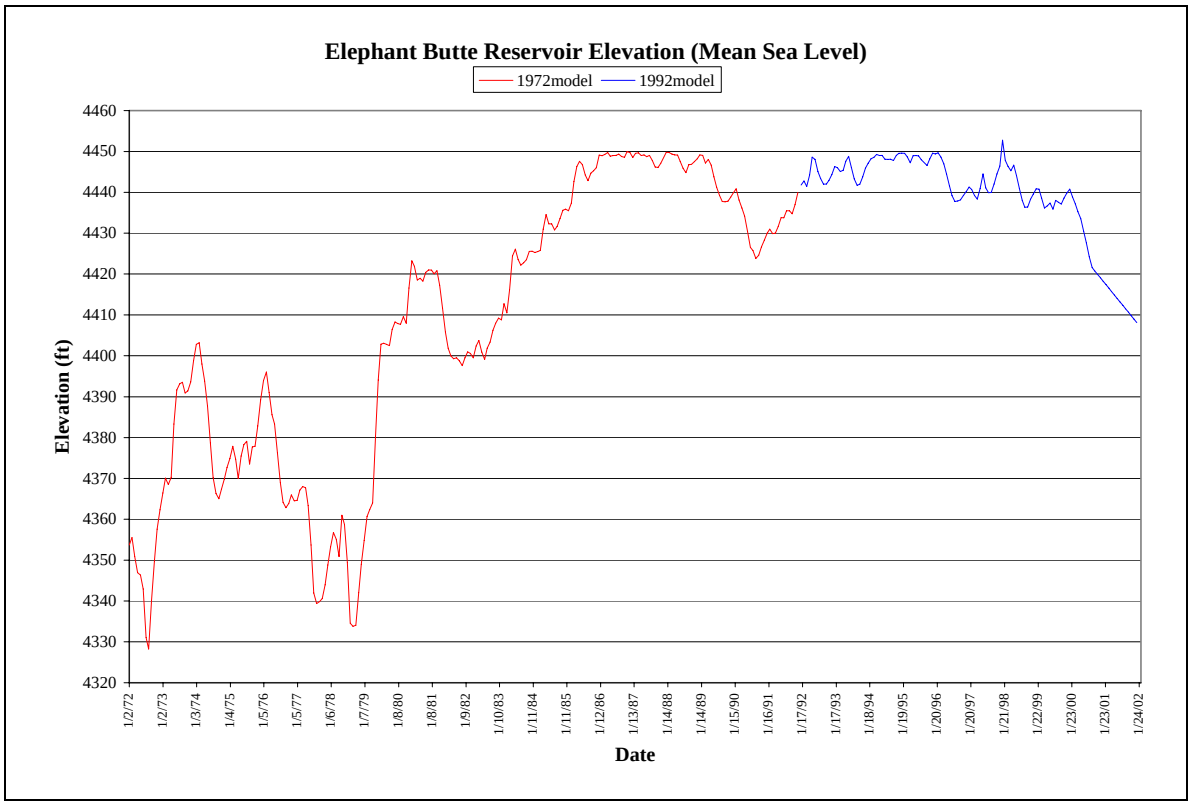

Figure 32: Elephant Butte Reservoir elevations for 1972 to 2002.

The flows developed for the predictive modeling (2002 to 2022) were a series of synthetically generated flows that potentially could take place in the future for three hydrology types; wet, average, and dry (Lane, 2004). They were based on the application of standard time series models to the observed historical flows and the subsequent generation of potential future traces using the statistical properties estimated from the historical data. The stochastic model was developed using stream flow data on the Rio Grande at San Acacia Diversion Dam from the period 1896 to 2001. A total of 40 traces were generated and analyzed to determine which traces best represented the three hydrologic periods of interest (Figure 33). The results of the stochastic analysis for each hydrology type are shown in Figure 34- Figure 37. It should be noted that the peaks and flood flows do not include flow regulation, especially at Cochiti Dam. Some impact of regulation is included because of the inclusion of flows post 1972, after construction of Cochiti Dam, but since the period of record extends from 1896 to 2001 there is a large period of non-regulated flows that influence the pattern and magnitude of the stochastic flows. Therefore, the stochastic hydrology produces peaks and flood flows that are greater than shown in the 1972 to 2002 measured data (Figure 38).

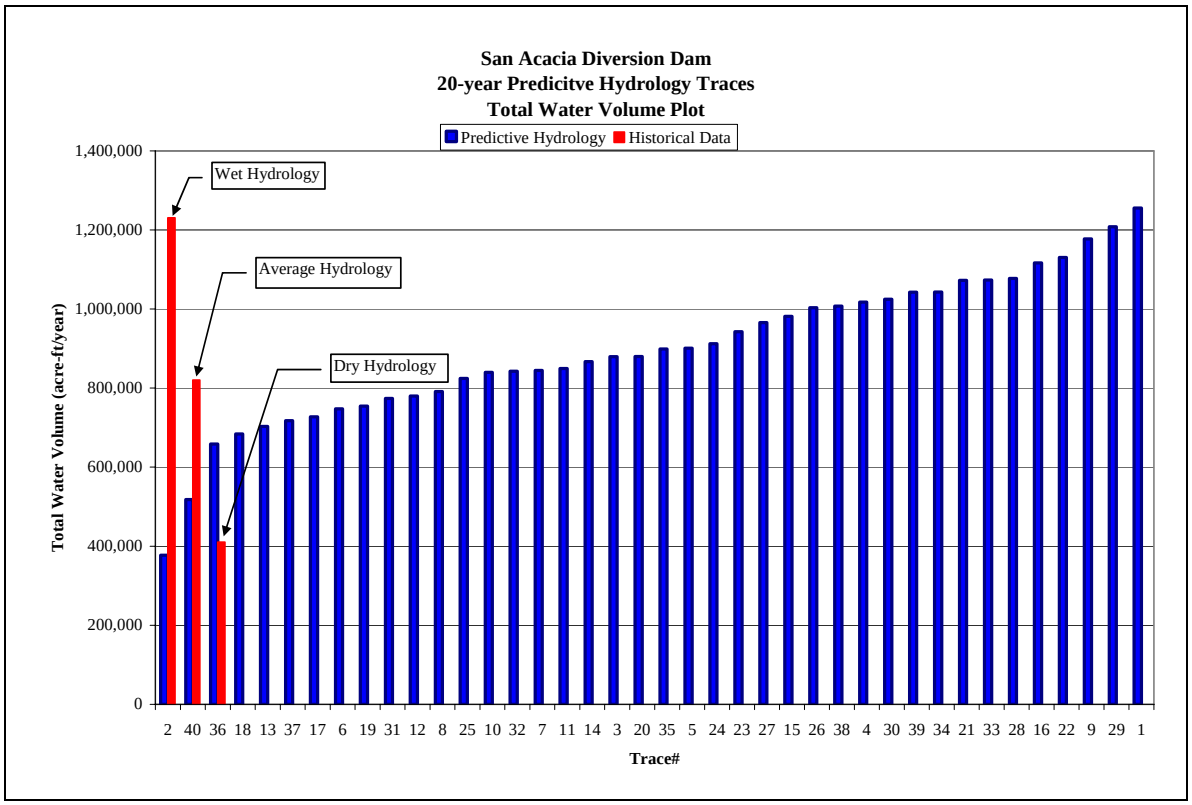

Figure 33: Historical vs. predictive stochastic total water volume.

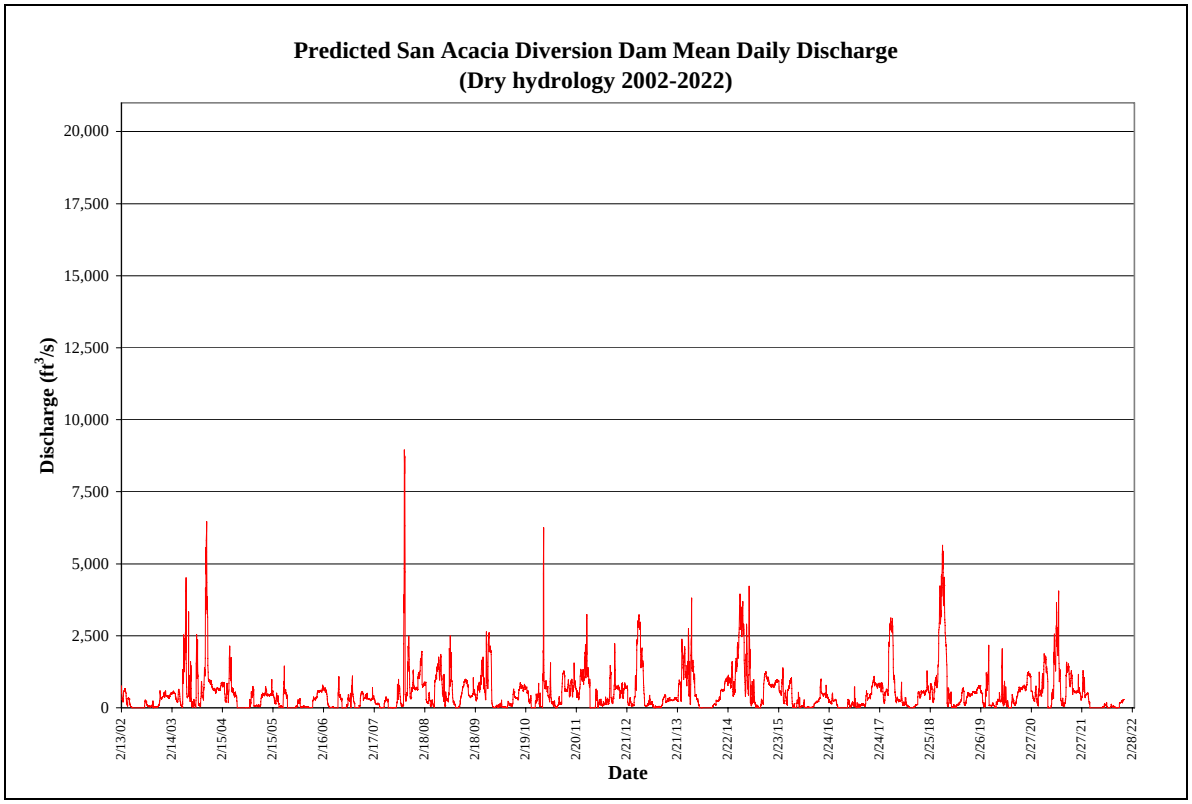

Figure 34: Generated stochastic mean daily discharge for dry hydrology.

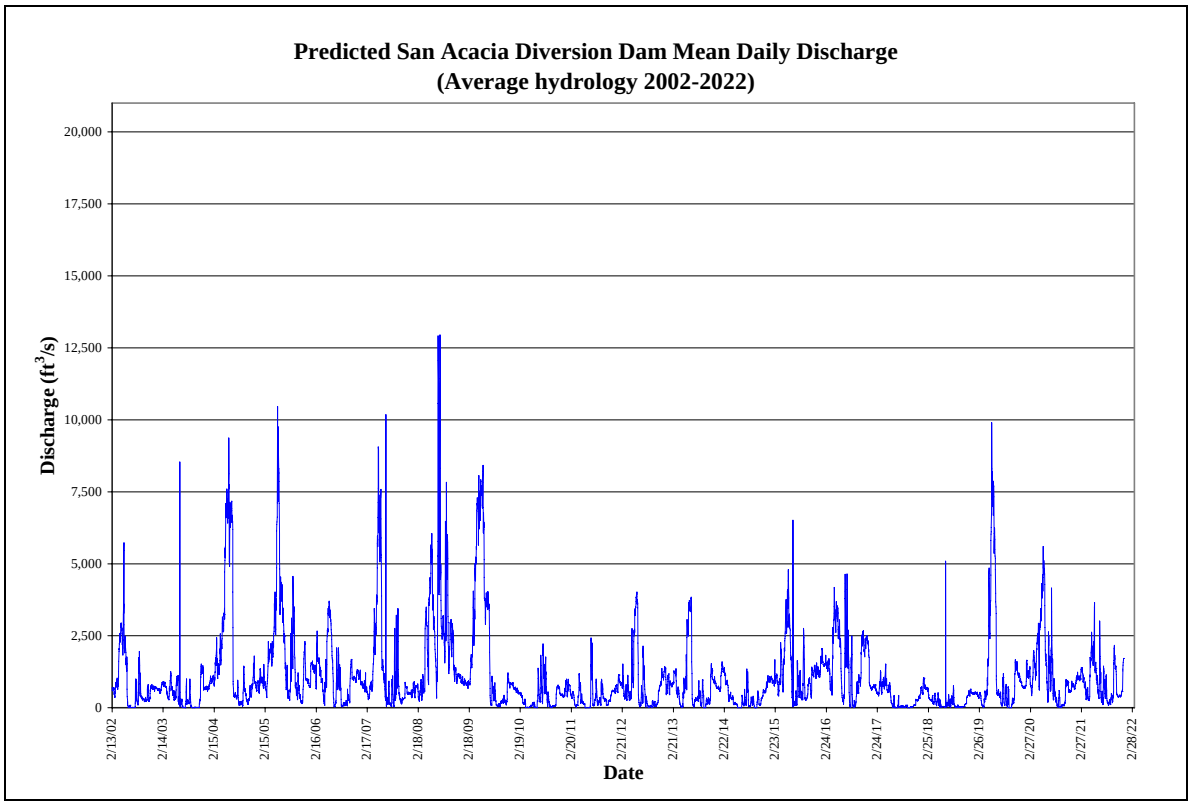

Figure 35: Generated stochastic mean daily discharge for average hydrology.

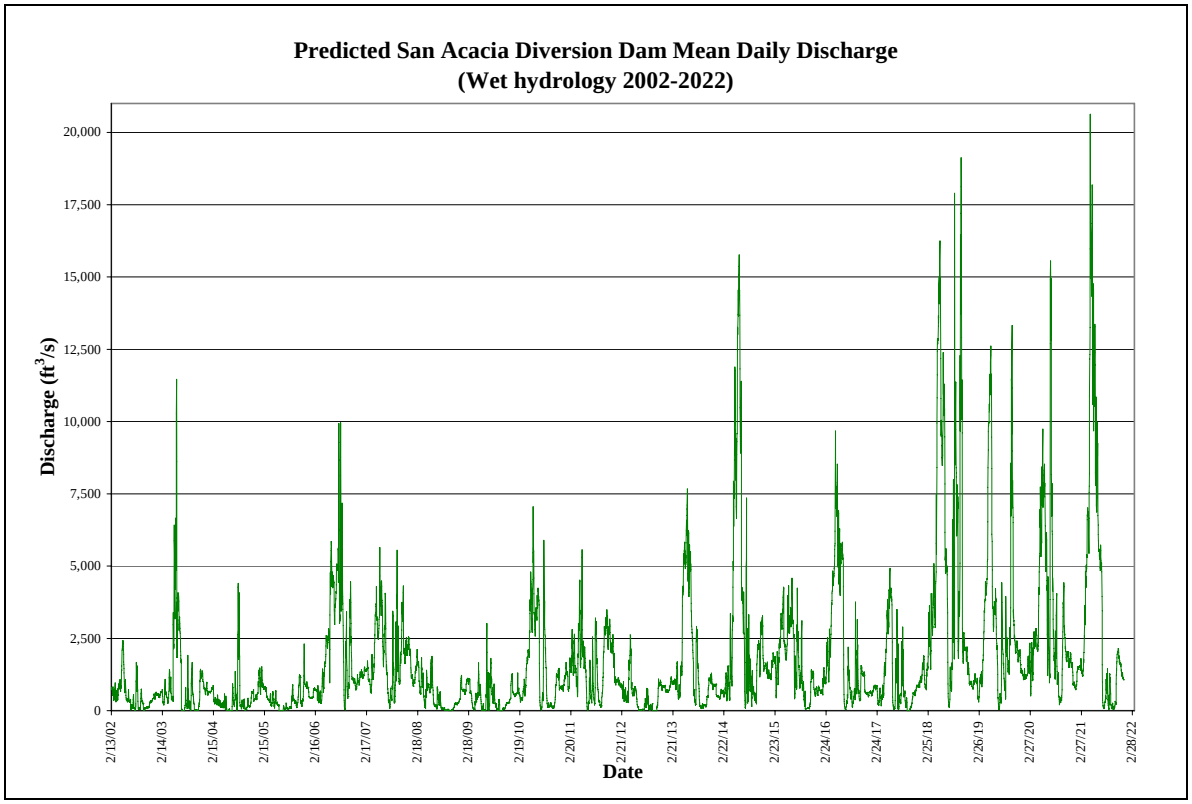

Figure 36: Generated stochastic mean daily discharge for wet hydrology.

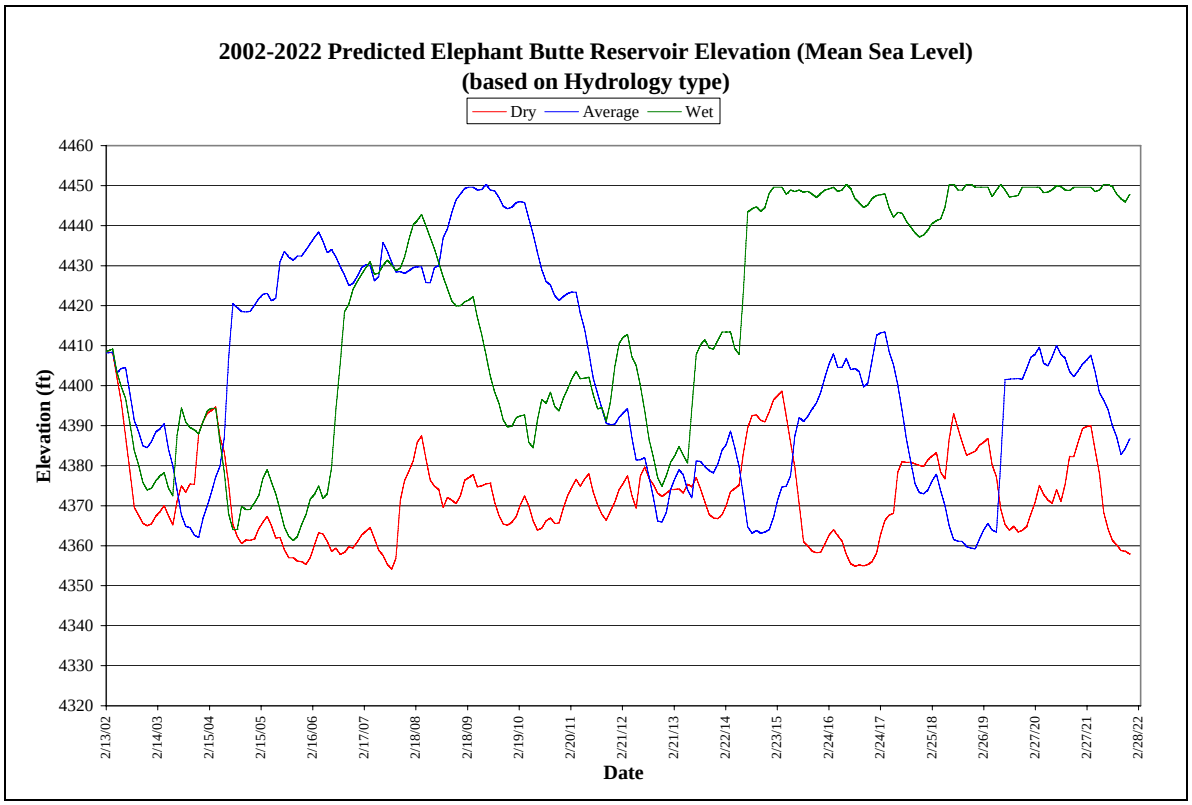

Figure 37: Generated stochastic Elephant Butte Reservoir elevations.

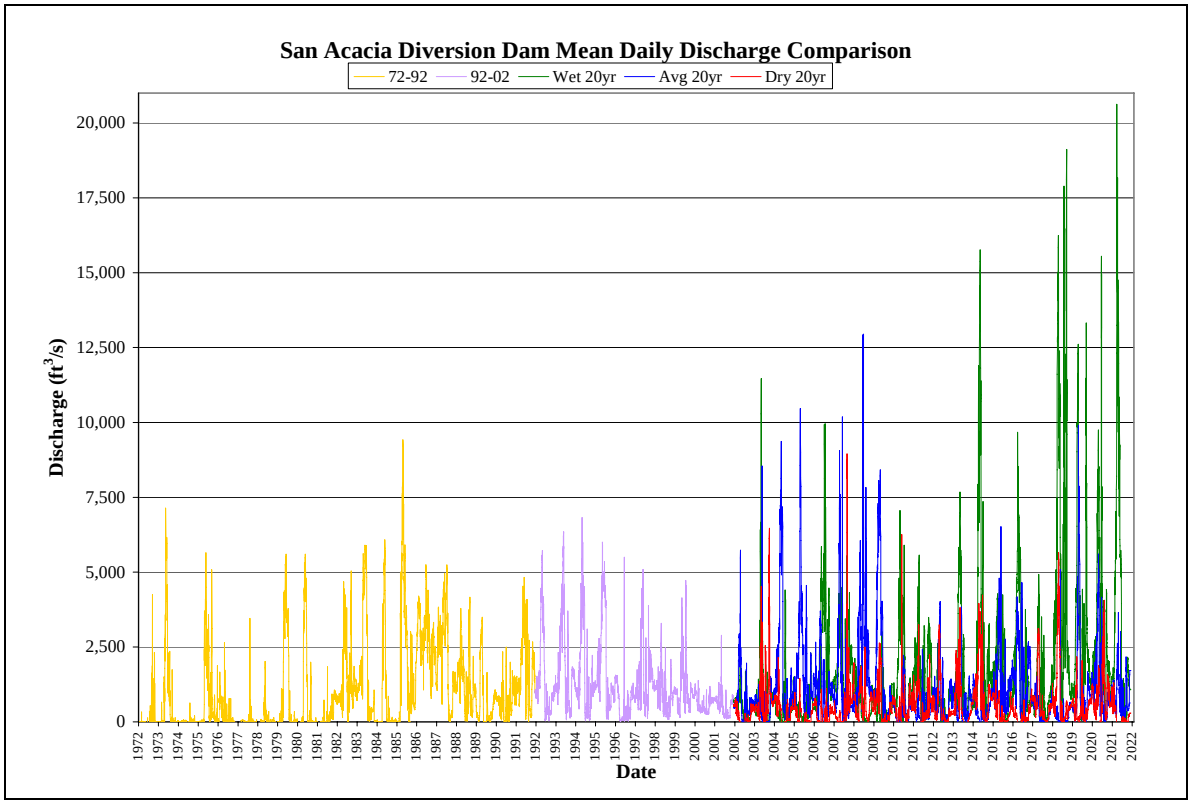

Figure 38: Historical vs. generated stochastic mean daily discharges.

4 Model Calibration

Two hydrologic periods were used to calibrate the model: dry period from 1972 to 1992 and a wetter period from 1992 to 2002. Hydrology consisted of mean daily flows recorded at the San Acacia floodway gage with extremely low flows (<100 ft^3/s) eliminated to maximize the chance of convergence and model stability. The 1972 and the 1992 cross-section data were the basis for calibration.

4.1 Model Input

The models used the 1972 and 1992 photogrammetric Agg/Deg cross-section data; average bed material gradation data; total load rating curve and sediment gradation; daily flow data developed from the San Acacia floodway gage; and monthly reservoir elevations at Elephant Butte Reservoir. The model consists of 226 cross-sections starting at San Acacia Diversion Dam (AggDeg#1208) and ending at the lower end of Elephant Butte Reservoir (EB#74). General considerations in these models included the number of sediment size fractions, number of bed material layers, minimum flow, length of simulation, and time step. The model simulations are very computationally intensive; for example, using a time step of 0.5 hrs, the numerical simulation took ~18 hours running on a PC computer with dual 2.4 GHz Xeon processors and 1.0 GB memory. The following describes data and assumptions used to create the input files for the model.

4.1.1 Hydrology and Boundary Conditions

Flow data are input at the upstream boundary in the form of a flow table. The table lists a time and an associated flow. For the calibration simulations, mean daily flow values from the San Acacia floodway gauge from 1972 to 1992 and 1992 to 2002 were used. These periods coincide with the collection dates of the Agg/Deg cross-section data. The period from 1972 to 1992 represents a dry decade followed by a relatively wet decade. Flow statistics for each of the model periods is shown in Table 5.

Table 5: Flow statistics for calibration models.

	Discharge (ft^3/s)			
	Minimum	**Maximum**	**Average**	**Std Deveation**
72-92	0	9,420	955	1,406
92-02	17	6,820	1,190	1,165

It should be noted that the LFCC was operated for more than half of the 20-year period from 1972 to 1992. Almost 46 percent of daily flow values are less than 100 ft^3/s (Figure 39).

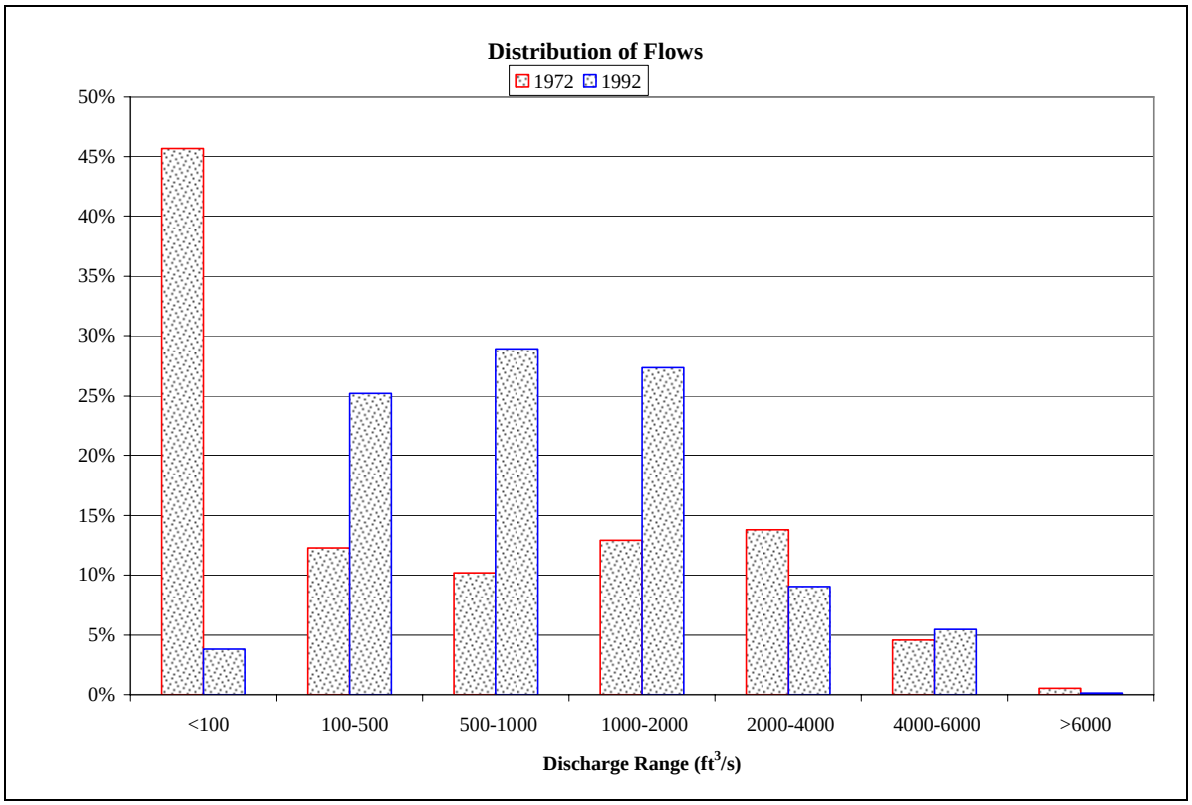

Figure 39: Distribution of flows for calibration models.

Monthly water surface elevation data from Elephant Butte Reservoir are used as the downstream boundary condition. These data are input in the form of an elevation table; the table lists a time and an associated water surface elevation. The minimum (~4330 ft.) and maximum (~4450 ft.) pool elevations for each time period can be seen in Figure 32.

4.1.2 Cross-section Geometry

The initial channel geometry was taken from the 1972 and 1992 photogrammetric surveys. Defining main channel limits (bank stations), levees, ineffective flow areas, and blocked obstructions were a critical step in defining the cross-section geometry for the sediment model. The bank stations were chosen based on the width of the vegetation in the cross-section observed from the 1972 and 1992 aerial photography. As previously stated, some adjustments were made to create a gradual transition in width for numerical stability. Additionally, levees and ineffective flows were used in the overbanks to account for the flow transitions from in-bank to out-of-bank, especially in the perched channel portion of the system. Levees and ineffective flows were used to better define and model the portion of the overbank considered active and transporting sediment. The LFCC was not included in this study and therefore blocked obstructions were used to restrict water from entering the LFCC. A representative cross-section showing all of these parameters is shown in Figure 40.

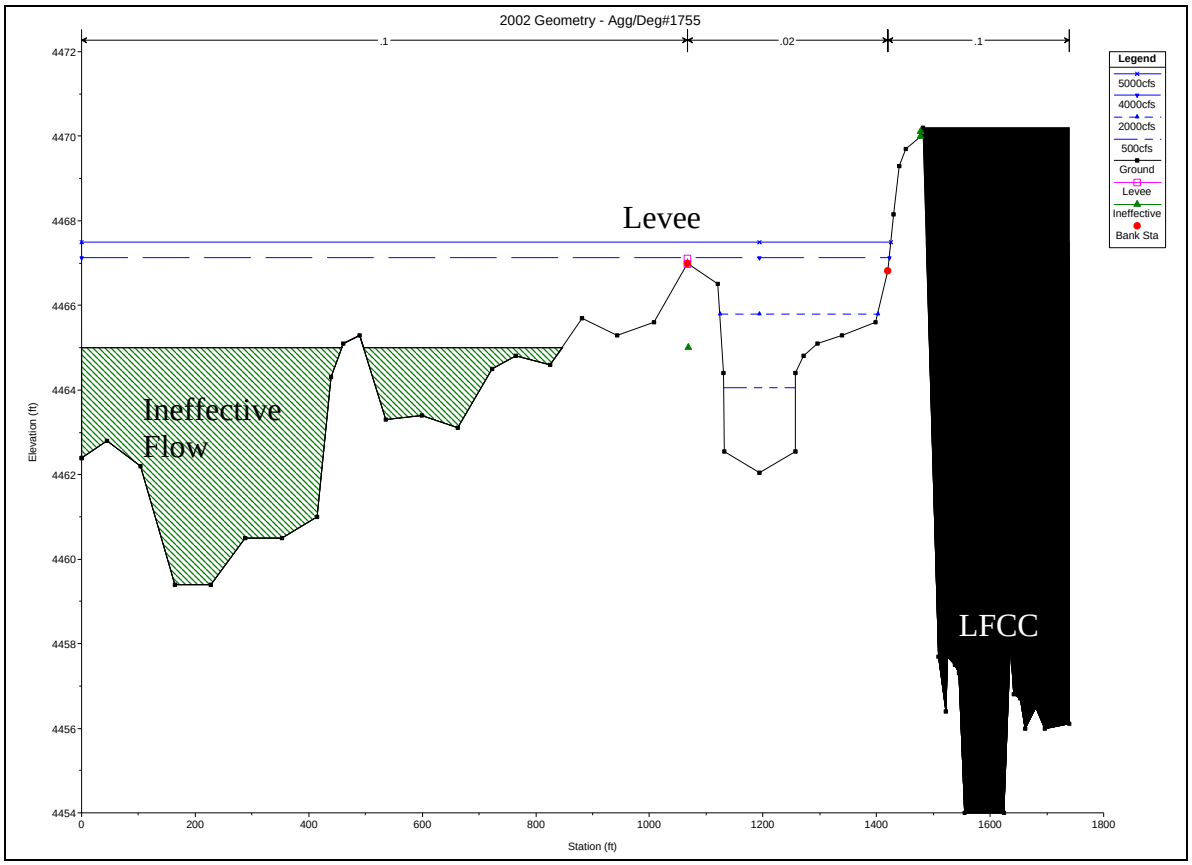

Figure 40: Example cross-section with channel limits, levee, ineffective flow, and blocked obstruction designations.

4.1.3 Sediment

A total of 10 grain sizes were used, ranging from clay to coarse gravel. The relationship between sediment load and flow rate was assumed to follow a power function given as:

$$Q_s = aQ^b$$

where Q_s is the sediment load in tons/day, Q is the flow rate in ft^3/s, and a and b are coefficients. The a and b coefficients were determined by fitting them to the total load data (Figure 41) derived from applying the Modified Einstein procedure to the San Acacia floodway gage data. The resulting rating curves significantly under predicted the total volume of sediment deposited in Elephant Butte Reservoir based on Agg/Deg data: 28,547 acre-ft vs. ~50,000 acre-ft for 1972 to 1992 and 9,082 acre-ft vs. ~20,000 acre-ft for 1992 to 2002. As a result, the amount of incoming fines was increased by multiplying the "*a*" coefficient by a constant and increasing the percentage of fines to match the total measured deposition in the reach while maintaining the total amount of coarse sediment entering the model to remain similar to the original input (Table 6). In addition, the fraction of the load within each size class was determined by increasing the amount of fines and then adjusting the remaining classes using a weighting scheme (Table 7).

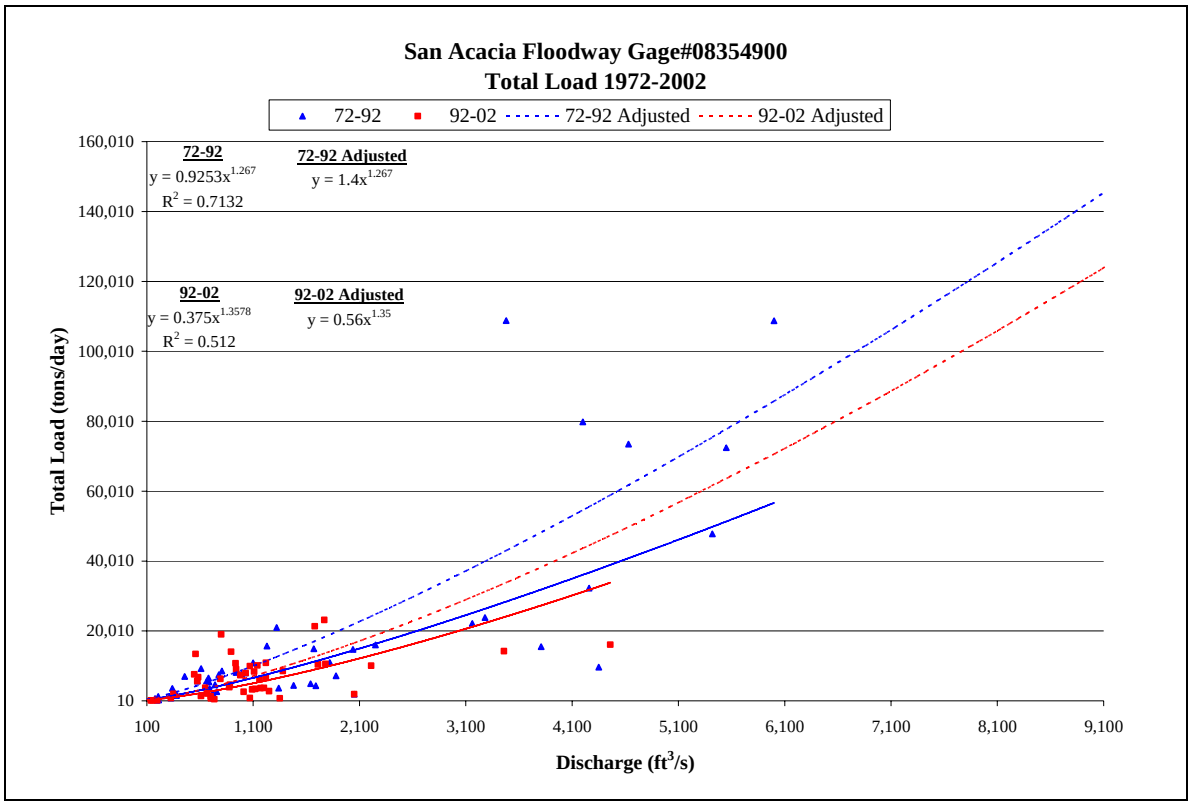

Figure 41: Total sediment load with adjusted rating curve.

Table 6: Adjusted total sediment load comparison.

Original Data			Model Input (adjusted fines by discharge)		
1972 input data					
Qs=0.92Q^1.267			Qs=1.4Q^1.267		
total incoming sediment			**total incoming sediment (Model)**		
28,547.86	acre-ft	bulk	**45,925.53**	acre-ft	bulk
total incoming coarse			**total incoming coarse**		
15,936.01	acre-ft	bulk	**14,224.39**	acre-ft	bulk
1992 input data					
Qs=0.375Q^1.35			Qs=0.56Q^1.35		
total incoming sediment			**total incoming sediment (Model)**		
9,082.93	acre-ft	bulk	**18,947.07**	acre-ft	bulk
total incoming coarse			**total incoming coarse**		
6,128.02	acre-ft	bulk	**5,084.94**	acre-ft	bulk

Table 7: Incoming sediment load data from Modified Einstein calculations.

	Original Data										
	Discharge	fines	vfs	fs	ms	cs	vcs	vfgrv	fgrv	grv	cgrv
	(ft^3/s)	**<0.0625**	**0.0625-0.125**	**0.125-0.25**	**0.25-0.5**	**0.5-1.0**	**1-2**	**2-4**	**4-8**	**8-16**	**16-32**
72-92	101-500	34.97	32.44	21.79	10.06	0.71	0.02	0.00	0.00	0.00	0.00
	501-1000	35.08	36.85	20.31	7.54	0.22	0.00	0.00	0.00	0.00	0.00
	1001-2000	36.06	31.68	21.16	10.22	0.83	0.03	0.02	0.00	0.00	0.00
	2001-4000	48.67	25.75	21.06	3.98	0.53	0.02	0.00	0.00	0.00	0.00
	4001-6000	56.56	18.50	16.32	7.34	1.20	0.09	0.00	0.00	0.00	0.00
92-02	101-500	32.17	6.65	27.42	26.61	6.65	0.50	0.00	0.00	0.00	0.00
	501-1000	31.64	10.55	26.60	26.14	4.63	0.41	0.03	0.00	0.00	0.00
	1001-2000	21.51	9.34	32.17	30.81	5.52	0.56	0.09	0.00	0.00	0.00
	2001-4000	38.78	21.30	25.24	11.56	2.45	0.41	0.16	0.09	0.01	0.00
	Model Input with adjusted gradations										
	Discharge	fines	vfs	fs	ms	cs	vcs	vfgrv	fgrv	grv	cgrv
	(ft^3/s)	**<0.0625**	**0.0625-0.125**	**0.125-0.25**	**0.25-0.5**	**0.5-1.0**	**1-2**	**2-4**	**4-8**	**8-16**	**16-32**
72-92	101-500	60	19.96	13.40	6.19	0.44	0.01	0.00	0.00	0.00	0.00
	501-1000	63	21.00	11.57	4.30	0.13	0.00	0.00	0.00	0.00	0.00
	1001-2000	65	17.34	11.58	5.60	0.46	0.01	0.01	0.00	0.00	0.00
	2001-4000	70	15.05	12.31	2.33	0.31	0.01	0.00	0.00	0.00	0.00
	4001-6000	80	8.52	7.51	3.38	0.55	0.04	0.00	0.00	0.00	0.00
92-02	101-500	70	2.94	12.13	11.77	2.94	0.22	0.00	0.00	0.00	0.00
	501-1000	75	3.86	9.73	9.56	1.70	0.15	0.01	0.00	0.00	0.00
	1001-2000	60	4.76	16.39	15.70	2.81	0.29	0.05	0.00	0.00	0.00
	2001-4000	80	6.96	8.25	3.78	0.80	0.13	0.05	0.03	0.00	0.00

The bed material data set used for the calibrations consist of bed material samples from the San Acacia gage, San Marcial gage, and additional cross-section bed material samples taken at various locations along the reach. The resulting distributions for the bed material are shown in Table 8. GSTAR-1D linearly interpolates, according to stream distance, bed material gradations between the cross-sections given below.

Table 8: Bed material for the San Acacia reach.

		fines	vfs	fs	ms	cs	vcs	vfgrv	fgrv	grv	cgrv
	Agg/Deg#	**<0.0625**	**0.0625-0.125**	**0.125-0.25**	**0.25-0.5**	**0.5-1.0**	**1-2**	**2-4**	**4-8**	**8-16**	**16-32**
72-92	1208	12.03	20.72	41.53	20.03	3.48	0.56	0.34	0.43	0.45	0.42
	1552	18.24	24.40	46.45	10.53	0.27	0.05	0.03	0.03	0.00	0.00
	1731	32.01	22.53	37.19	7.05	1.19	0.03	0.00	0.00	0.00	0.00
92-02	1208	3.70	4.76	8.50	21.11	12.63	7.57	8.08	9.24	10.93	13.49
	1259	3.82	6.94	35.31	43.87	6.84	1.39	0.76	0.55	0.52	0.00
	1552	5.90	11.18	42.72	34.86	5.03	0.28	0.03	0.00	0.00	0.00
	1661	20.16	10.01	41.42	26.66	1.54	0.15	0.06	0.01	0.00	0.00
	1792	19.29	23.03	40.29	13.88	3.50	0.00	0.00	0.00	0.00	0.00

4.1.4 Lateral Water and Sediment Inflow

Lateral flow and sediment from arroyos are input in the form of a time-flow and time-sediment table. The table lists input location, time, and an associated flow/sediment load. Flow and sediment statistics for each of the arroyos are shown in Table 9. These flows were estimated to occur once a year over a three day period between the months of July and September (during summer thunderstorm events). Details on how arroyo inflows and sediment transport were estimated were provided in section 3.1.3.

Table 9: Arroyo flow and sediment statistics.

	Discharge (ft^3/s)			Sediment Load (tons/day)		
	Day 1	**Day2**	**Day3**	**Day 1**	**Day2**	**Day3**
Alamillo	652	193	12	105,081	18,448	532
Parida	507	78	1	28,805	2,312	8
NSDC	328	86	4	136,464	35,831	1,864
Canas	461	112	5	24,627	3,425	77
Brown	257	62	3	51,297	12,371	562

	fines	vfs	fs	ms	cs	vcs	vfgrv	fgrv	grv	cgrv
	<0.0625	**0.0625-0.125**	**0.125-0.25**	**0.25-0.5**	**0.5-1.0**	**1-2**	**2-4**	**4-8**	**8-16**	**16-32**
Alamillo	80	10.00	8.00	2.00	0.00	0.00	0.00	0.00	0.00	0.00
Parida	70	10.16	6.51	3.81	2.00	5.18	1.24	0.95	0.13	0.02
NSDC	80	10.00	10.00	0.00	0.00	0.00	0.00	0.00	0.00	0.00
Canas	70	3.97	4.52	2.20	0.98	0.82	6.77	4.81	4.43	1.49
Brown	70	20.00	10.00	0.00	0.00	0.00	0.00	0.00	0.00	0.00

4.1.5 Transport Calibration Parameters

Several parameters in this section of the input file are used to calibrate the model. Model parameters were set so that one stream tube was used in the simulation and the bank angle of repose above and below the water surface was set to 60 and 45 degrees, respectively. Yang's sand (1973) and gravel (1984) and Engelund-Hansen (1972) transport formulas were used to calculate the sediment transport capacity. The active layer thickness is equal to a constant times the diameter of the largest sediment size with a bed fraction of at least 0.01 percent. Based on results from initial calibration simulations, in order to replicate the aggradation/degradation trends along the reach, the constant was set equal to 21 downstream of San Acacia Diversion Dam, 14 in the middle of the reach, and 7 in the lower portion of the reach near Elephant Butte Reservoir.

There are large uncertainties in the transport parameters for cohesive sediments (assumed here to be those sediments with a diameter less than 0.062 mm). The experimental data of Vermeyen (1995) was used in the numerical model for the consolidated sediment in the lower portion of the reach below San Marcial. The experimental values for the critical shear stress for erosion and deposition are 0.125 lb/ft^2 and 0.02 lb/ft^2 respectively. The critical shear stress for erosion and deposition was varied along the reach depending upon the anticipated opportunity for consolidation. Lower values were used in the upper reach to allow the unconsolidated fines that are deposited during low flows to erode during larger flows.

4.2 Sensitivity Analysis

After input to the model was complete, simulations were run and input parameters were adjusted until results were stable and consistent with expected trends. Sensitivity tests were then run with respect to sediment transport equation, bed material gradation, incoming sediment load and gradation, levee/ineffective flow designation, and silt and clay transport parameters. The results show the predicted deposition and erosion is more sensitive to changes in the incoming sediment load (incoming sediment rating curve), incoming sediment load gradation, and time step than any other parameters. It should be noted that portions of the reach containing a perched channel system were found to be very sensitive to levee/ineffective flow designation when comparing main channel and floodplain aggradation/degradation.

4.2.1 Sediment Transport Equation

The selection of the sediment transport equation was based on matching the total volume of deposition. Engelund – Hansen (1972) and Yang (1973) were used in the calibration phase. It was determined that the Engelund – Hansen formula best predicted the sediment transport in the San Acacia reach of the Rio Grande (Figure 42).

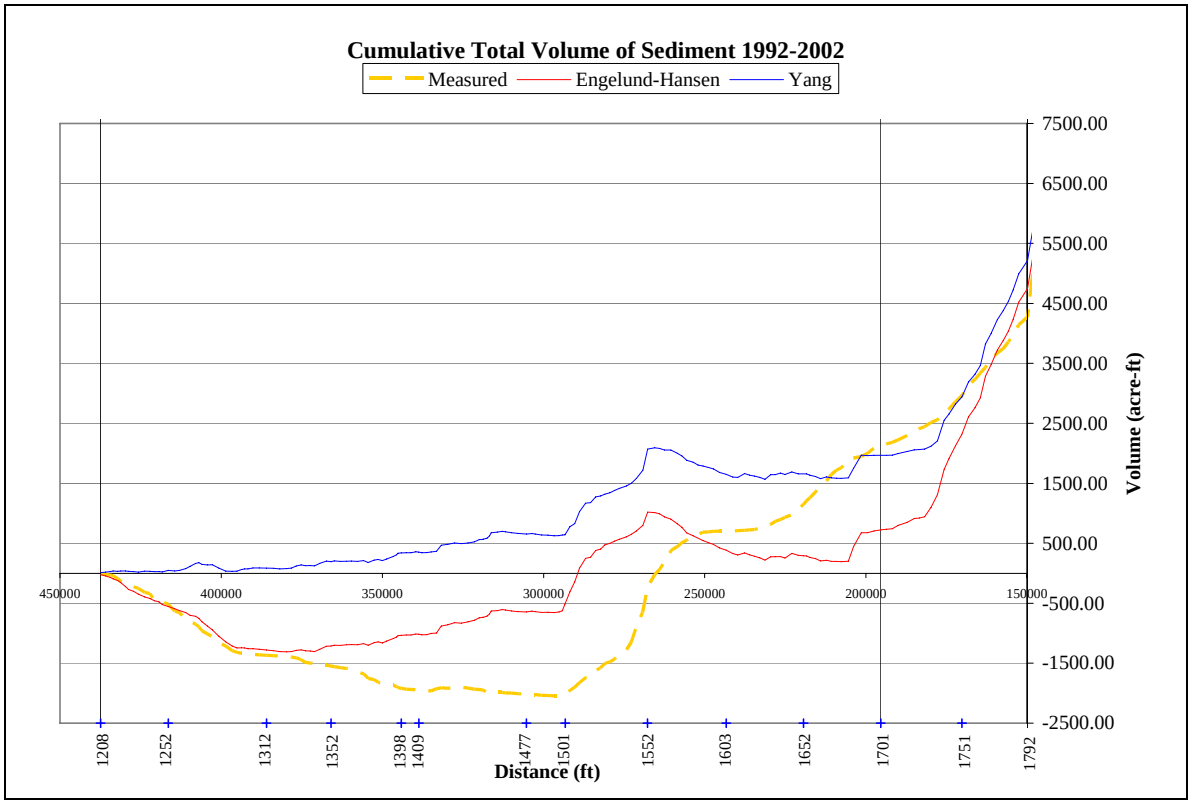

Figure 42: Affects of sediment transport equation on model results.

4.2.2 Incoming sediment load

The incoming sediment load gradation in the model was varied from coarse to fine within the limits of the scatter of the collected data. This change did not affect the total volume of deposition for the entire reach. However, the amount of material eroded in the upstream portion of the model was affected by changing the percentage of fines. In general, a greater percentage of fines increased the erosion predicted in the upstream portion of the model and a smaller percentage of fines resulted in decreased erosion in the upstream portion of the model. The results of this analysis are shown in Figure 43. From the results, it was determined that using 80% fines produced results similar to the measured data.

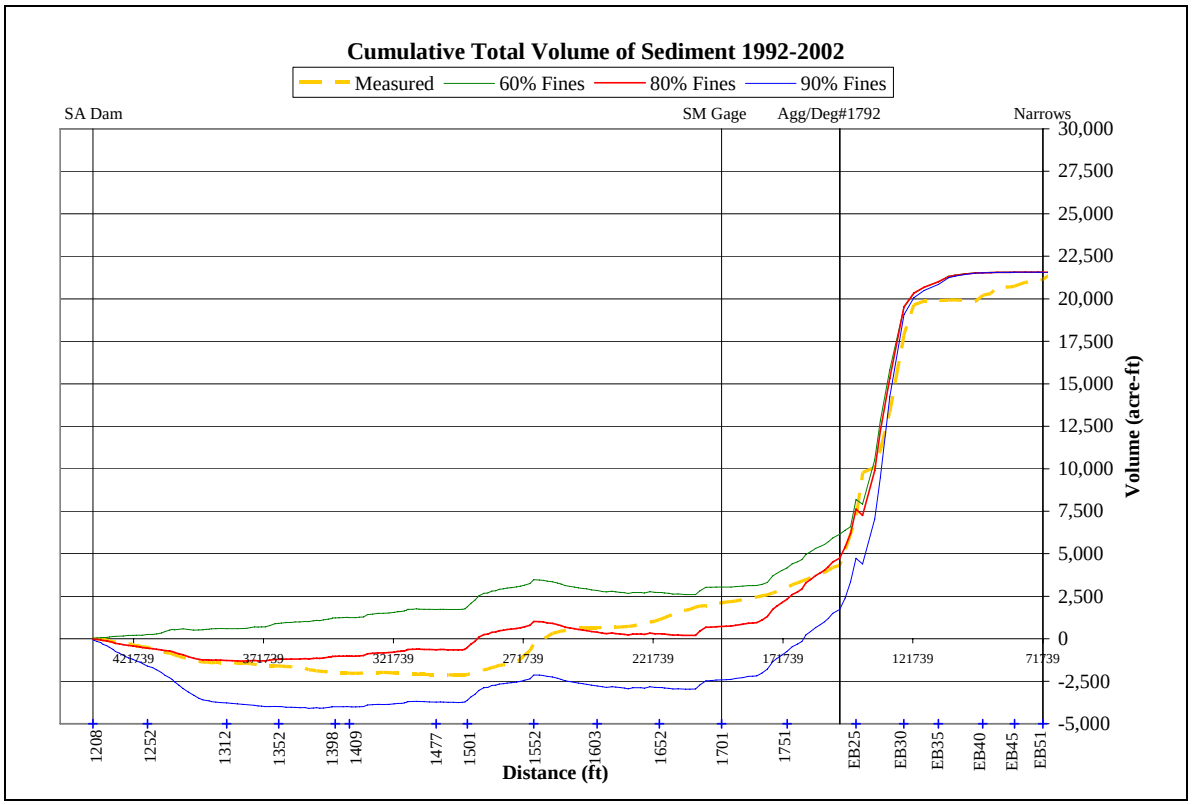

Figure 43: Affects of incoming sediment load on total sediment volume.

4.2.3 Silt/clay transport parameters

The parameters for silt and clay erosion were also varied within the limits of the data obtained from the laboratory tests. The model results were not sensitive to these parameters except for in the upstream reach of the model where fines that deposited during low flows were considered to be consolidated in the model and not allowed to be transported at the next larger flow. In order to account for this change, the critical shear stress values for erosion and deposition were adjusted accordingly from the beginning of the reach, 0.04 lb/ft^2 and 0.02 lb/ft^2 respectively, where the fines are freshly deposited to the downstream reach where the fines have become consolidated and therefore require higher shear stresses for erosion (0.125 lb/ft^2).

4.2.4 Time Step

The time step used for sediment modeling is based on many parameters. The most important parameters include; cross-section spacing, flow rate, flow data frequency (15 minute or daily average) and the active layer thickness. An improper time step will cause instabilities and lead to erroneous results. The method of testing the model to the sensitivity of the time step was to decrease the time step until the results did not change. This analysis indicated that a 0.5 hour time step was appropriate.

4.3 Final Results

The overall results of the final calibration runs reproduce the general shape and magnitude of the cumulative erosion and deposition in both the main channel and the total channel including the floodplains. Though the base runs show the deposition for the entire reach is similar to that of the historical record, the reach by reach volumes of deposition differ slightly from the historical volumes of deposition. Detailed results for each of the final calibration runs are discussed in the following sections.

4.3.1 1972-1992 Final Results

The numerical model reproduces the general shape and magnitude of the cumulative erosion and deposition in both the main channel and the total channel including the floodplains (Figure 44 - Figure 49). The difference between the main channel and total channel deposition is the floodplain deposition. While the final calibration run shows the deposition for the entire reach is similar to that of the historical record, the reach by reach volumes of deposition differ slightly from the historical volumes of deposition.

In the upper portion of the reach, from Agg/Deg#1208 to 1312, the field measurements show that the main channel experienced erosion and the floodplains experienced a small amount of deposition. In general, the numerical model predicts the total cross-section erosion accurately but slightly under-predicts erosion in the main channel.

From Agg/Deg#1312 to 1603, the field measurements show that the main channel experienced little erosion or deposition, but the floodplain experienced a large amount of deposition. The numerical model predicted slight aggregation in the main channel from Agg/Deg#1312 to 1552. From Agg/Deg# 1552 to 1603, the model predicted erosion in the main channel as a result of the deep, narrow channel present in 1972. In reality, the river from Agg/Deg#1552 to 1603 became wider and not as deep in 1992 due to channel clearing prior to 1985 and pilot channel construction through sediment plugs that formed in 1991 near Tiffany Junction. The sediment plugs that formed in 1991 resulted in large amounts of sediment deposition along this reach causing the channel to fill and required pilot channels to be constructed in order to reconnect the river and convey water downstream. The model does not account for artificial channel realignment or artificial channel change without stopping the model and manually making the modifications. The channel clearing and pilot channel construction were not incorporated into the model and therefore the effects of the clearing and sediment plugs on the channel geometry were not modeled.

In the reach from Agg/Deg#1603 to the reservoir (Agg/Deg#1792) both the main channel and the floodplains experienced large amounts of deposition because of the reservoir backwater and the increase in the concentration of sediment transported downstream as a result of the sediment plug and pilot channel construction in 1991. Since the sediment plug and channel clearing were not incorporated into the model, the numerical model under-predicts the main channel deposition downstream of Agg/Deg#1603. The under prediction of the main channel deposition results in less overbank interaction and therefore the floodplain deposition is also under predicted.

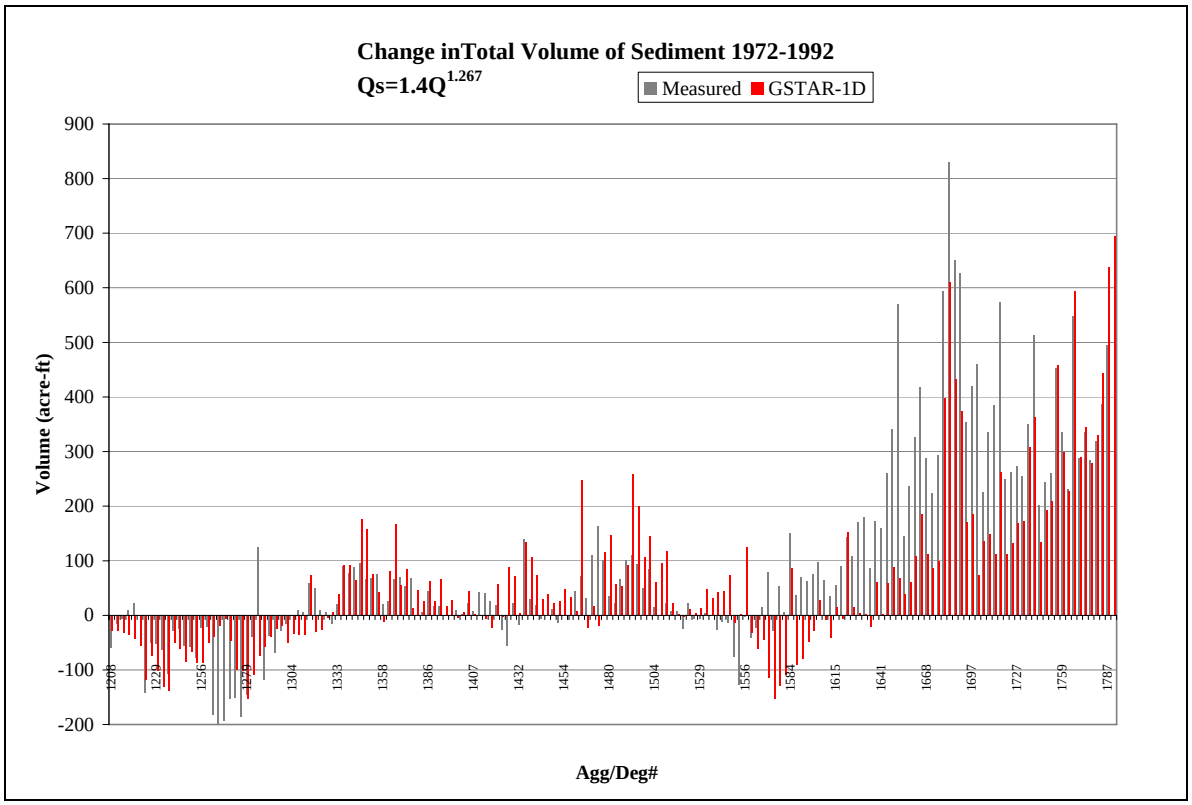

Figure 44: Change in total volume of sediment 1972-1992.

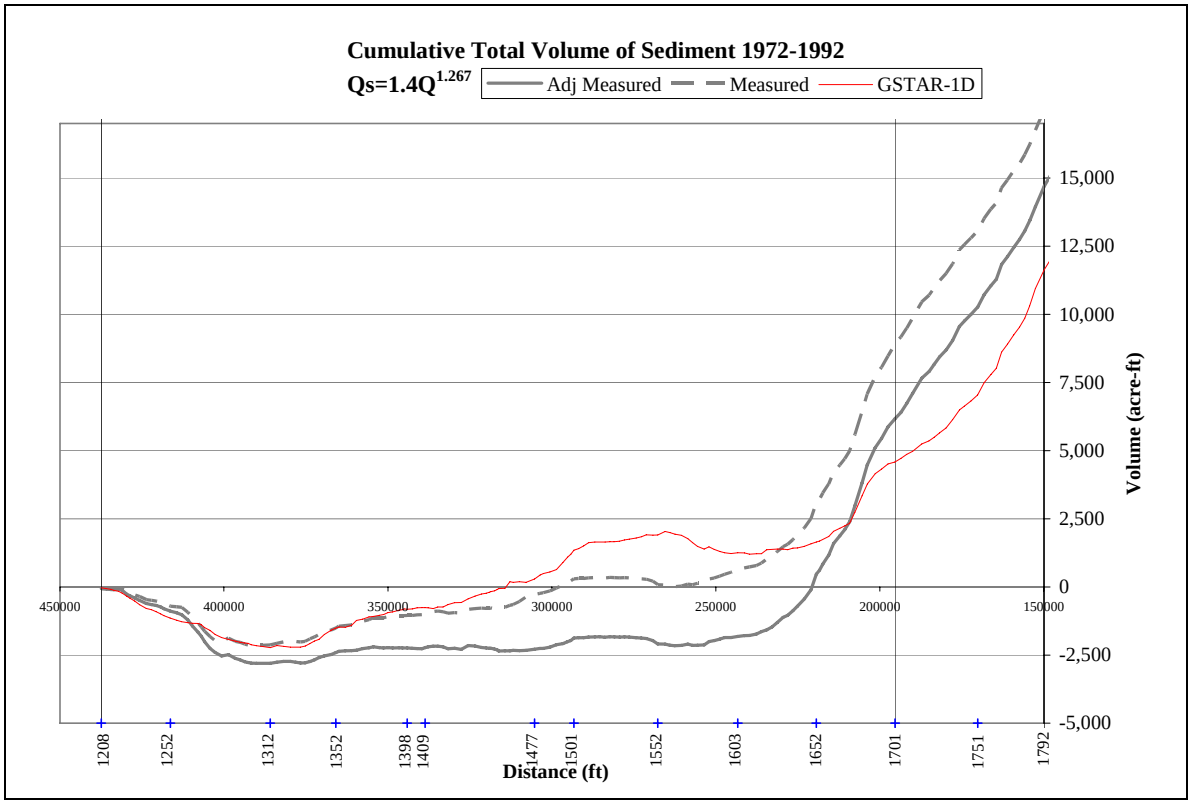

Figure 45: Cumulative total volume of sediment 1972-1992.

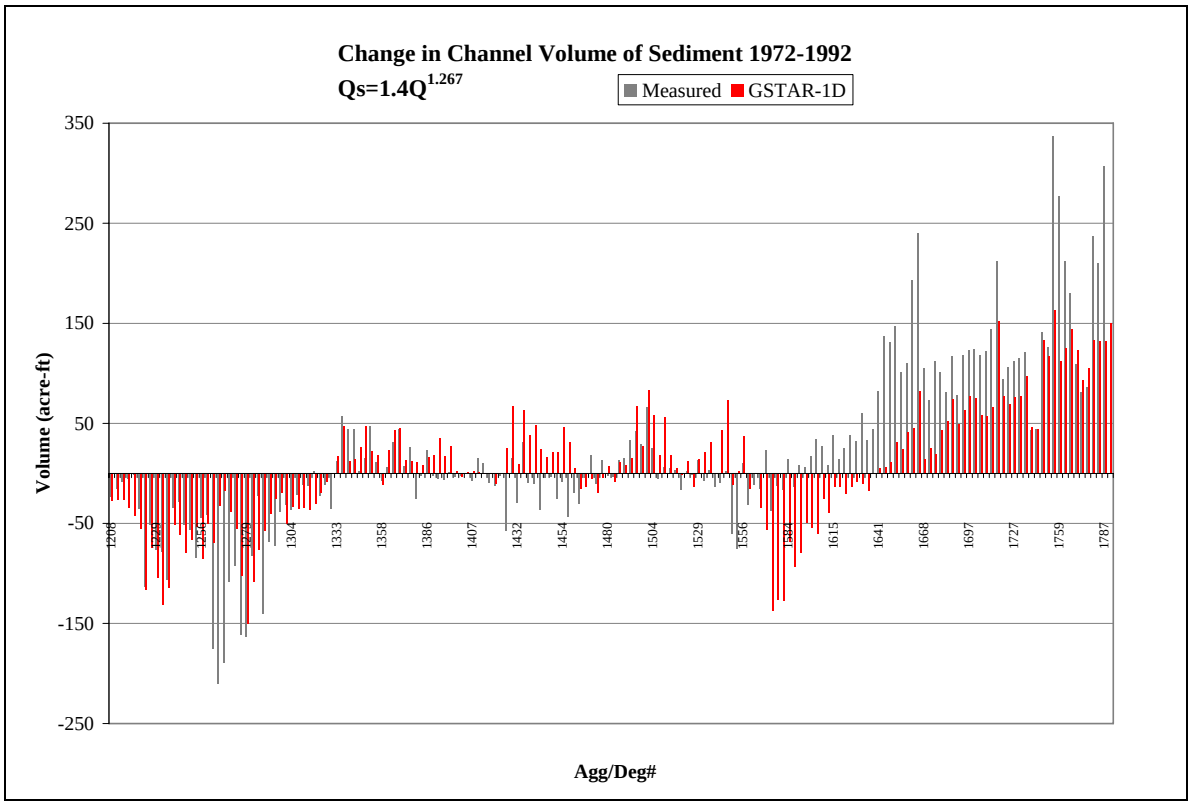

Figure 46: Change in main channel volume of sediment 1972-1992.

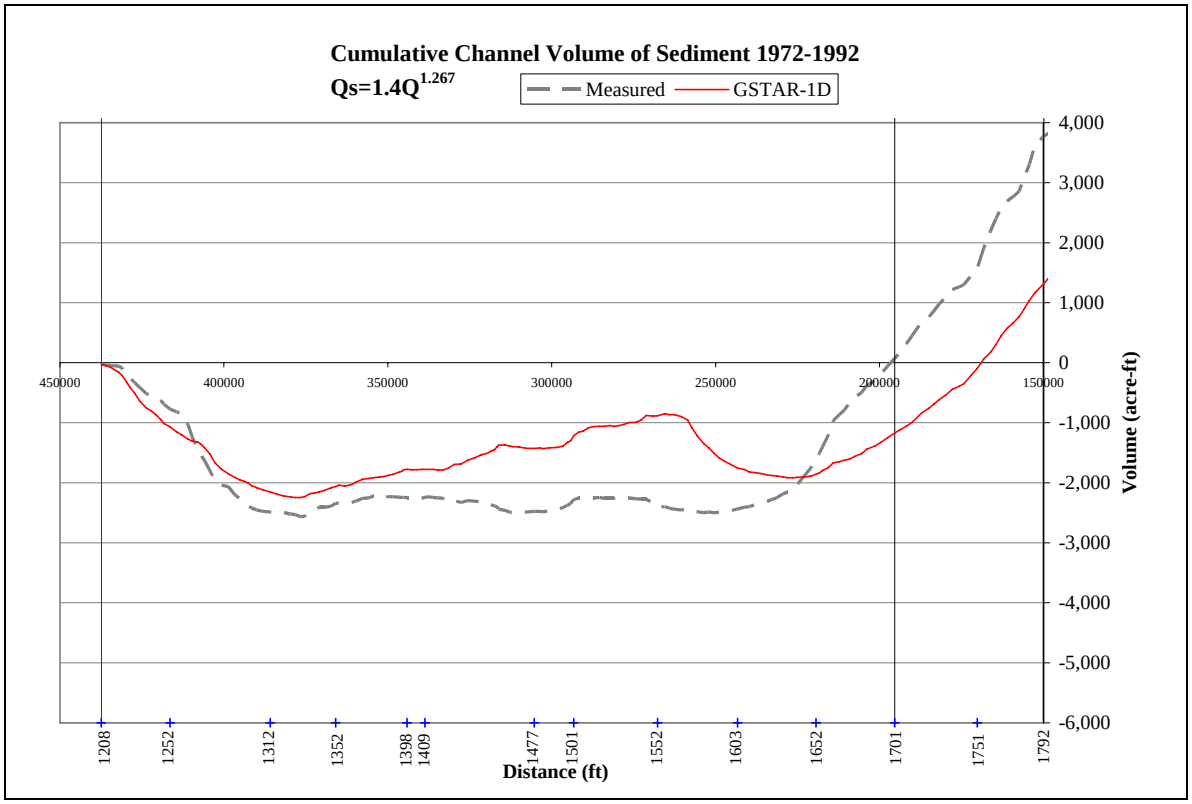

Figure 47: Cumulative main channel volume of sediment 1972-1992.

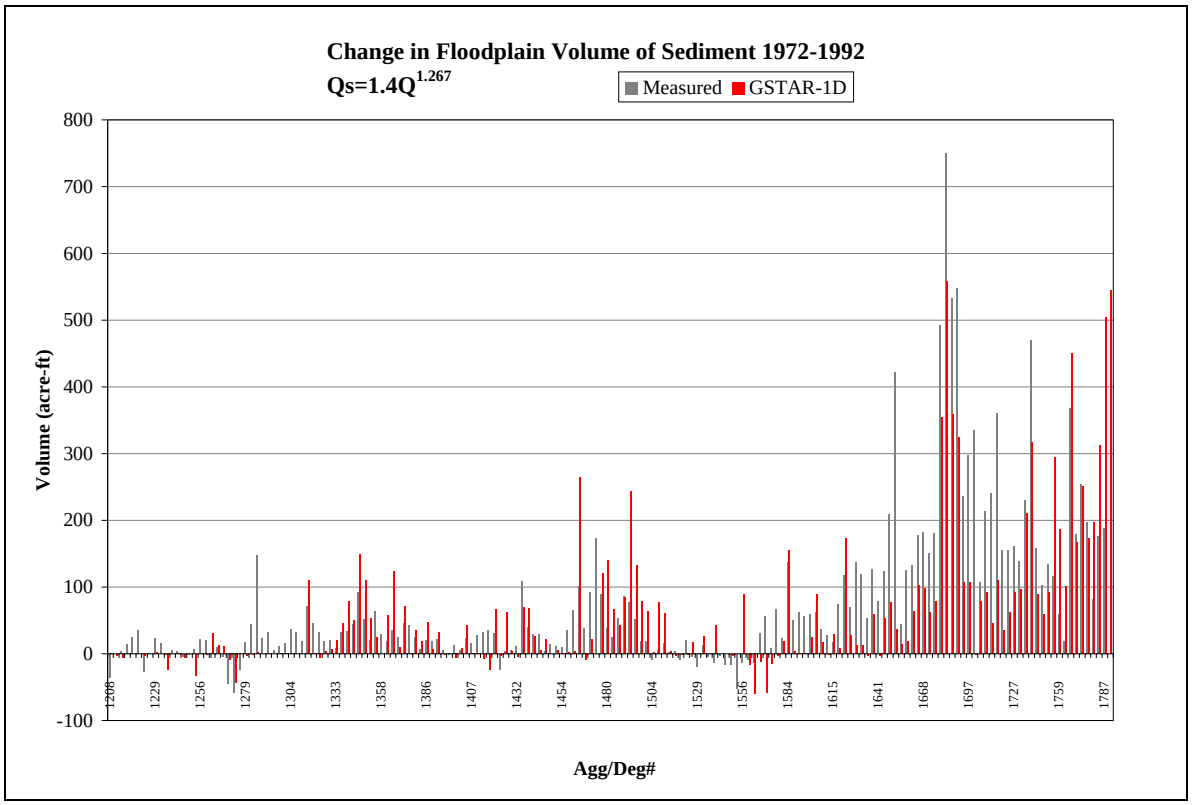

Figure 48: Change in floodplain volume of sediment 1972-1992.

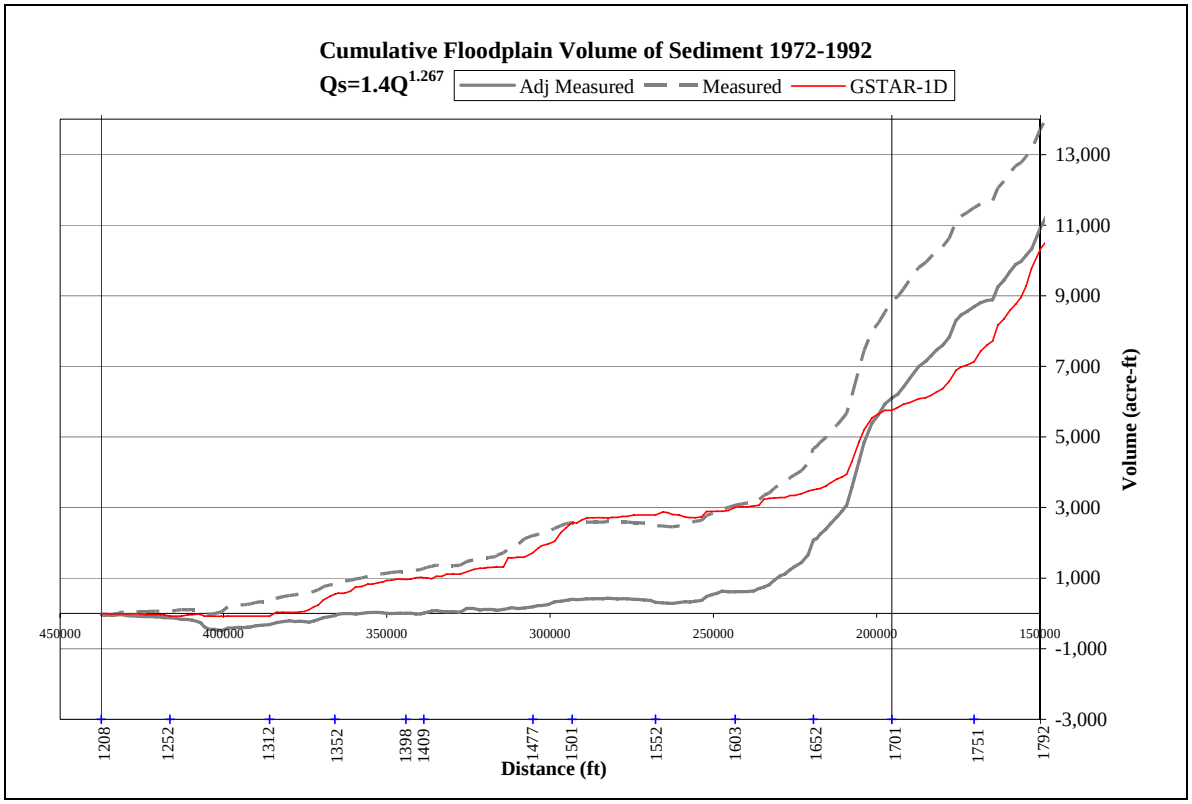

Figure 49: Cumulative floodplain volume of sediment 1972-1992.

Figure 50 shows the total change in mean bed from the start (1972) of the simulation to the end (1992). Overall, the numerical model reproduces the mean bed profile change (Figure 51). The increase in bed elevation in the lower reach is simulated accurately; however, the cross-sections between Agg/Deg#1552 and 1632 show degradation in the channel whereas the survey data shows a stable channel. The average difference in mean bed between 1992 measured and the 20 year simulation is only 0.26 ft. and has a standard deviation of 1.75 ft. (Figure 52). The degradation of the channel downstream from San Acacia Diversion Dam and the channel aggradation in the reach upstream from Elephant Butte Reservoir has resulted in an overall decrease in channel slope. The modeled change in slope from 1972 to 1992 matches the historical decrease in slope reasonably well (Figure 51).

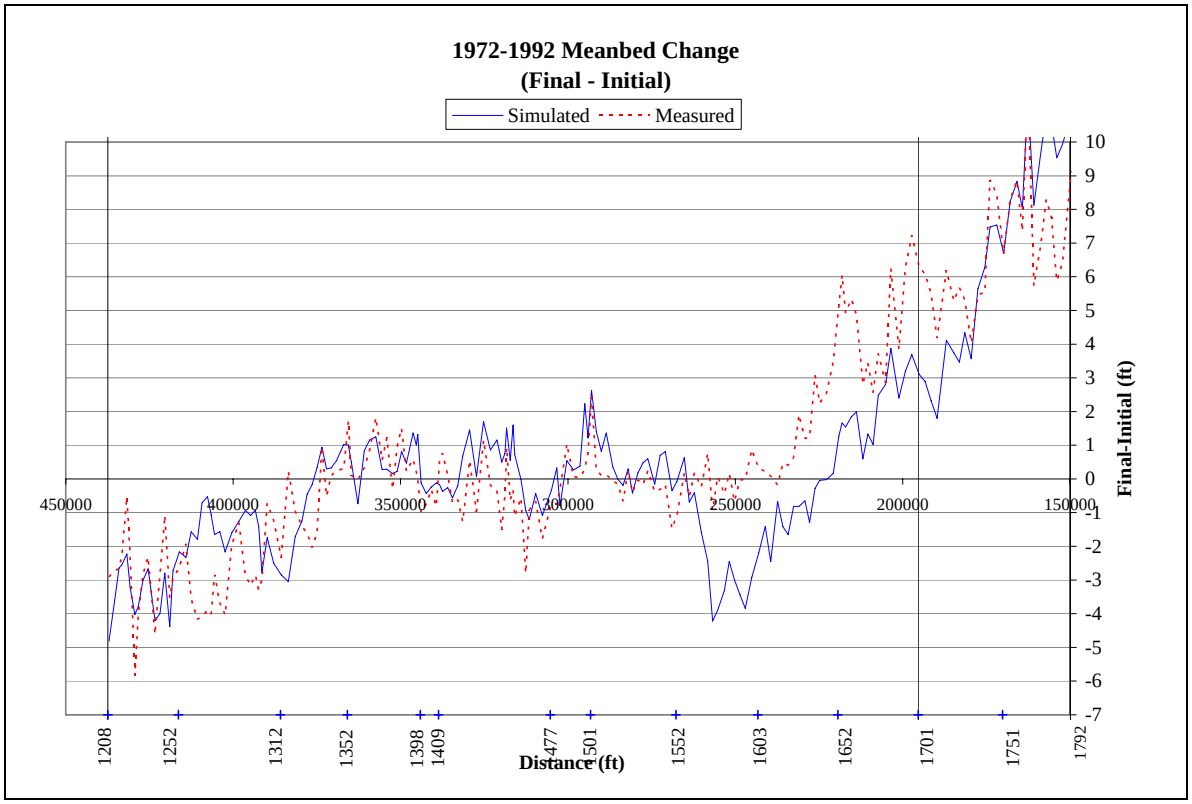

Figure 50: 1972-1992 change in mean bed.

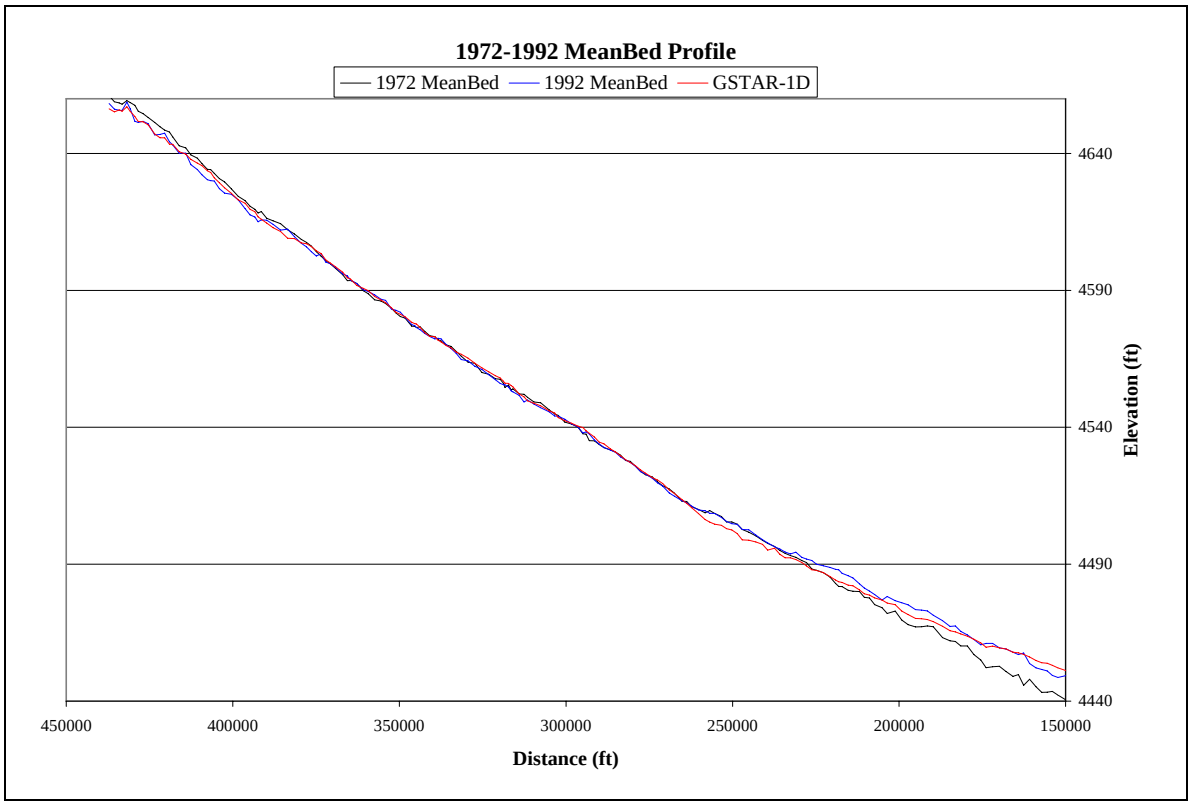

Figure 51: 1972-1992 mean bed elevation profile.

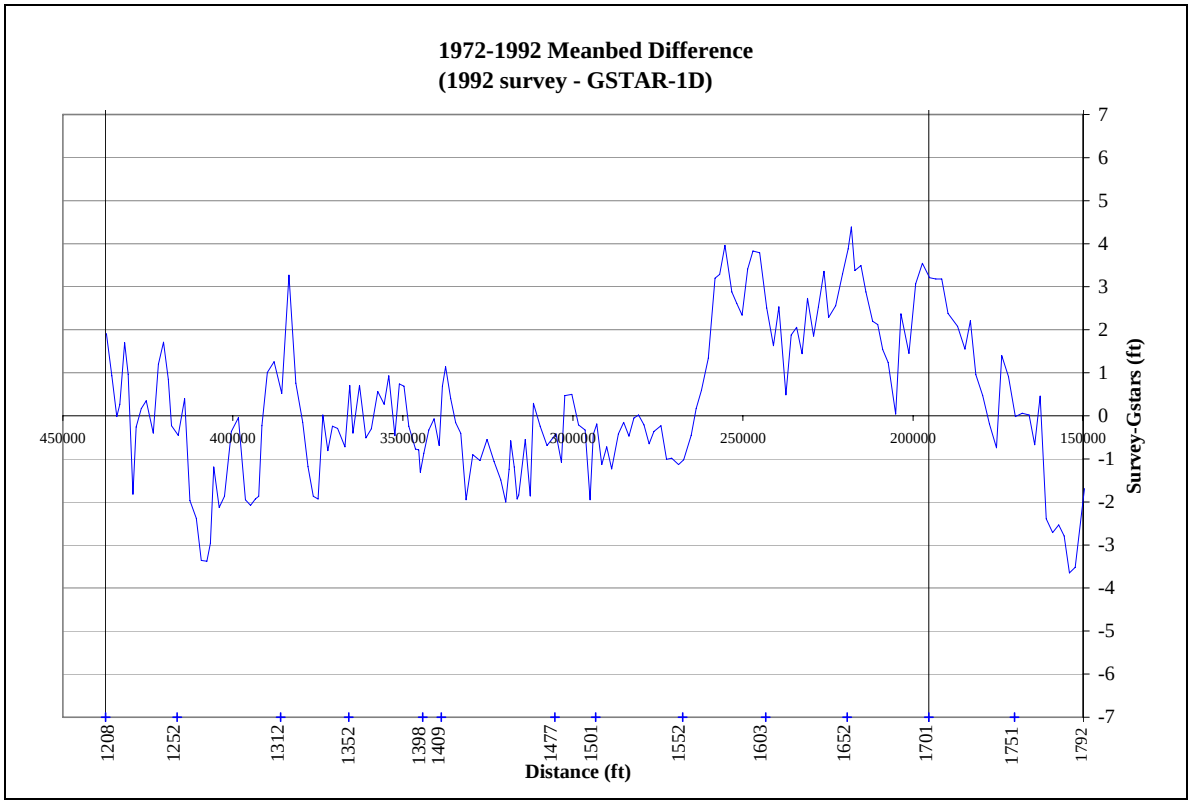

Figure 52: 1972-1992 mean bed elevation difference.

The median diameter of bed sediment, d_{50}, for three sub-reaches is shown in Figure 53 below. In most cases, the bed material becomes coarser with high flows and finer during low flows. Overall, there is a trend for coarsening, but the model results do not show coarsening as much as the measured data. There are two likely reasons for not capturing the coarsening of the bed: 1) the initial bed material and incoming load in 1972 does not contain enough coarse sediment, and/or 2) the bed mixing processes may not be represented correctly in the model. The bed mixing processes may not be represented in the model correctly because the cycles of erosion during high flows may leave armoring layers of coarse sediment. As the low flows follow the model will mix the fines with the coarser material. However, in reality the fines may pass over the top of the coarser material and not mix.

During the low to moderate flows, sand is deposited in the channel whereas at the higher flows the incoming sediment is transported downstream and additional sediment is eroded from the channel bed causing degradation. An example of this process can be seen in Figure 54 for Agg/Deg#1276.

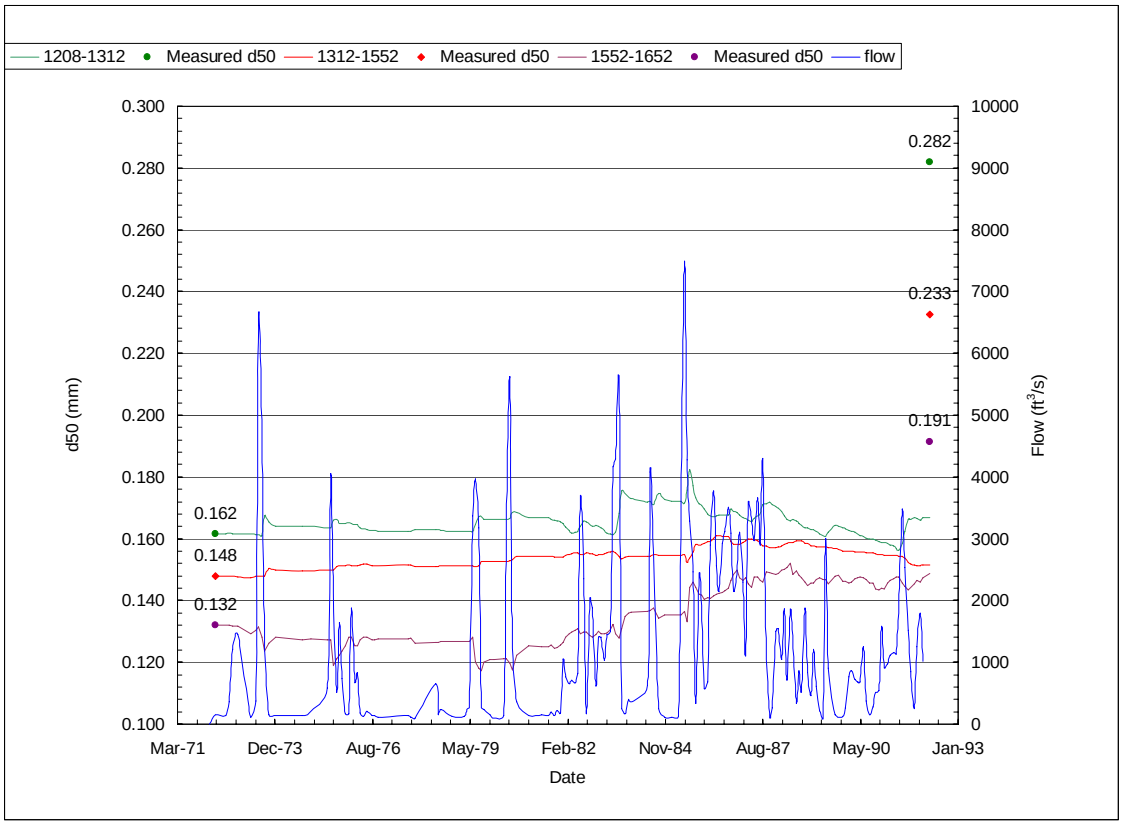

Figure 53: Change in bed material size (d_{50}) during model simulation.

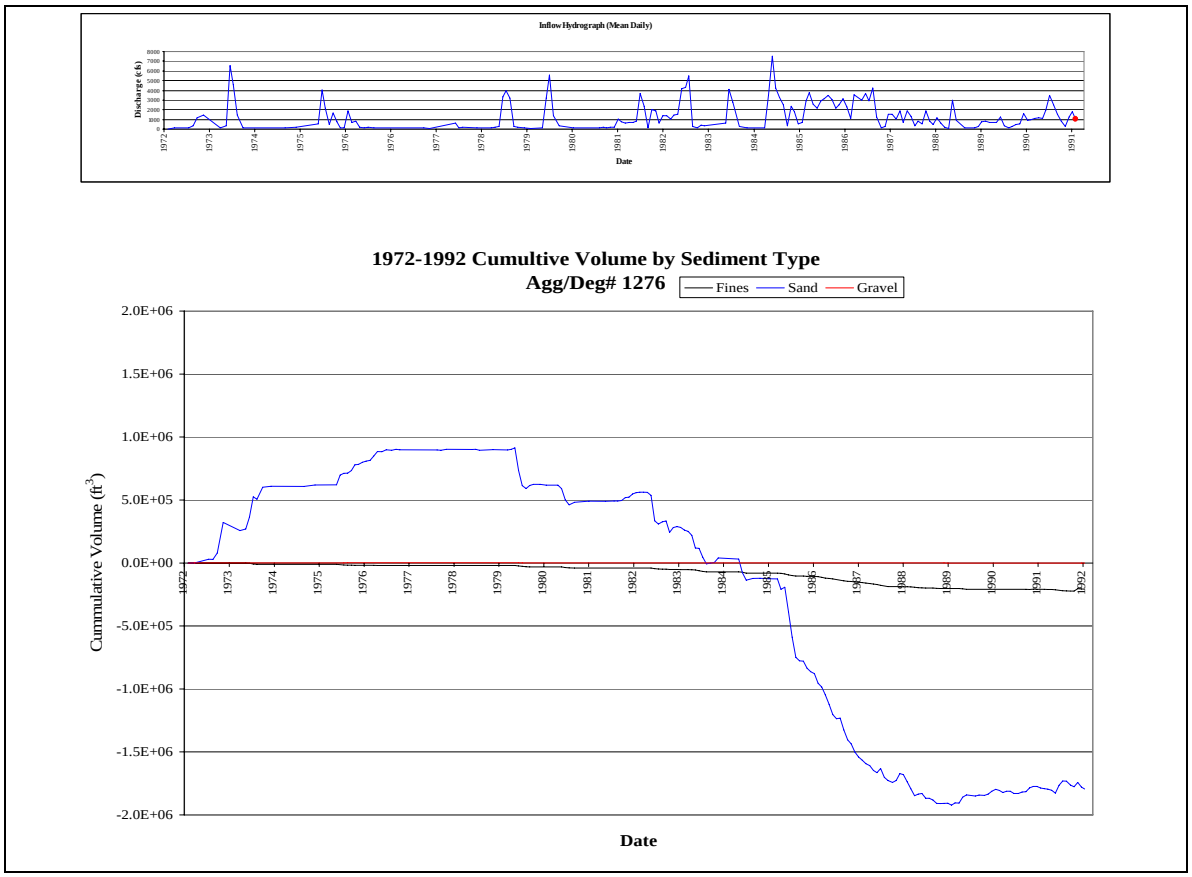

Figure 54: Plot of cumulative volume change by sediment type (Agg/Deg#1276).

Four typical river cross-section changes are shown in Figure 55 – Figure 58. The right sides of the cross-sections are behind the levee, include the low flow conveyance canal and therefore are not modeled. Figure 55 shows the cross-section at Agg/Deg#1214, just downstream from San Acacia Diversion Dam, where field data show that the main channel experienced erosion and the main channel shifted to the left. The model results also show erosion in the main channel, however, channel migration is a phenomenon that cannot be predicted with the current model. Figure 56 shows the cross-section at Agg/Deg#1276, where field data show that both main channel and floodplains experienced erosion and the main channel widened. The numerical model reproduces the total main channel erosion fairly well but the addition of the smaller channels in the 1992 data set cannot be predicted with the current model since the erosion/deposition along the cross section is distributed evenly over the entire wetted perimeter. Figure 57 shows the cross-section at Agg/Deg#1494, where field data show that the main channel shifted to the left and the floodplains experienced deposition. The numerical model reproduces the floodplain deposition fairly well. Additionally, while the shift in the channel and the resulting change in slope cannot be predicted with the current model, the over all shape of the predicted channel (thalweg and mean bed elevation) is similar to the channel in 1992. Figure 58 shows the cross-section at Agg/Deg#1792 and shows the deposition in the entire cross-section induced by the downstream reservoir.

The difference between the 1972 and 1992 water surface widths at 5,000 ft^3/s varied along the study reach. From Agg/Deg#1208 to Agg/Deg# 1312 the water surface width for the channel tends to decrease with a more incised and narrow channel with less

floodplain interaction. From Agg/Deg#1316 to Agg/Deg#1584 the water surface width remains fairly constant and from Agg/Deg#1587 to Agg/Deg#1972 the water surface width tends to increase due to the deposition in the main channel resulting in more floodplain interaction in the lower portion of the study reach. Overall, the results show that the numerical model reproduces the general channel characteristics such as channel width, water surface width, thalweg elevation, and mean bed elevations fairly well.

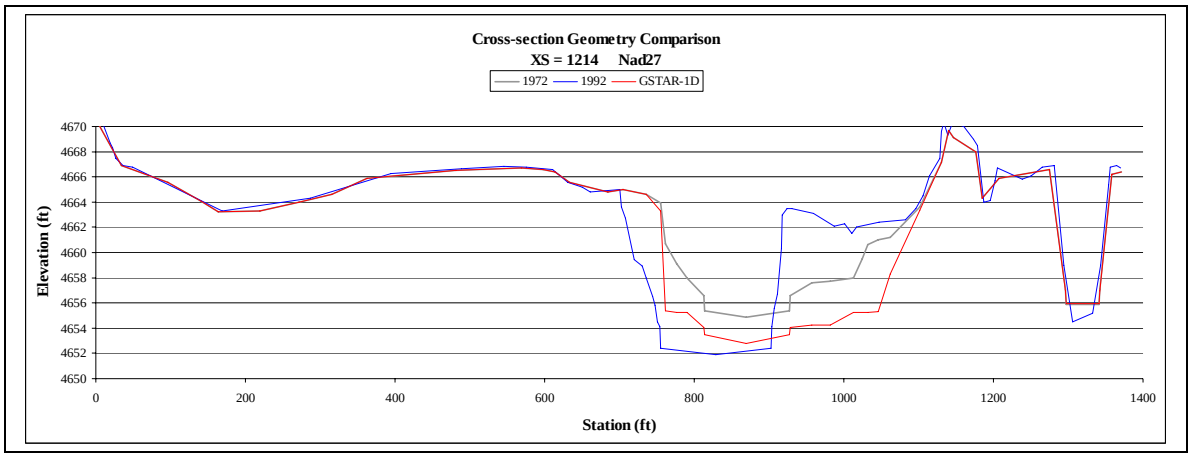

Figure 55: 1972-1992 cross-section change at Agg/Deg#1214.

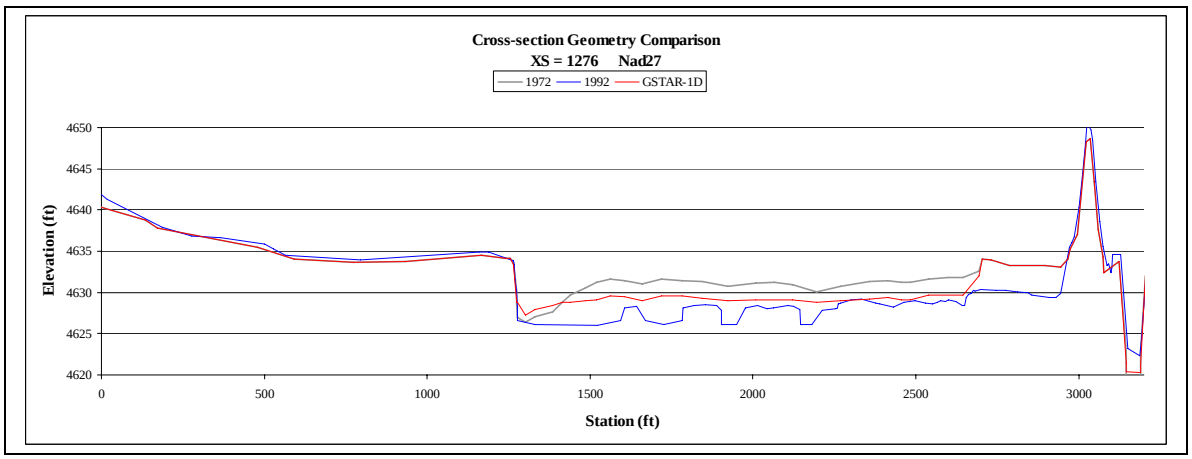

Figure 56: 1972-1992 cross-section change at Agg/Deg#1276.

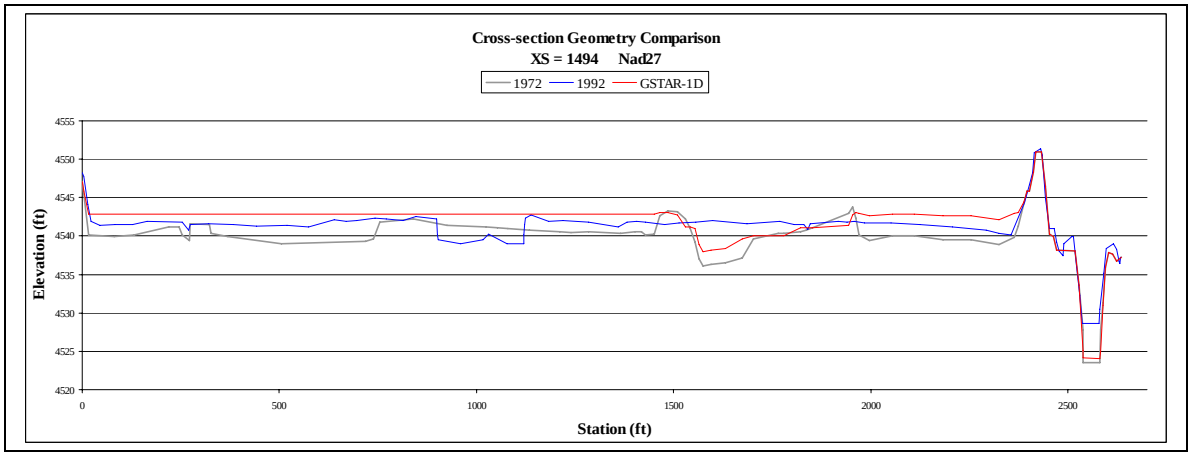

Figure 57: 1972-1992 cross-section change at Agg/Deg#1494.

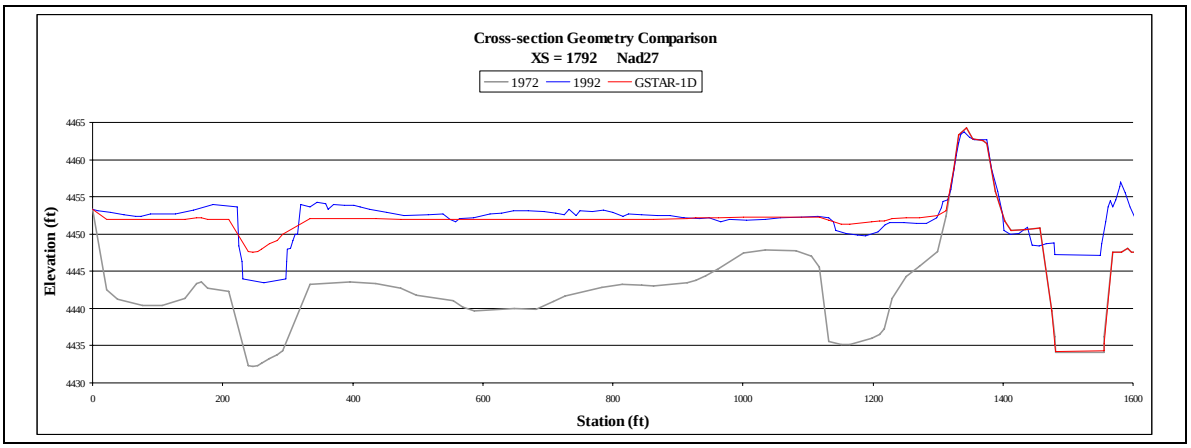

Figure 58: 1972-1992 cross-section change at Agg/Deg#1792.

The results presented above show that the model reasonably matched (16,741 acre-feet historical vs. 12,036 acre-feet simulated) the total historical deposition within the reach and predicted the overall geometry changes along the reach fairly well. As discussed above, the possible errors associated with estimating the observed floodplain elevations along portions of the reach in the 1992 survey could result in an overestimation of the floodplain deposition. This potential overestimation in the 1972-1992 model accounts for ~2,000 acre-ft of floodplain deposition in the measured data.

4.3.2 1992–2002 Final Results

The numerical model reproduces the general shape and magnitude of the cumulative erosion and deposition in both the main channel and the total channel including the floodplains (Figure 59 -Figure 64). The difference between the main channel and total channel depositions is the floodplain deposition. Though the base runs show deposition for the modeling reach as does the historical record, the reach by reach volumes of deposition are somewhat different from the historical volumes of deposition.

From Agg/Deg#1208 to Agg/Deg#1409, the field measurements show that the main channel experienced erosion. In general, the numerical model predicts the main channel erosion accurately up to Agg/Deg#1352 but under-predicts the erosion from Agg/Deg#1352 to 1409. From Agg/Deg#1409 to Agg/Deg#1552, the field measurements show that the main channel experienced little erosion or deposition whereas the numerical model tends to over-predict the deposition in this reach. In the remaining channel, both the main channel and the floodplains experienced deposition because of the downstream reservoir. The numerical model under-predicts the main channel deposition but predicts the total deposition well.

As discussed above, the possible errors associated with estimating the floodplain elevations along portions of the reach in the 1992 survey could result in an overestimation of the floodplain erosion. Therefore, the adjusted measured aggradation/degradation volumes are used for comparing the model results; both the original and adjusted aggradation/degradation volumes are shown. This potential overestimation in the 1992-2002 model accounts for ~2,000 acre-ft of floodplain erosion in the measured data. Overall, the model reasonably matched (4,274 acre-feet historical adjusted vs. 4,745 acre-feet simulated) the adjusted total historical deposition within the reach.

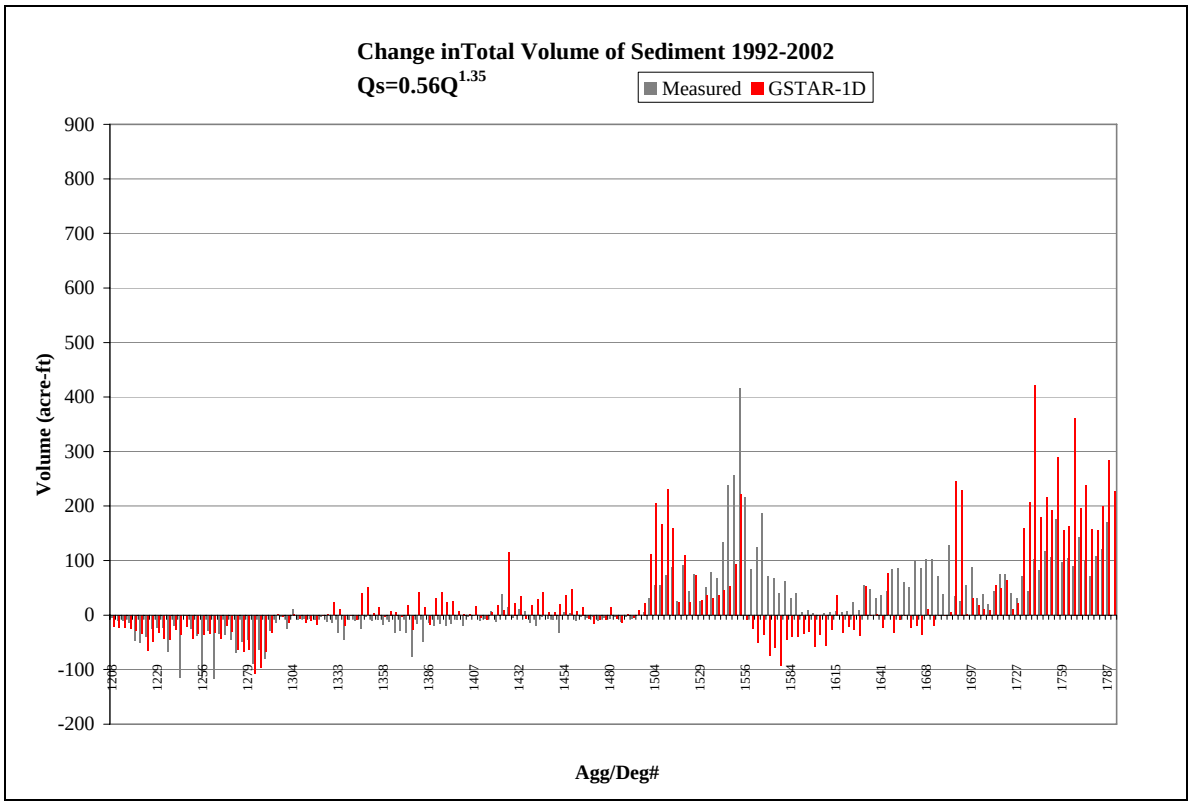

Figure 59: Change in total volume of sediment 1992-2002.

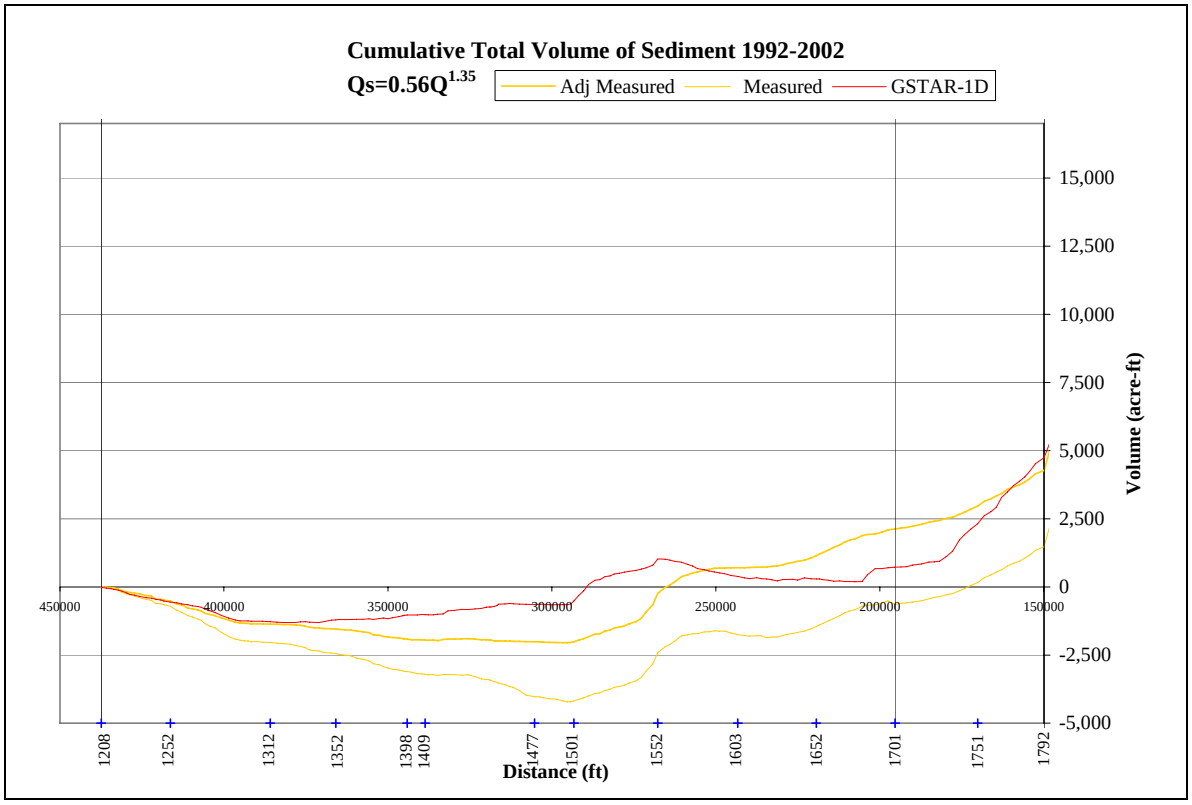

Figure 60: Cumulative total volume of sediment 1992-2002.

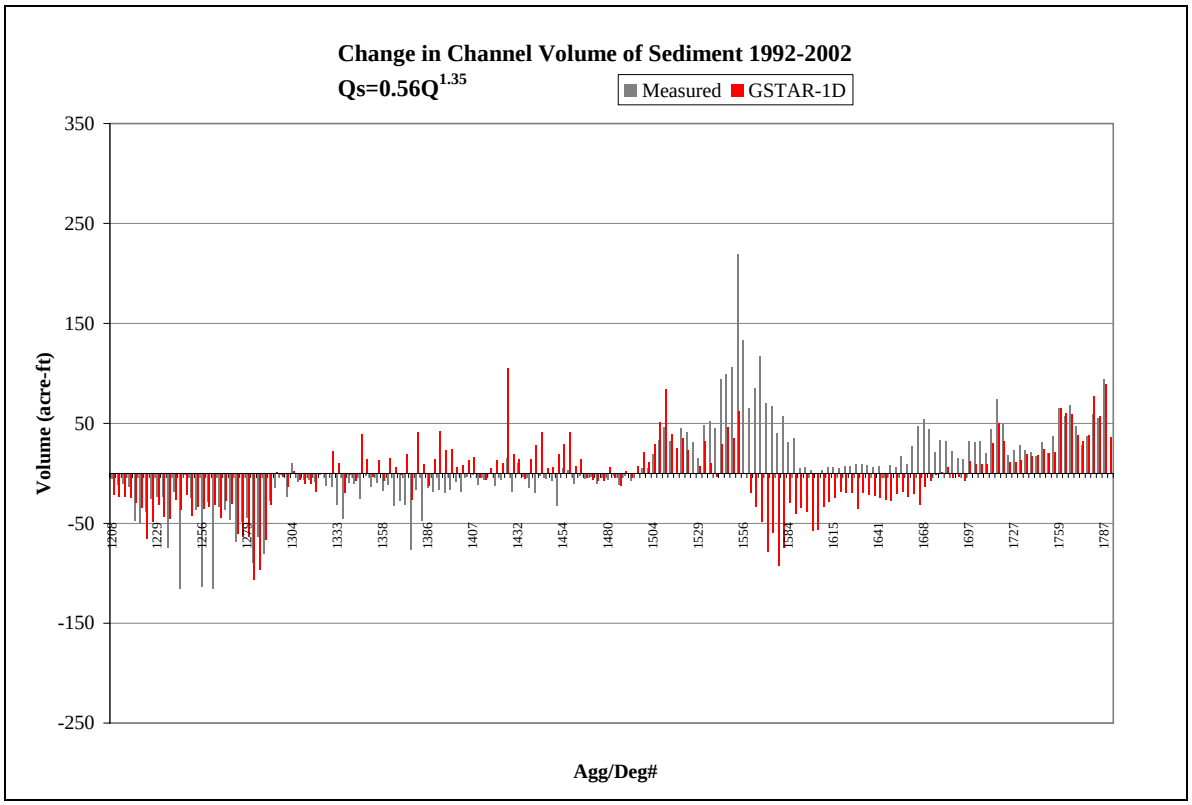

Figure 61: Change in main channel volume of sediment 1992-2002

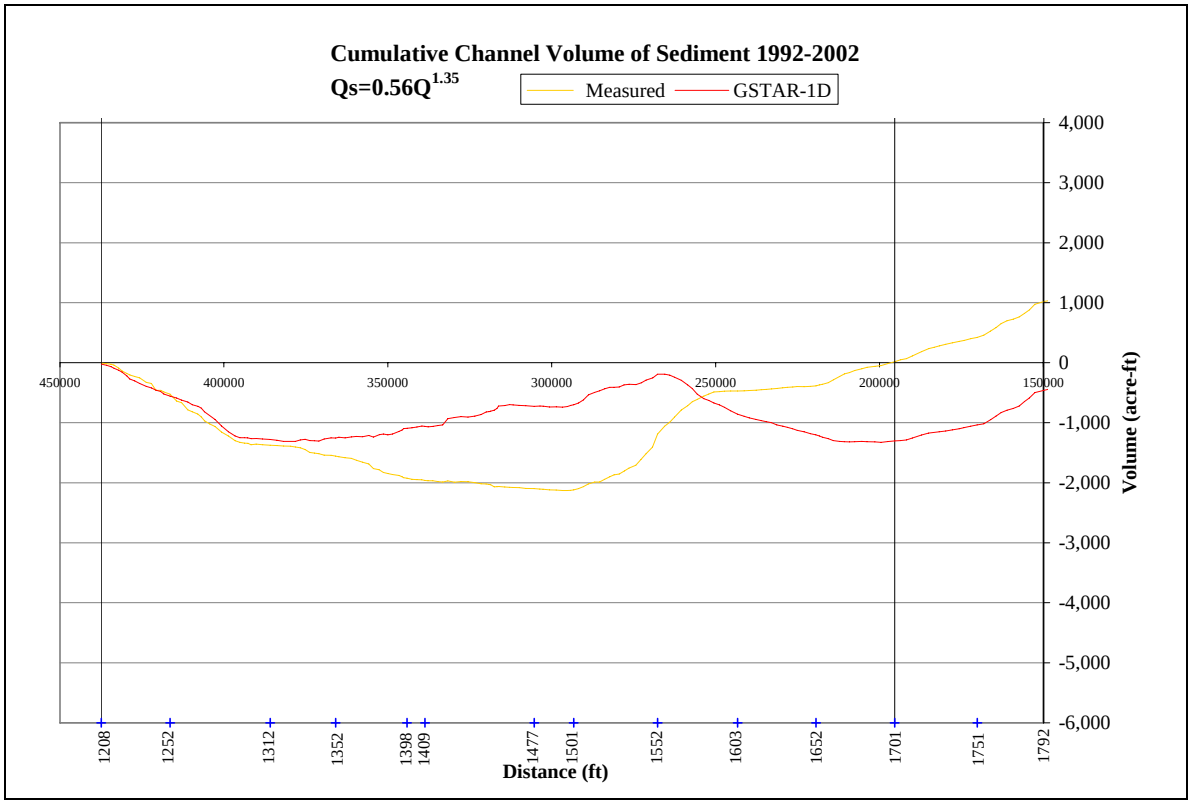

Figure 62: Cumulative main channel volume of sediment 1992-2002

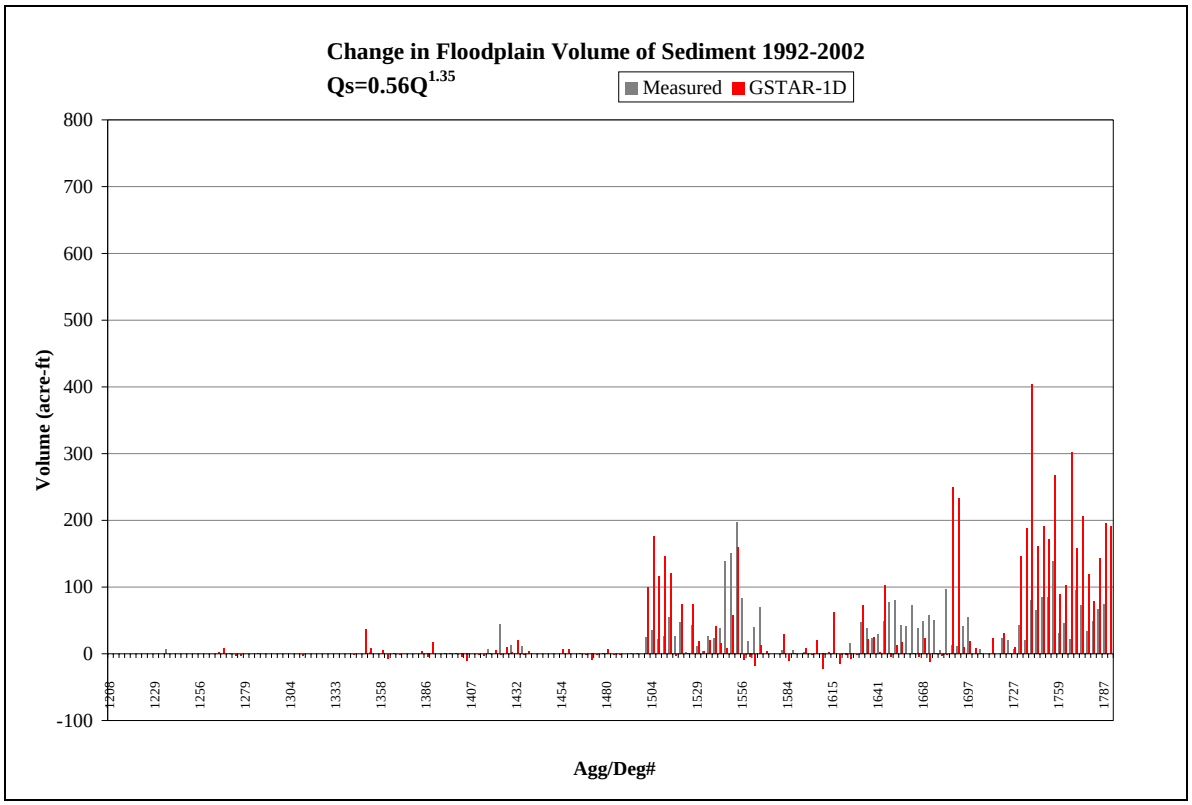

Figure 63: Change in floodplain volume of sediment 1992-2002

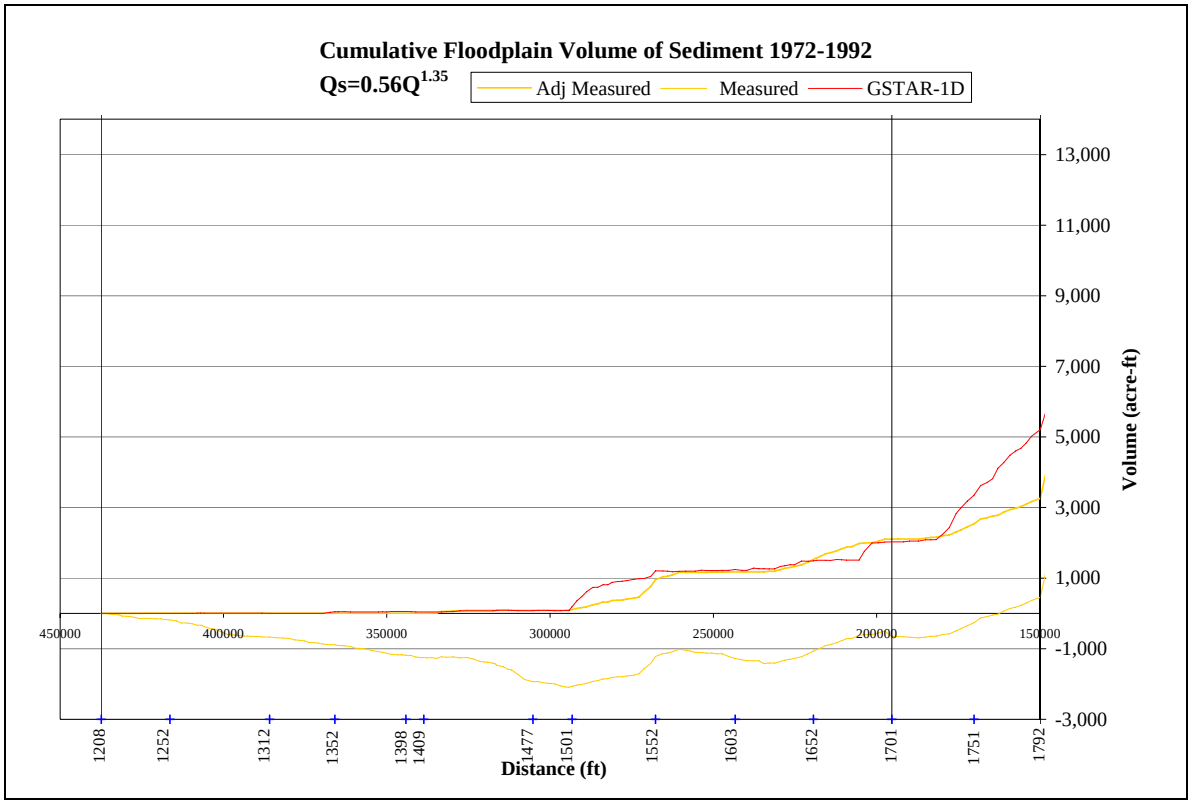

Figure 64: Cumulative floodplain volume of sediment 1992-2002

Figure 65 shows the total change in mean bed from the start (1992) of the simulation to the end (2002). Overall, the numerical model reproduces the mean bed profile change (Figure 66). However, the bed elevation increase in the lower reach is under estimated, especially in the area of Agg/Deg#1552 to Agg/Deg#1701. The average bed elevation is similar to the survey and for the 10 year simulation; the average difference in mean bed is only 0.94 ft. and has a standard deviation of 2.05 ft. (Figure 67).

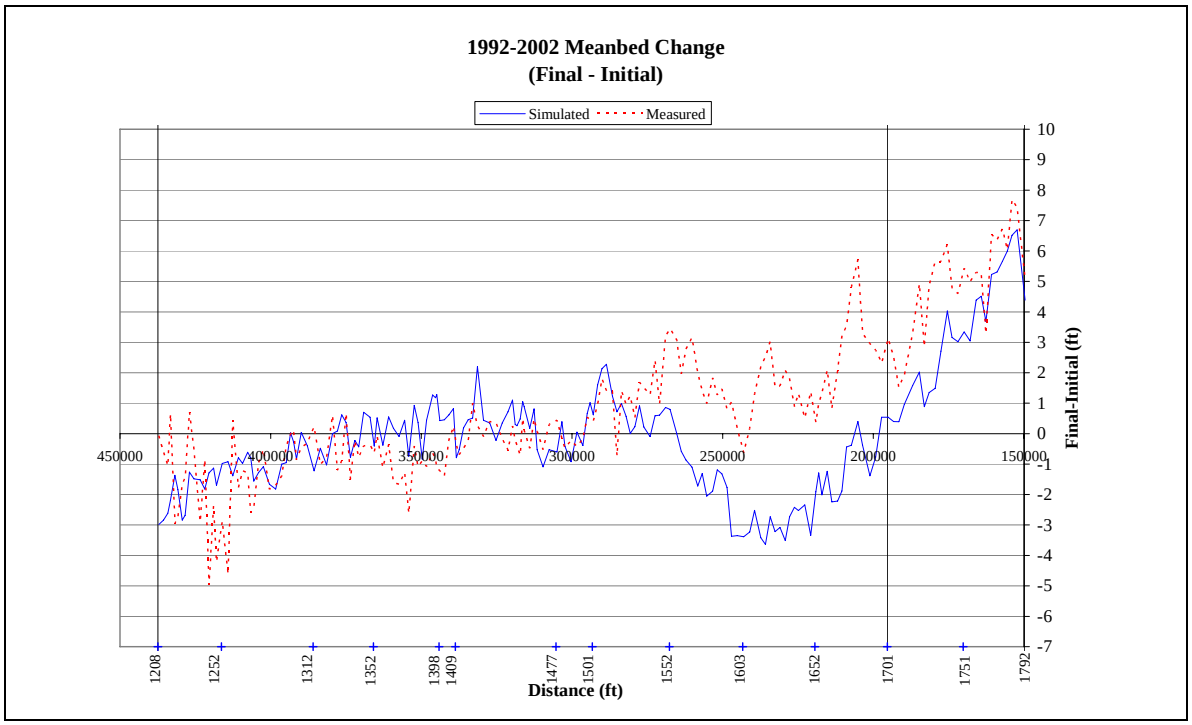

Figure 65: 1992-2002 change in mean bed.

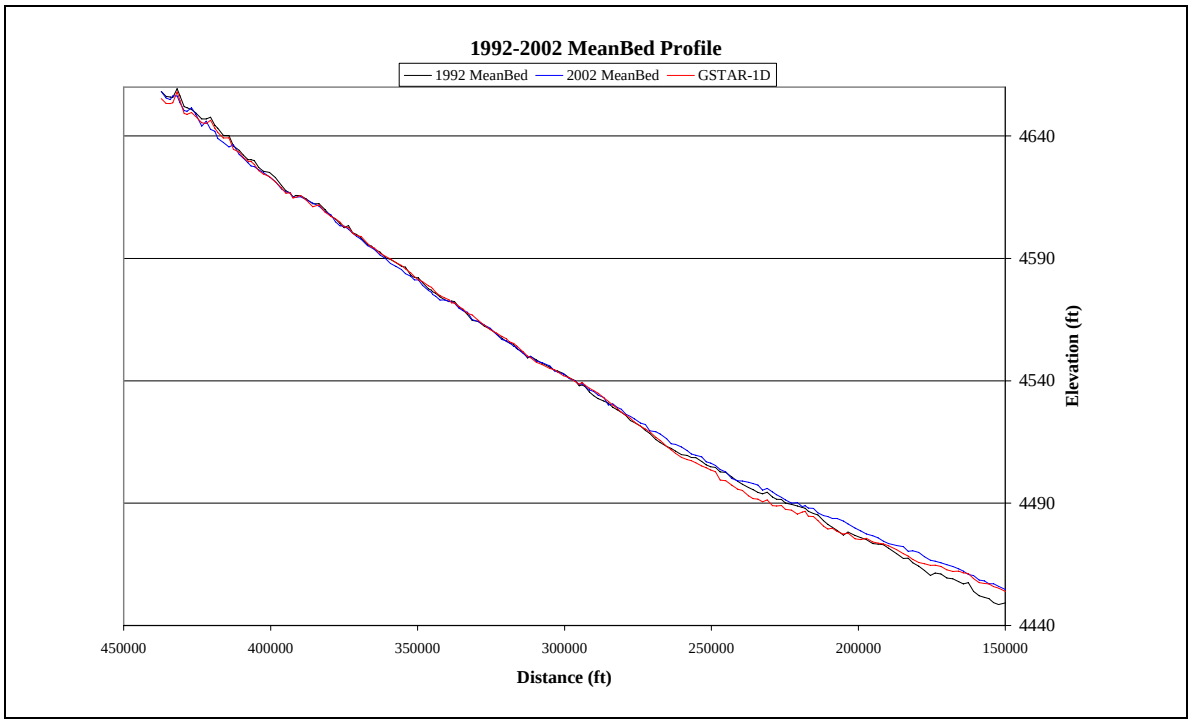

Figure 66: 1992-2002 mean bed elevation profile.

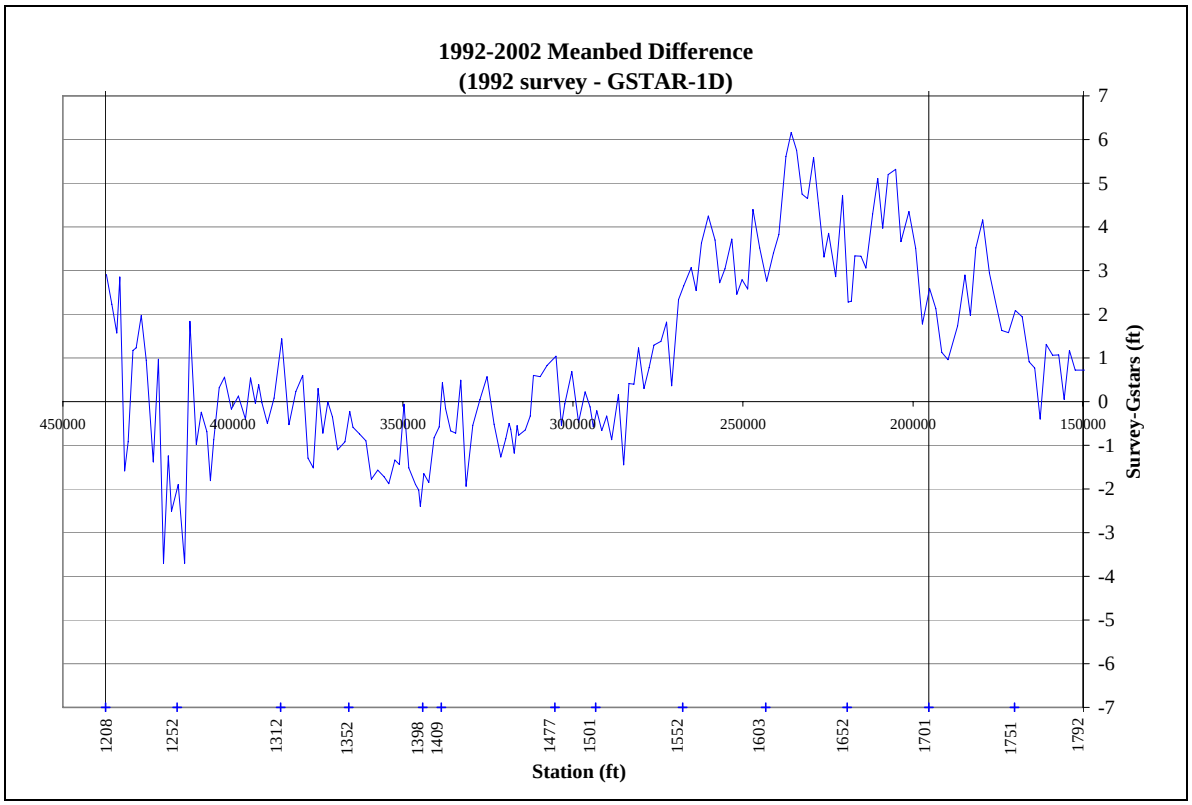

Figure 67: 1992-2002 mean bed elevation difference.

The median diameter of bed sediment, d_{50}, for three sub-reaches is shown in Figure 68 below. Similar to the 1972-1992 model results, the bed material becomes coarser in response to high flows and finer during low flows. This is much more predominate in the upper reach then the lower portion of the reach Overall, there is a trend for coarsening, but the model results do not show coarsening as much as the measured data for the same reasons stated above. During the low flows, sand is deposited in the channel whereas at the higher flows the incoming sediment is transported downstream and additional sediment is eroded for the channel bed causing degradation (Figure 69).

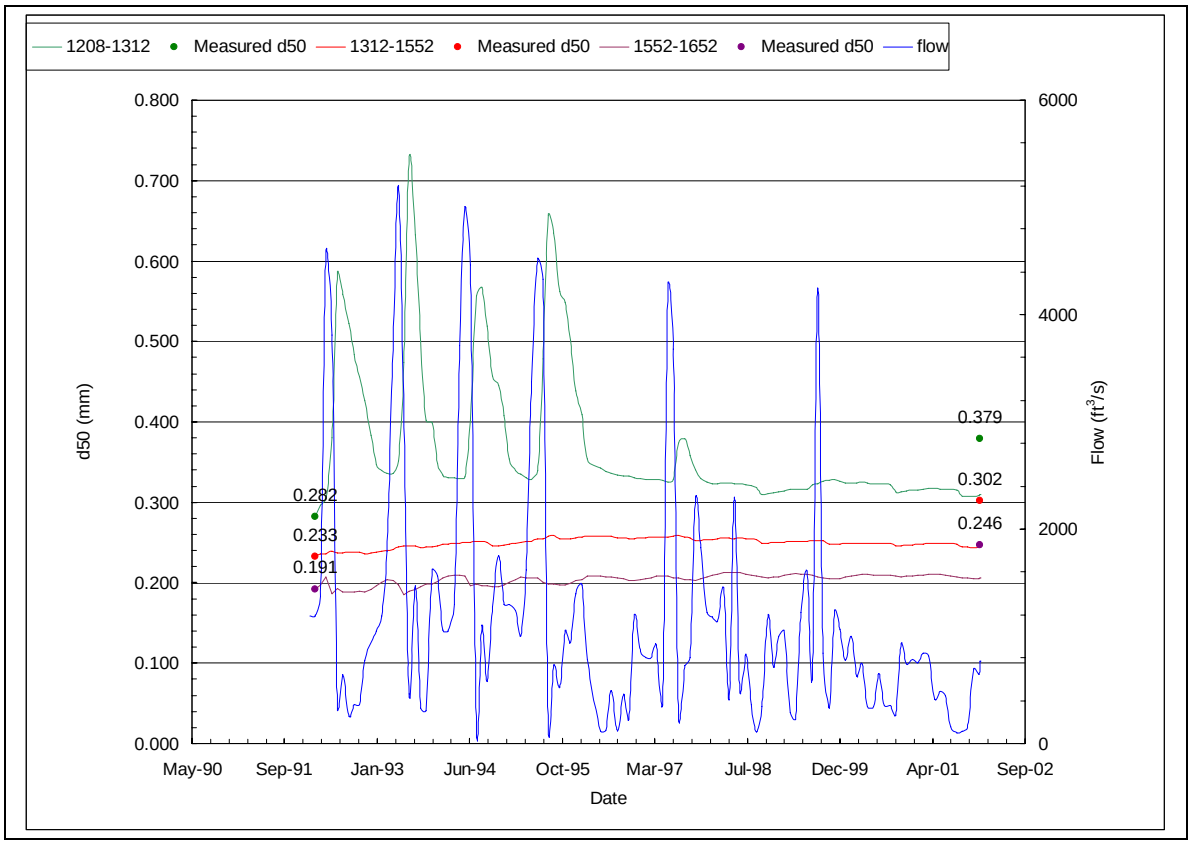

Figure 68: Change in bed material size (d_{50}) during model simulation.

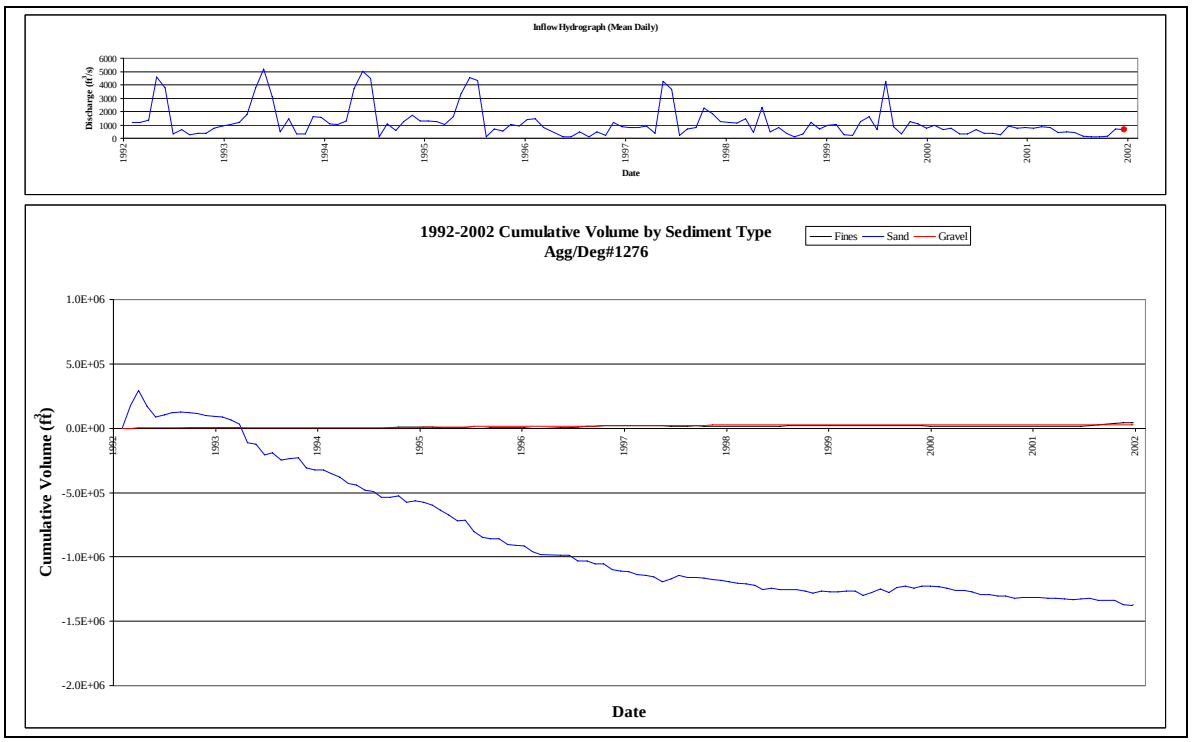

Figure 69: Plot of cumulative volume change by sediment type (Agg/Deg#1276).

Similar to the 1972-1992 model results, four typical river cross-section changes are shown in Figure 70 – Figure 73. The right sides of the cross-sections are behind the levee, include the low flow conveyance channel and therefore are not modeled. Figure 70 shows the cross-section at Agg/Deg#1214, just downstream from the San Acacia Diversion Dam, where field data show that the main channel experienced erosion. The model results match the degradation fairly well. Figure 71 shows the cross-section at Agg/Deg#1276, where field data show that both main channel and floodplains experienced erosion. The numerical model reproduces the main channel changes with good accuracy while under predicting the floodplain erosion. Figure 72 shows the cross-section at Agg/Deg#1501, where field data show that the main channel remained stable and the floodplains experienced deposition. The numerical model reproduces the phenomena fairly well, slightly overestimating the amount of deposition in the floodplain. Figure 73 shows the cross-section at Agg/Deg#1792. The numerical model reproduces the deposition in the main channel induced by the downstream reservoir but over predicts the floodplain deposition as a result of the slightly perched channel providing additional interaction between the main channel and the floodplains.

The differences in water surface width along the study reach from 1992 to 2002 are similar in trends to the 1972 to 1992 period but are smaller. Overall, the results show that the numerical model reproduces the general channel characteristics such as channel width, water surface width, thalweg elevation, and mean bed elevations fairly well.

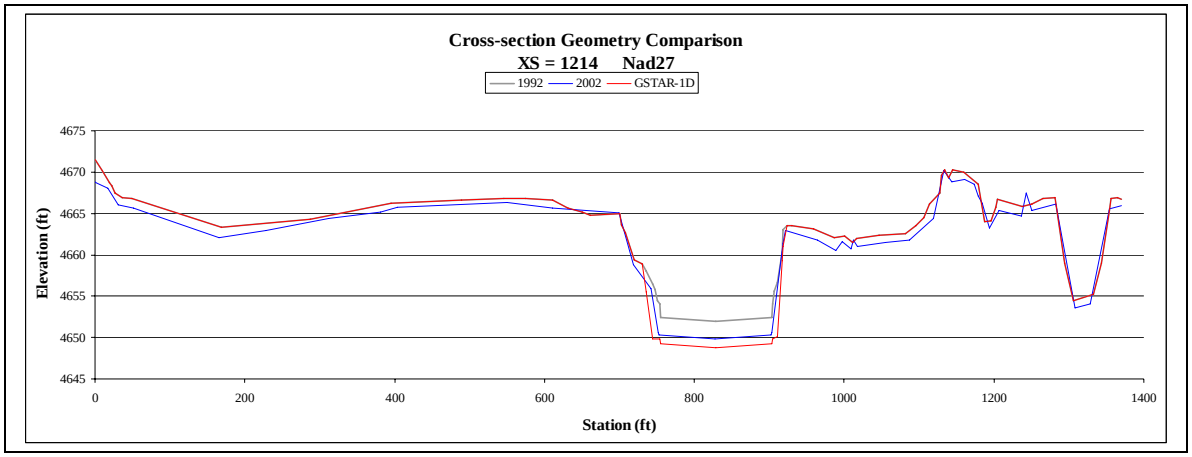

Figure 70: 1992-2002 cross-section change at Agg/Deg#1214.

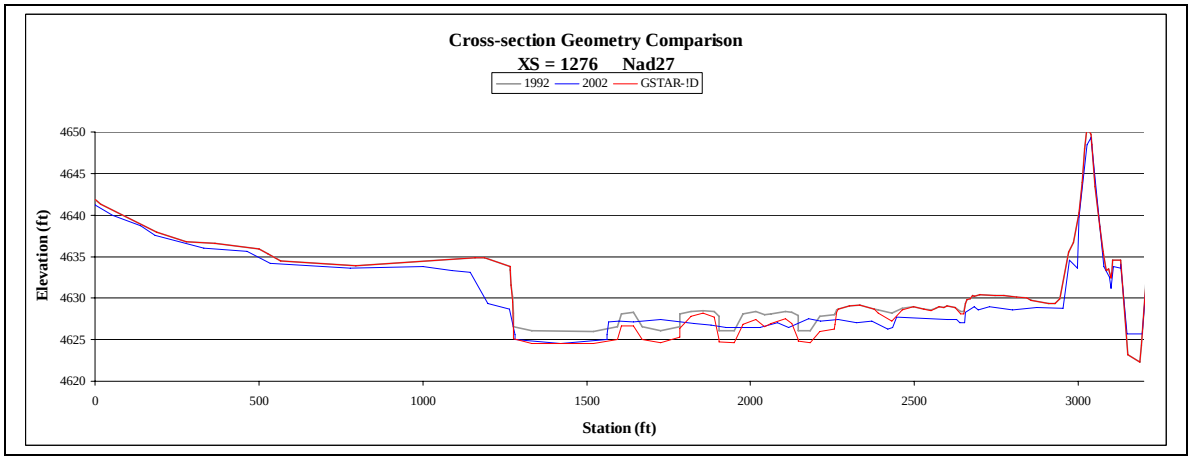

Figure 71: 1992-2002 cross-section change at Agg/Deg#1276.

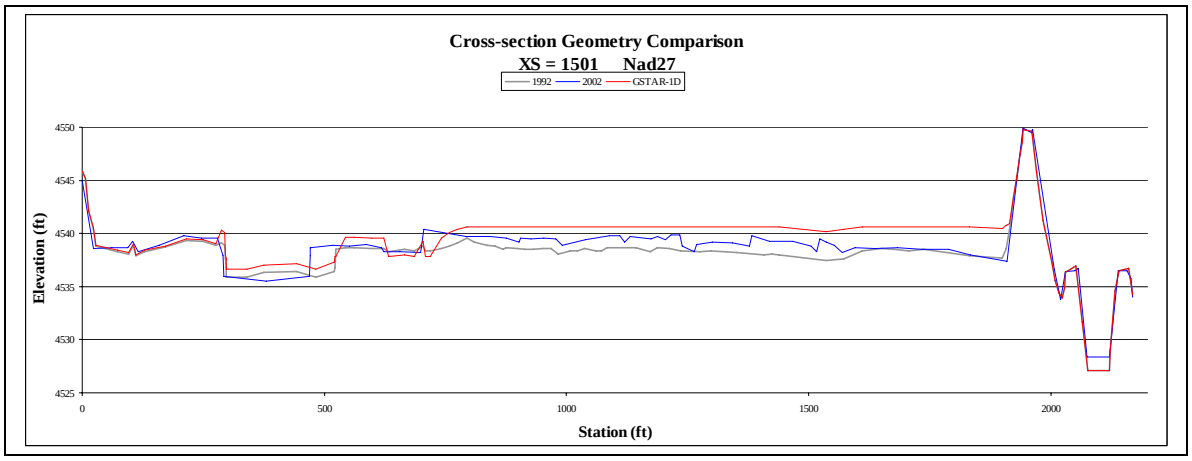

Figure 72: 1992-2002 cross-section change at Agg/Deg#1501.

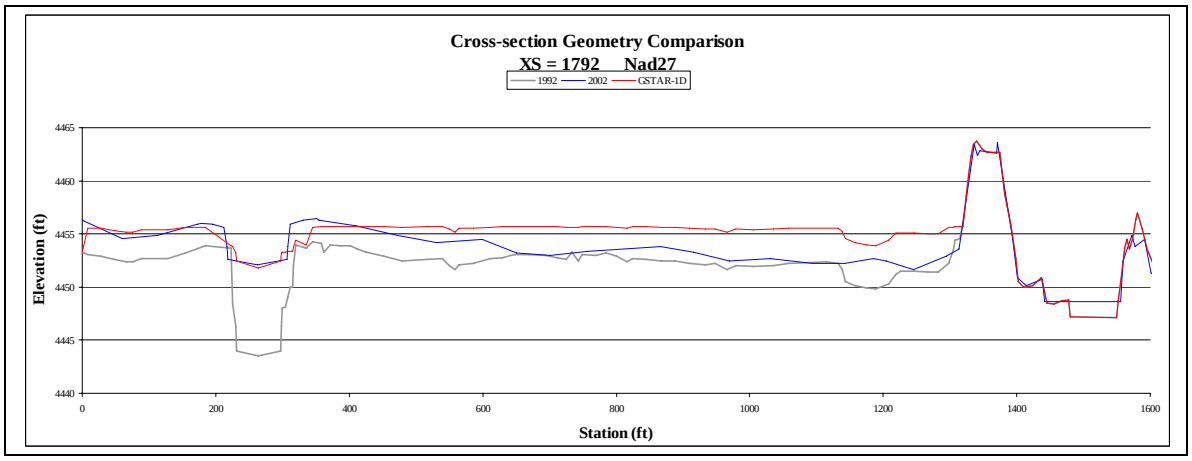

Figure 73: 1992-2002 cross-section change at Agg/Deg#1792.

5 Predictive Modeling

5.1 No Action Option

5.1.1 Model input

The model input included: 2002 Agg/Deg cross-section data, 2002 average bed material gradation data, the total load rating curve and sediment gradation data from the 1992 calibration model, the predicted daily flow data at San Acacia, and the predicted daily reservoir elevations at Elephant Butte Reservoir. The 20-year simulation was performed using the cross-sections at the same locations as the 226 cross-sections used in the calibration models to represent the 80 mile river reach and a time step of 0.5 hrs. The following describes the modifications that were made to the hydrology, boundary conditions, cross-section geometry, and sediment data for the predictive models. All other input parameters were set to the values determined in the calibration phase.

5.1.2 Hydrology and Boundary Conditions

For the predictive simulations, mean daily flow values for three hydrological time periods (dry, wet, and average) were generated (Lane, 2004). Section 3.2.4 provides additional information regarding the generation of the predictive mean daily flow values. These hydrologic scenarios were used to model the affects 20-year dry, average, and wet hydrologic periods would have on the river. Flow statistics for each of the models are shown in Table 10.

Table 10: Flow statistics for hydrologic traces used in predictive modeling.

	Discharge (cfs)			
	Minimum	**Maximum**	**Average**	**Std Deveation**
Dry	0	8,953	516	701
Average	0	12,951	1,078	1,427
Wet	0	20,630	1,733	2,447

It should be noted that all three of the predictive hydrologic scenarios contain a large number of flows greater than 6,000 ft^3/s (Figure 74) and the duration of moderate to high flows are greater compared to the calibration runs for 1972 to 2002 (Figure 38).

Predicted daily reservoir elevation values for Elephant Butte Reservoir were used for the downstream boundary condition in the form of a time-elevation table. The range of pool elevations for each hydrology can be seen in Figure 37.

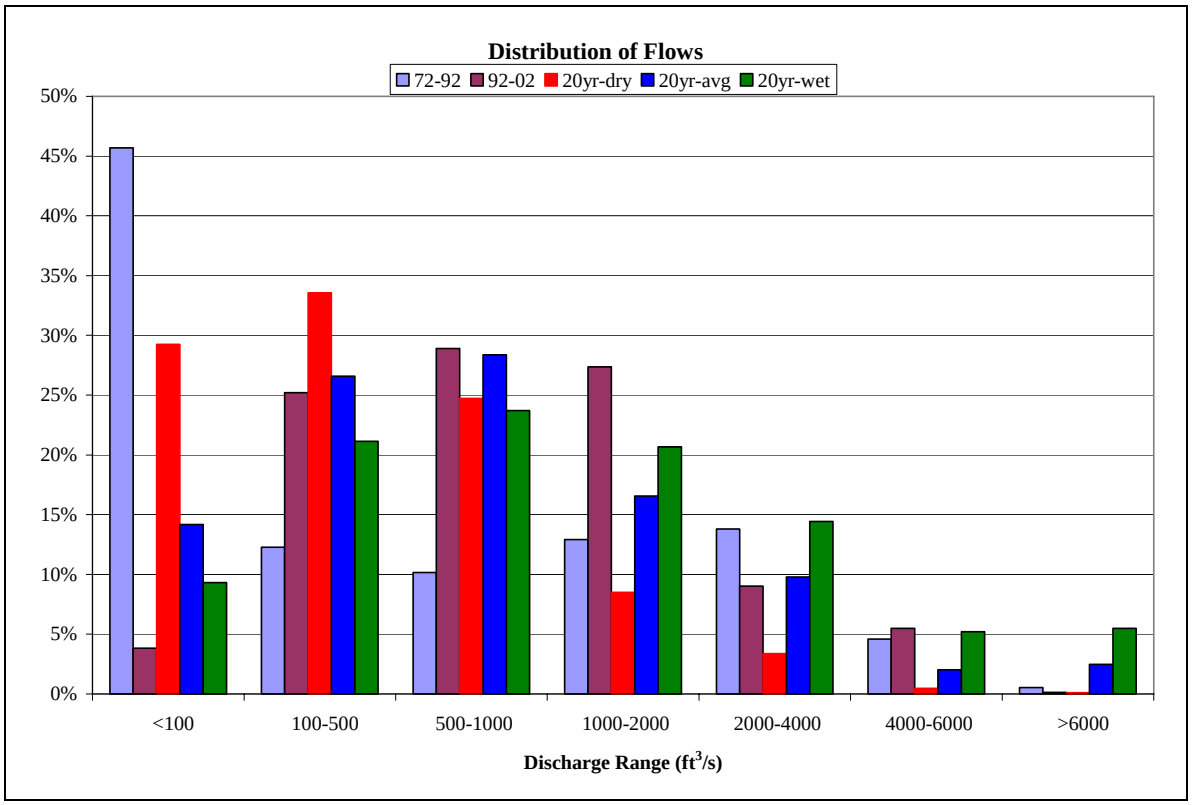

Figure 74: Distribution of flows for 20-year predictive models.

5.1.3 Sediment

A total of 10 grain sizes were used, ranging from clay to coarse gravel. The sediment loads were determined by using the 1992 sediment rating curve (Figure 41) and then adjusting the rating curve at higher flows (>4,000 ft^3/s) to account for the sediment transport at the higher discharges where field data were not available. To estimate the amount of sediment being transported at the larger flows, sediment transport capacity was calculated for various cross-sections at San Acacia Diversion Dam using the sediment transport capacity function in HEC-RAS. The incoming sediment load was reduced to match the sediment transport capacity calculated for discharges greater than 4,000 ft^3/s (Figure 75).

In addition, for discharges greater than the measured data (4,000 ft^3/s.), the fraction of the load within each size class was manually adjusted to estimate the change in the sediment transport gradation with increasing discharge. The results are given in Table 11.

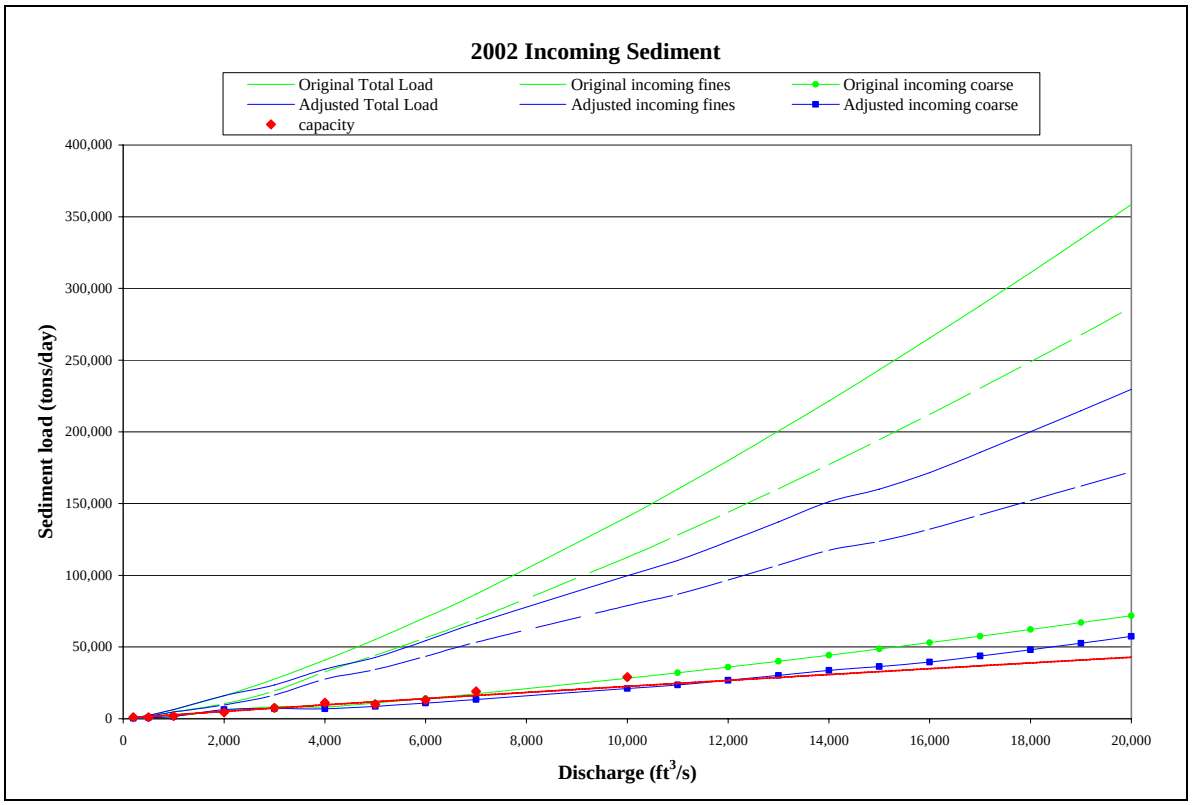

Figure 75: Adjusted total sediment load with capacity limits.

Table 11: Adjusted incoming sediment load data for predictive model.

Original Data										
Discharge	fines	vfs	fs	ms	cs	vcs	vfgrv	fgrv	grv	cgrv
(ft^3/s)	**<0.0625**	**0.0625-0.125**	**0.125-0.25**	**0.25-0.5**	**0.5-1.0**	**1-2**	**2-4**	**4-8**	**8-16**	**16-32**
101-500	32.17	6.65	27.42	26.61	6.65	0.50	0.00	0.00	0.00	0.00
501-1000	31.64	10.55	26.60	26.14	4.63	0.41	0.03	0.00	0.00	0.00
1001-2000	21.51	9.34	32.17	30.81	5.52	0.56	0.09	0.00	0.00	0.00
2001-4000	38.78	21.30	25.24	11.56	2.45	0.41	0.16	0.09	0.01	0.00
Model Input with Adjusted Gradations										
Discharge	fines	vfs	fs	ms	cs	vcs	vfgrv	fgrv	grv	cgrv
(ft^3/s)	**<0.0625**	**0.0625-0.125**	**0.125-0.25**	**0.25-0.5**	**0.5-1.0**	**1-2**	**2-4**	**4-8**	**8-16**	**16-32**
101-500	70	2.94	12.13	11.77	2.94	0.22	0.00	0.00	0.00	0.00
501-1000	75	3.86	9.73	9.56	1.70	0.15	0.01	0.00	0.00	0.00
1001-2000	60	4.76	16.39	15.70	2.81	0.29	0.05	0.00	0.00	0.00
2001-4000	80	6.96	8.25	3.78	0.80	0.13	0.05	0.03	0.00	0.00
4001-8000	80	6.25	6.95	4.69	1.17	0.31	0.23	0.16	0.16	0.08
8001-16000	77	6.72	7.43	4.95	1.59	0.71	0.62	0.35	0.35	0.27
16001-21000	75	6.92	7.69	5.00	1.92	1.06	0.77	0.58	0.58	0.48

The bed material data set consists of 2002 bed material samples from the San Acacia floodway gage, San Marcial floodway gage, and additional cross-section bed material samples taken at various locations along the reach in 2002. The resulting distribution for the bed material is shown in Table 12.

Table 12: Bed material gradation for predictive models.

	fines	vfs	fs	ms	cs	vcs	vfgrv	fgrv	grv	cgrv
Agg/Deg#	**<0.0625**	**0.0625-0.125**	**0.125-0.25**	**0.25-0.5**	**0.5-1.0**	**1-2**	**2-4**	**4-8**	**8-16**	**16-32**
1208	1.77	4.28	18.43	27.67	11.62	5.31	5.53	7.12	8.62	9.67
1262	2.38	3.61	20.60	37.85	18.33	2.77	2.58	4.41	6.10	1.37
1440	1.22	3.78	31.41	50.76	8.11	0.70	0.38	0.66	1.12	1.87
1562	11.00	6.00	32.00	42.00	5.25	0.80	0.50	0.65	0.80	1.00
1972	12.66	8.55	34.70	38.35	2.85	1.06	0.62	0.65	0.36	0.19

5.1.4 Results

The predicted erosion and deposition for the 20-year period are, in general, greater than historical trends (Figure 76-Figure 83). The numerical model shows the main channel to be relatively stable downstream from Agg/Deg#1327 with a general trend towards channel erosion at the furthest downstream cross sections.

Downstream from ~Agg/Deg#1327 the main channel volume calculations do not appear to be very sensitive to hydrology and are fairly stable. Therefore, future channel capacity should remain relatively stable downstream of ~Agg/Deg#1327. However, an extended dry period may cause channel deposition in the upstream reaches. And wetter hydrology will cause erosion to progress further downstream (notice that in Figure 82 the inflection point in the mass deposition curves moves downstream with wetter hydrology). Conversely, the model shows large amounts of deposition in the floodplains downstream of Agg/Deg#1327.

The major difference between the different hydrologic scenarios is in the overbanks and the main channel just downstream of San Acacia Diversion Dam at the upper portion of the modeled reach (Figure 82). Floodplain aggradation increases with higher flows as a result of additional floodplain interaction. The lower potion of the study reach exhibits excessive amounts of aggradation in the floodplain for the wet hydrology due to the complex interaction between the floodplain and main channel in a perched channel system. In a perched channel system, the interaction between the floodplain and main channel cannot be modeled properly with a 1-dimensional model because a 1-D model assumes a constant water surface for the entire cross-section resulting in a sediment transport capacity that is too low.

Floodplain deposition begins downstream of ~Agg/Deg#1327 in the 20-year simulations. This is upstream of the location where floodplain deposition began in the period 1992 to 2002. It is suspected that because the predictive hydrology contained larger flow rates of relatively long duration, floodplain deposition occurred in reaches that previously had not experienced floodplain flow. Agg/Deg#1327 is also where the channel capacity decreases below 8,000 ft^3/s. The predictive hydrology contains several flows larger than 8,000 ft^3/s and therefore, the floodplains become active at this point. Downstream of approximately Agg/Deg#1452, the floodplain deposition rate increases due to the further reduction in channel capacity to below 5,000 ft^3/s. The increase in floodplain aggradation rate downstream of Agg/Deg#1452 is shown by the increase in the slope of the cumulative total volume of sediment deposition (Figure 77). Downstream of Agg/Deg#1751 there is significant channel erosion predicted, but it is likely that the channel erosion is over predicted. The erosion in the main channel could be due to a low reservoir elevation and/or because the flows were confined to the main channel (temporary channel) when the flows should have been allowed to spread over the reservoir delta.

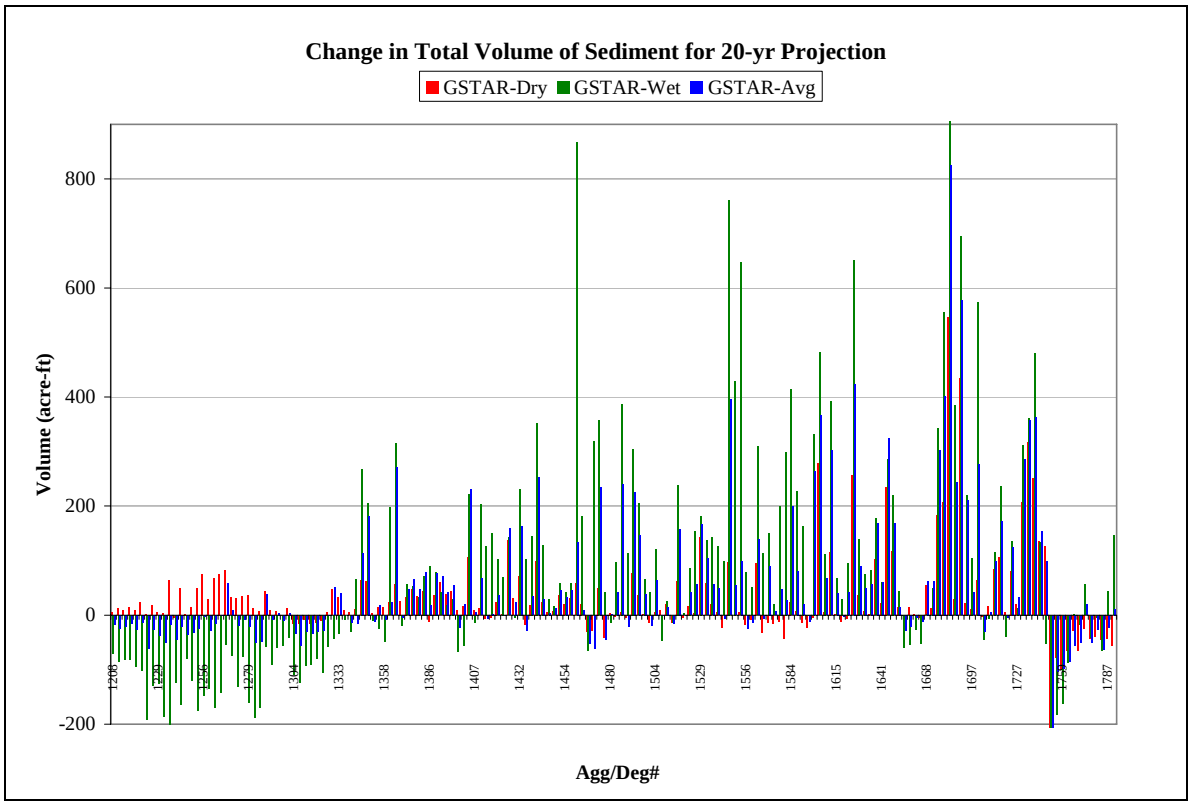

Figure 76: Change in total volume of sediment for 20-year projection.

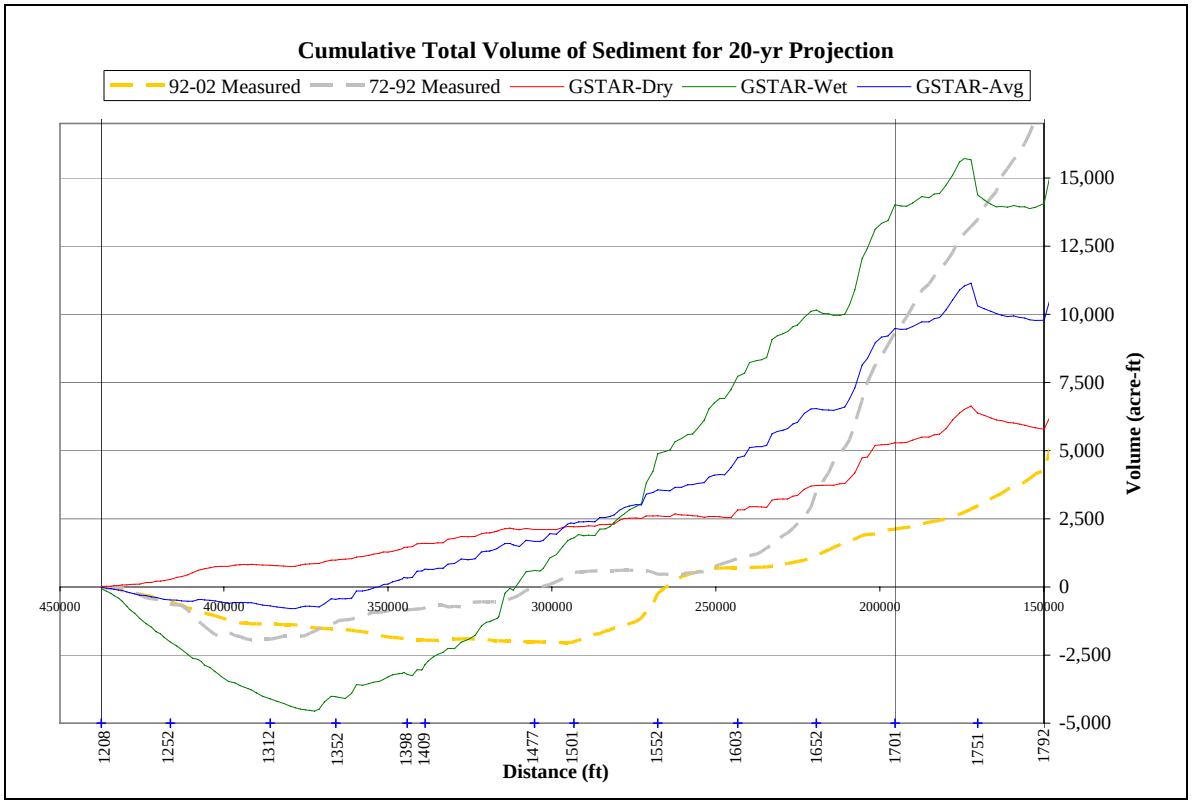

Figure 77: Cumulative total volume of sediment for 20-year projection.

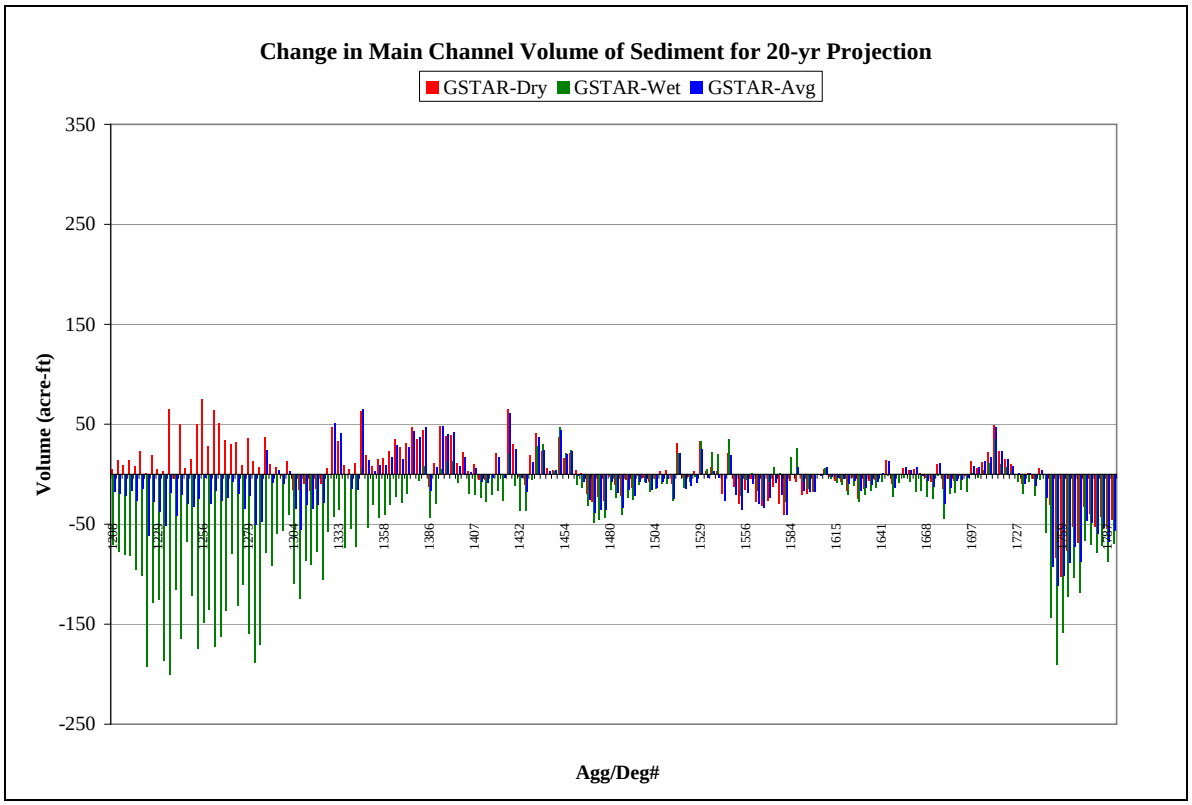

Figure 78: Change in main channel volume of sediment for 20-year projection.

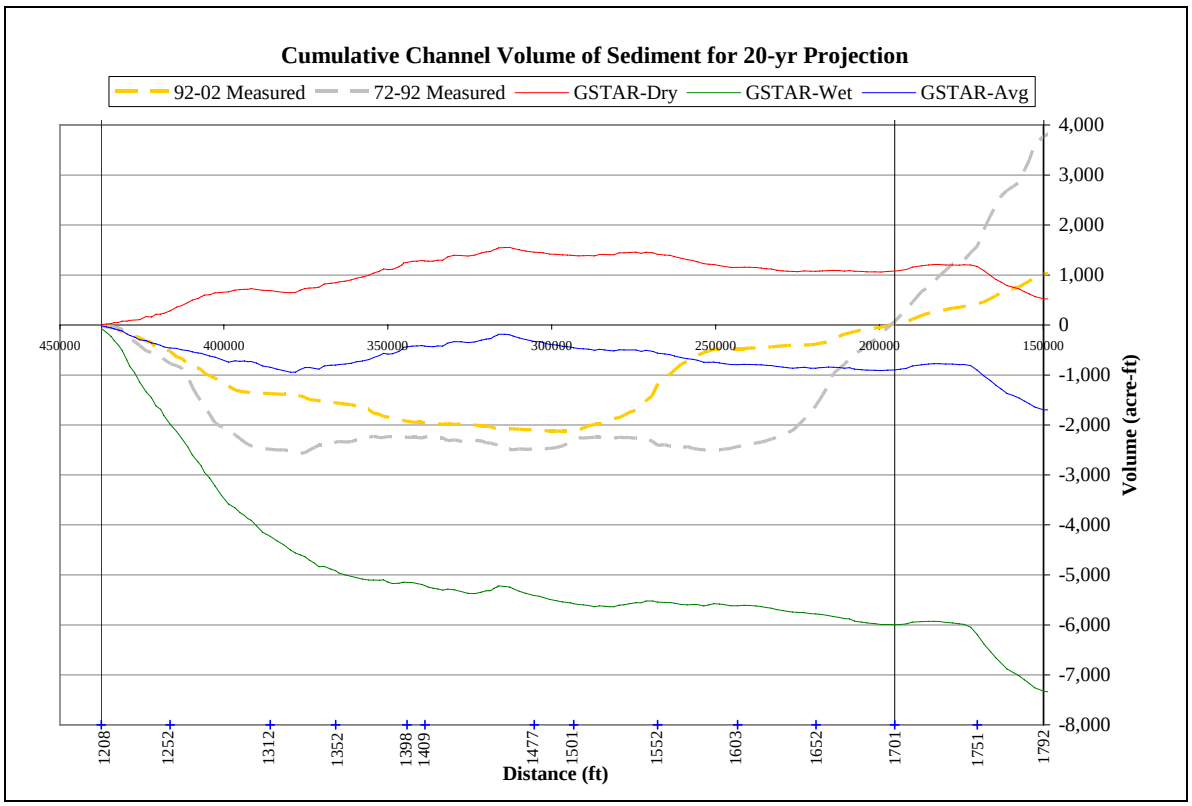

Figure 79: Cumulative main channel volume of sediment for 20-year projection.

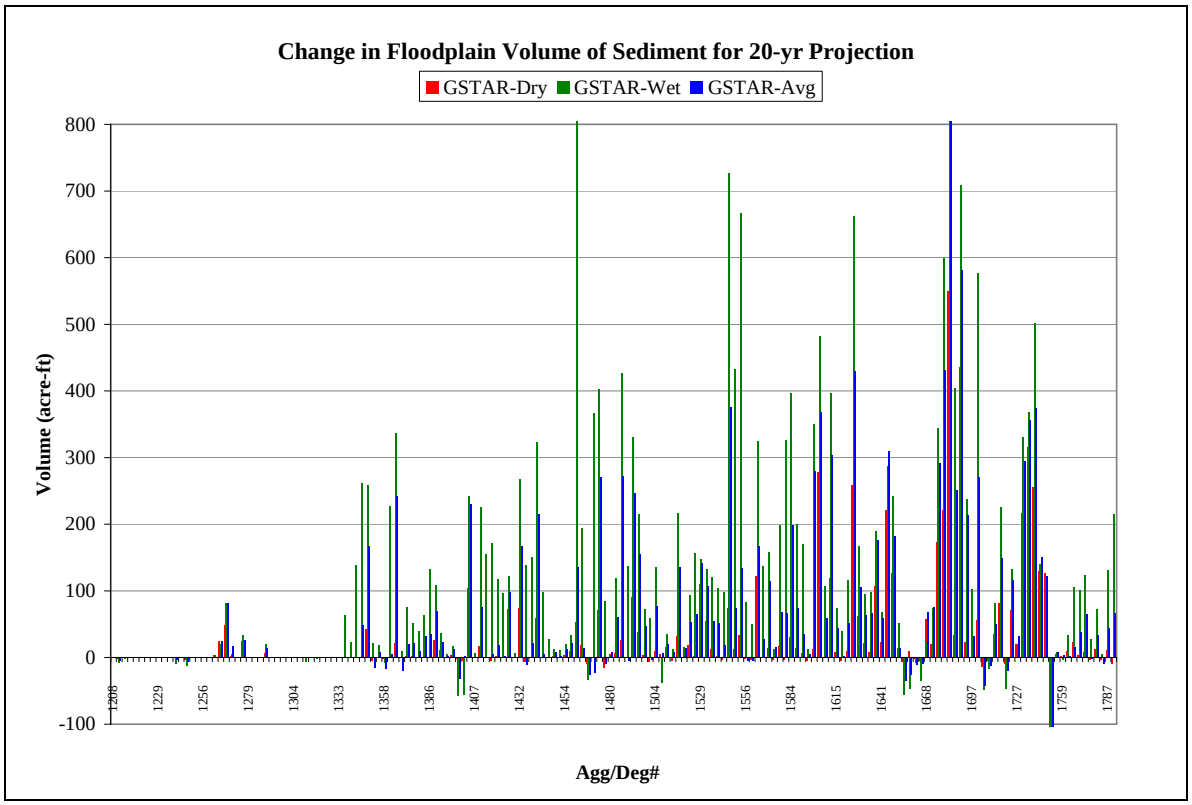

Figure 80: Change in floodplain volume of sediment for 20-year projection.

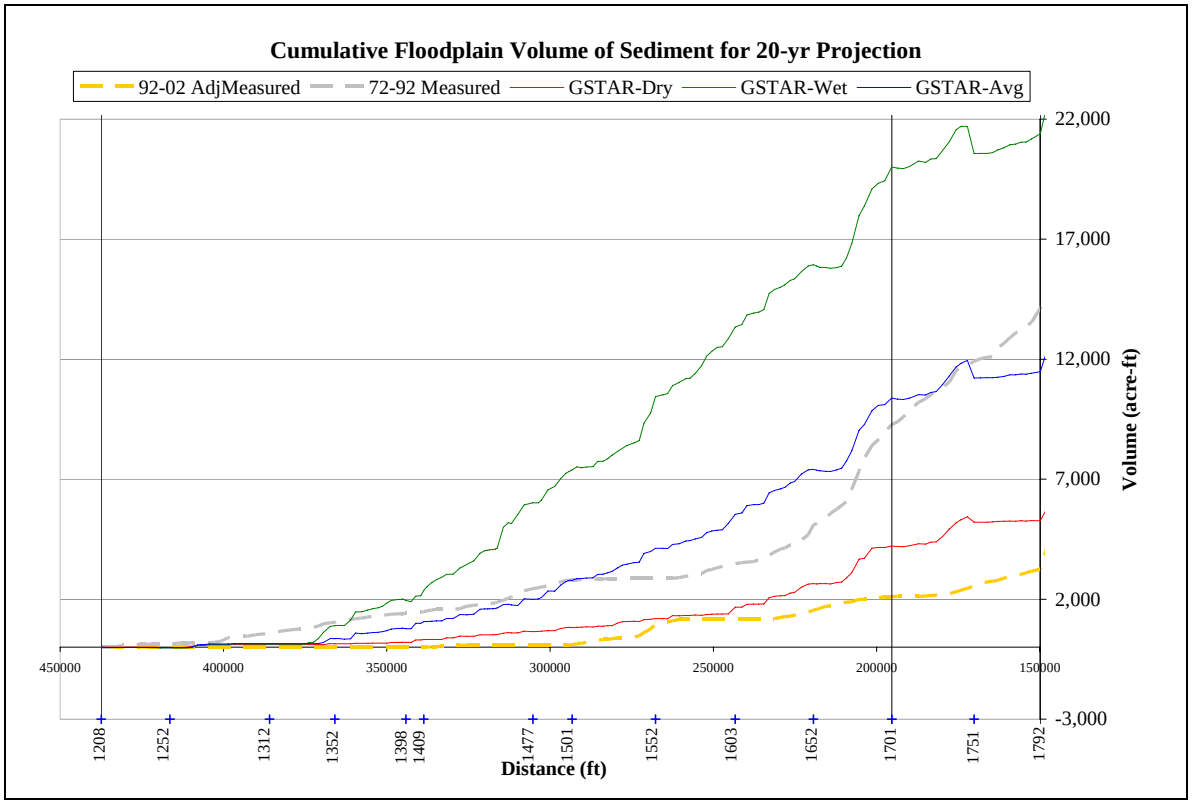

Figure 81: Cumulative floodplain volume of sediment for 20-year projection.

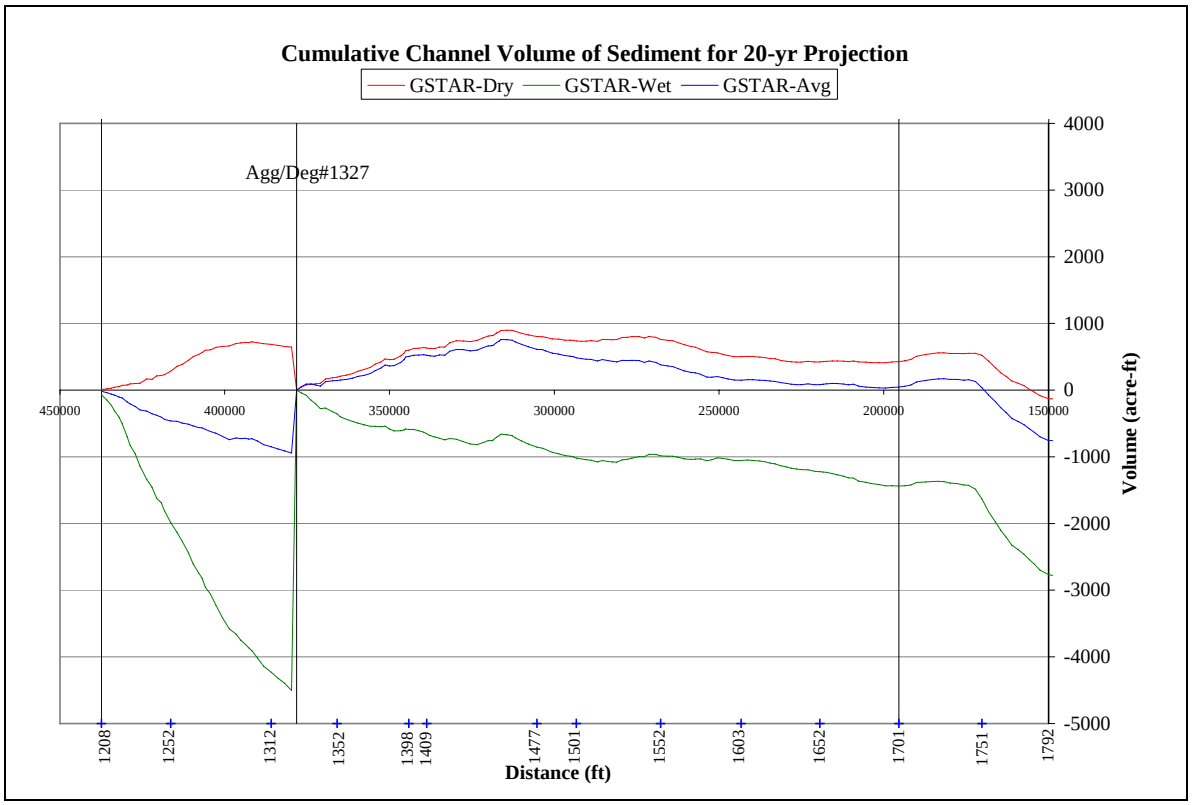

Figure 82: 20-year projected adjusted cumulative channel volume comparison.

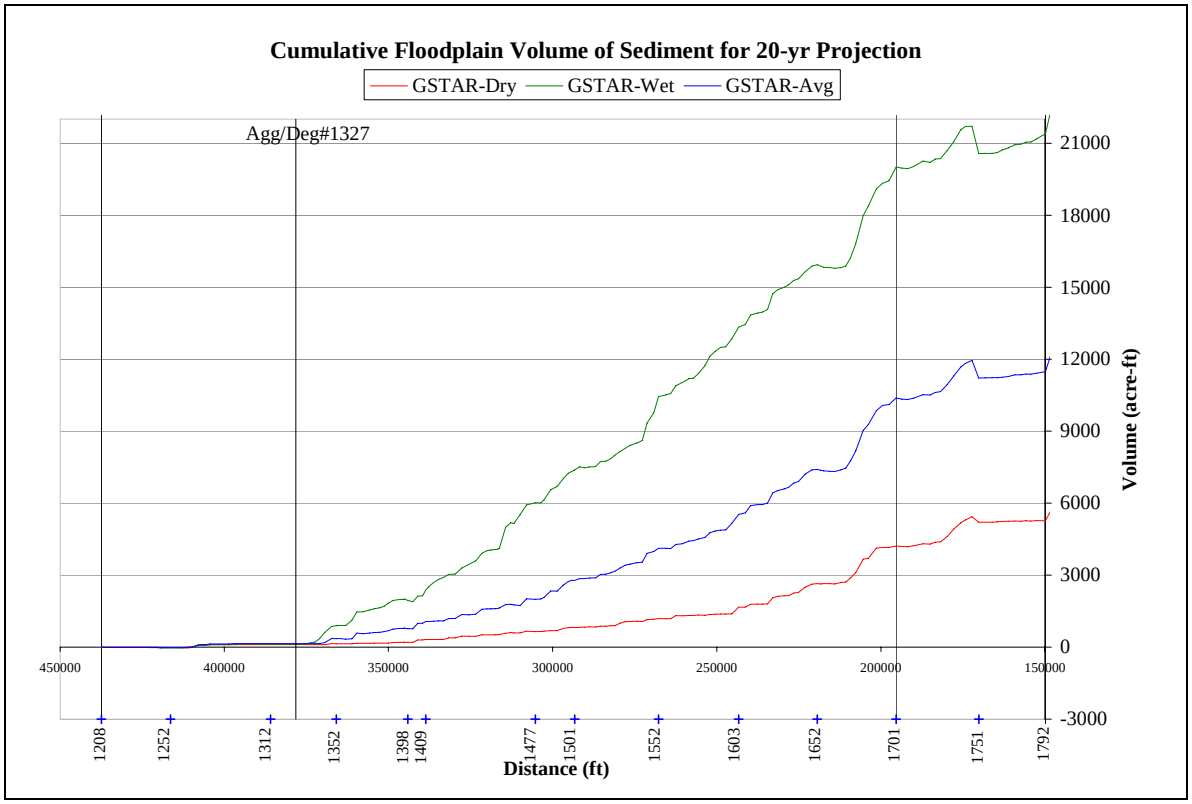

Figure 83: 20-year projected adjusted cumulative floodplain volume comparison

Figure 84 shows the total change in mean bed from the start (2002) of the simulation to the end of the 20-year modeling period for each hydrology. Figure 85 to Figure 87 shows the mean bed profile change for each hydrology.

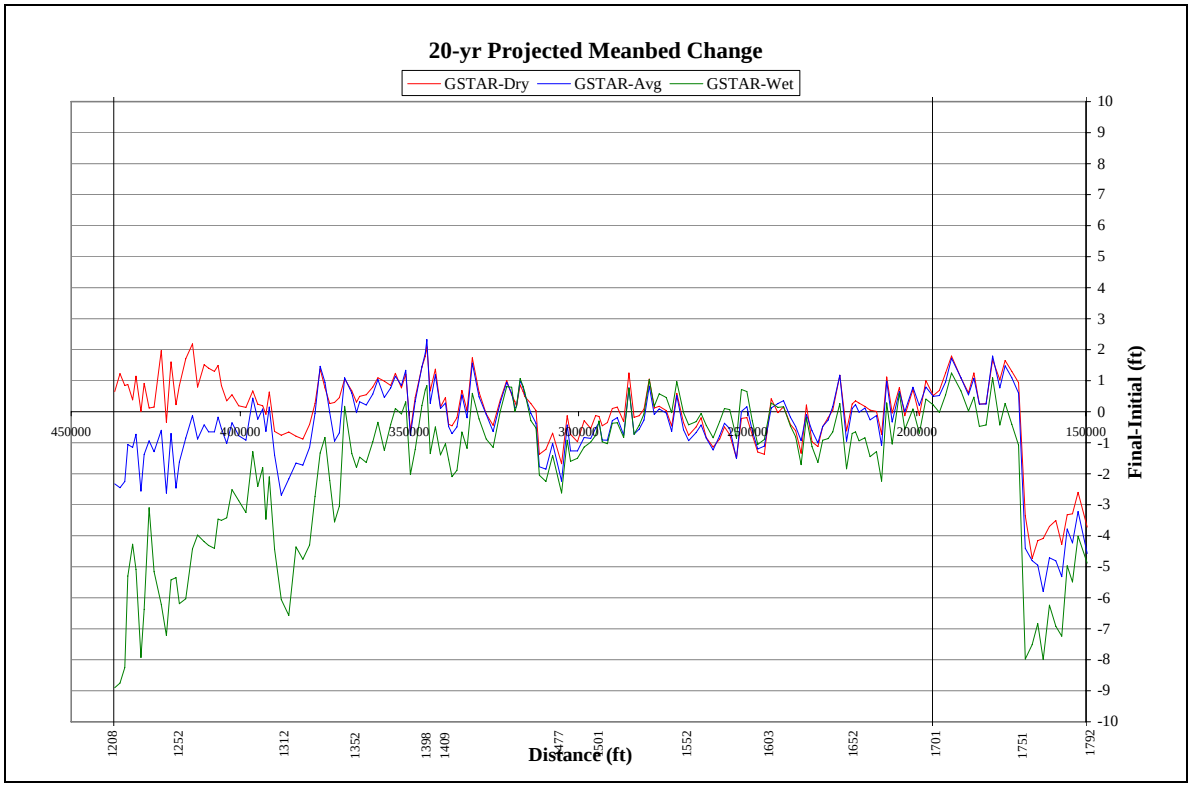

Figure 84: 20-year projected change in mean bed.

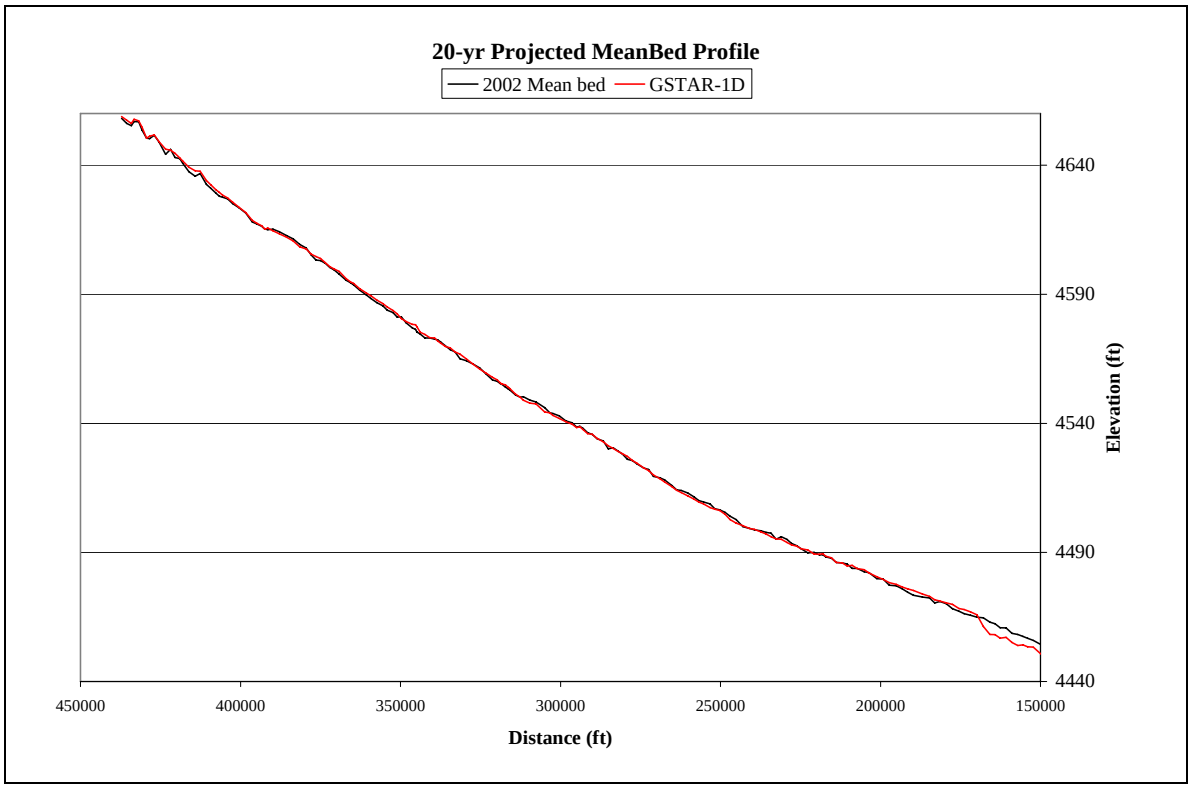

Figure 85: 20-year projected mean bed elevation profile (dry hydrology).

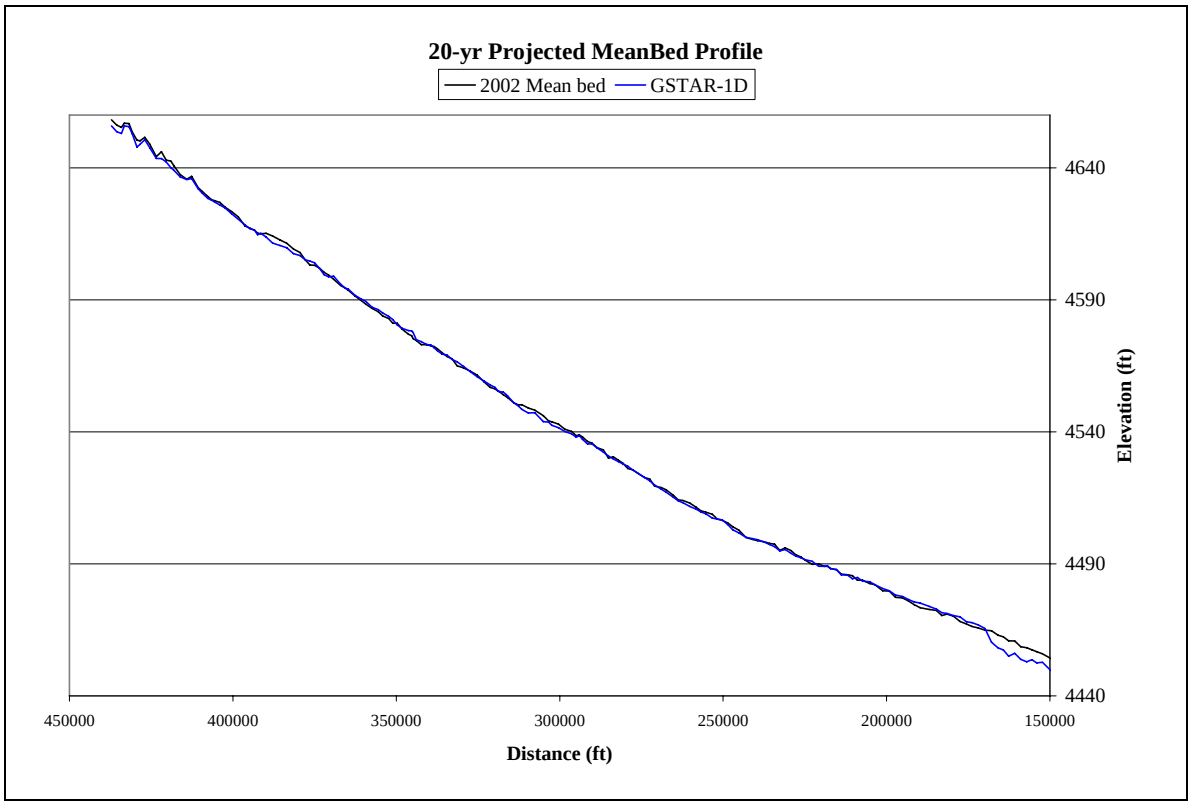

Figure 86: 20-year projected mean bed elevation profile (average hydrology).

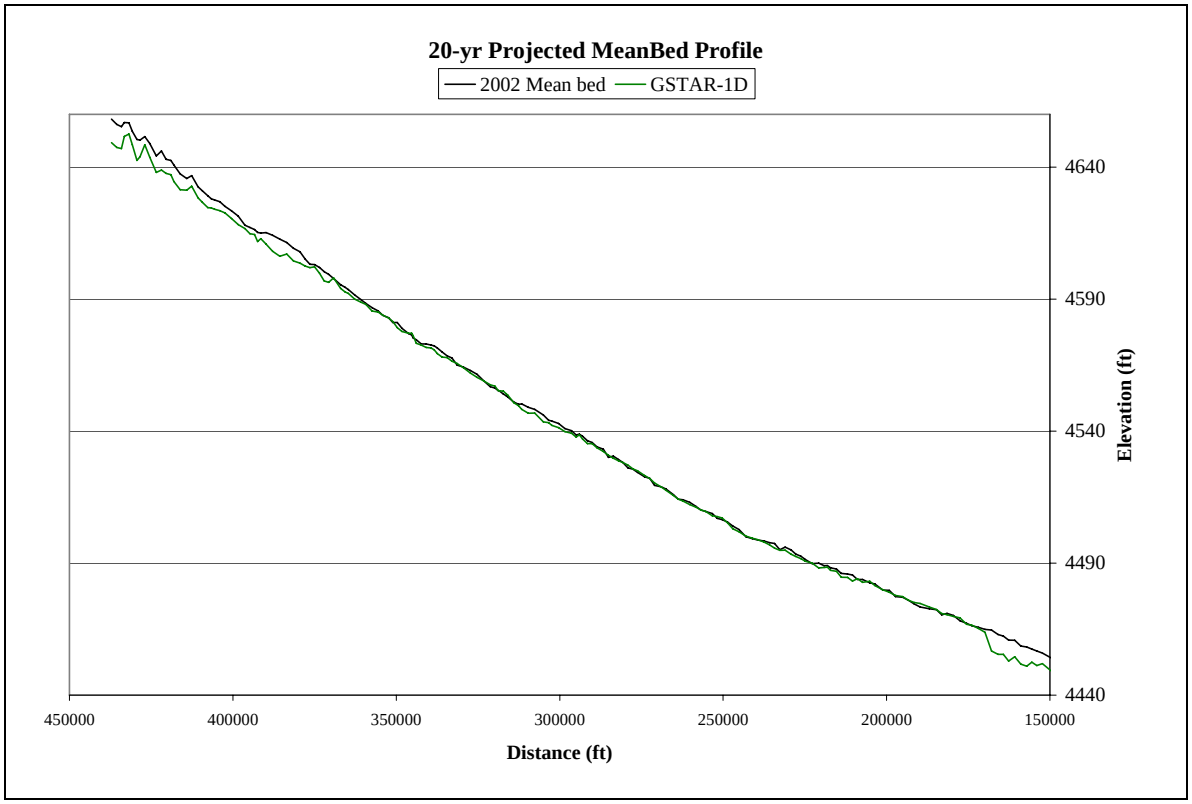

Figure 87: 20-year projected mean bed elevation profile (wet hydrology).

The median diameter of bed sediment, d_{50}, for three sub-reaches is shown in Figure 88 for the average hydrology. Similar to the calibration model results, the bed material becomes coarser following peak flows and finer during low flows. During the low flows, sand is deposited in the channel whereas at the higher flows the incoming sediment is transported downstream and additional sediment is eroded from the channel bed causing degradation (Figure 89). Because the upstream portion of the model coarsens during high flow, it is expected that the river will continue to coarsen upstream of Agg/Deg# 1327, decreasing the rate of degradation in the upstream reach.

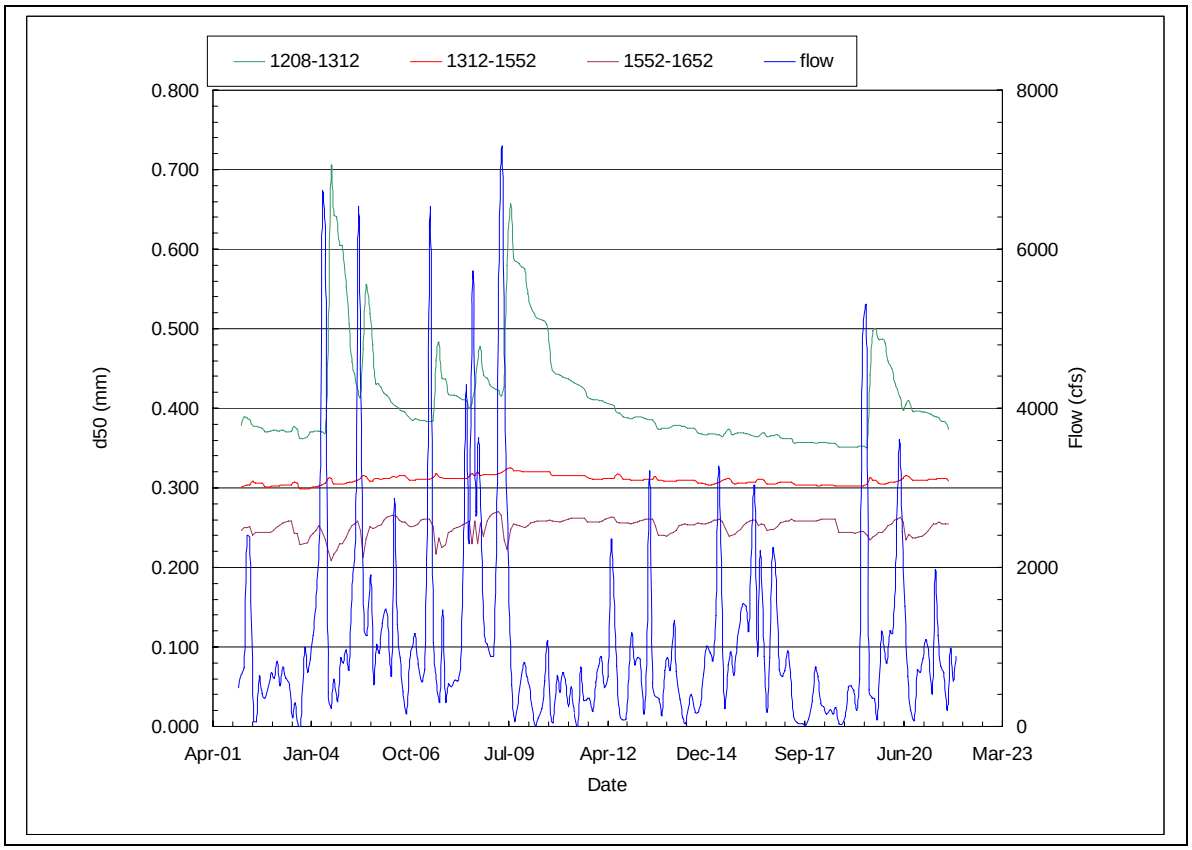

Figure 88: Change in bed material size (d_{50}) during model simulation.

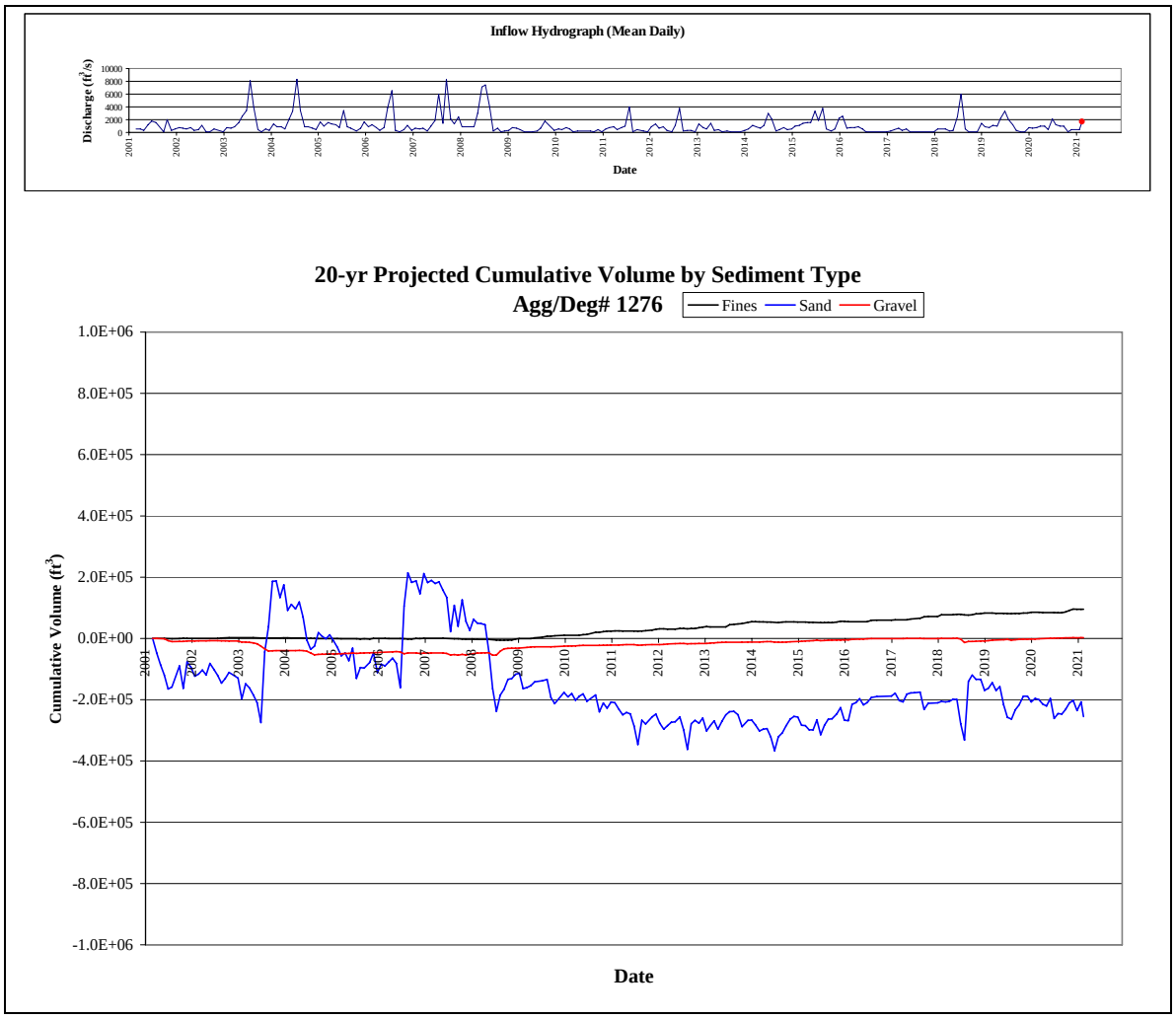

Figure 89: Plot of cumulative volume change by sediment type (Agg/Deg#1276).

Similar to the calibration model results, four typical river cross-section changes are shown in Figure 90 – Figure 93. Figure 90 shows the cross-section at Agg/Deg#1214, just downstream from the San Acacia Diversion Dam. The dry hydrology shows deposition in the main channel while the average and wet hydrology show erosion as would be expected. As noted above, the main channel in this reach is greatly affected by the incoming sediment load. Figure 91 shows the cross-section at Agg/Deg#1276, where again the dry hydrology produces deposition and the average and wet hydrology show erosion in the main channel. The floodplains experienced slight deposition for all three hydrologic scenarios. Figure 92 shows the cross-section at Agg/Deg#1501, where the main channel eroded for each hydrology and the floodplains remained stable except for the wet hydrology which produced floodplain deposition. Figure 93 shows the cross-section at Agg/Deg#1792. Historically, this section has continued to aggrade in both the main channel and the floodplains. However, with the inclusion of a channel through the delta deposits, the model predicts main channel erosion for each hydrology and floodplain deposition for the average and wet hydrology.

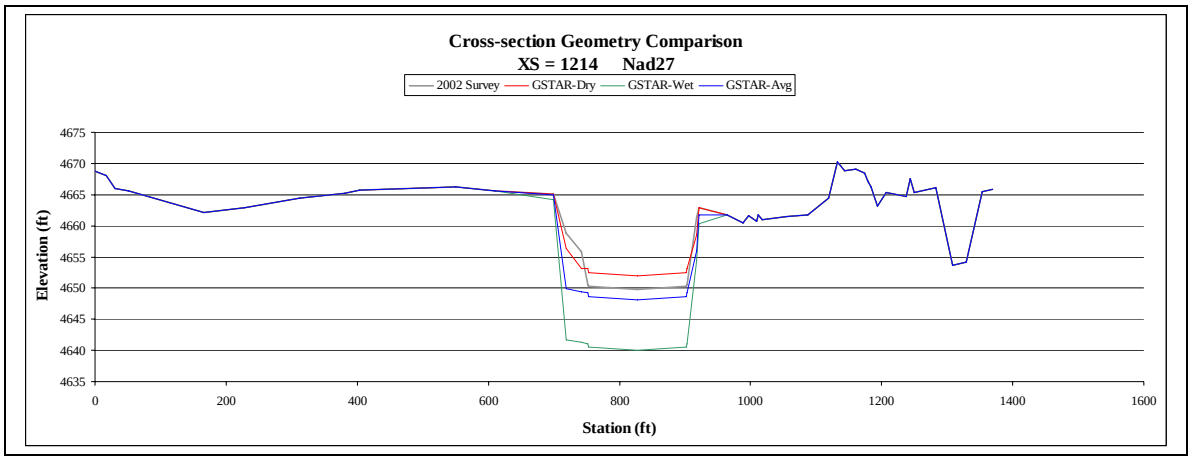

Figure 90: 20-year projected cross-section change at Agg/Deg#1214.

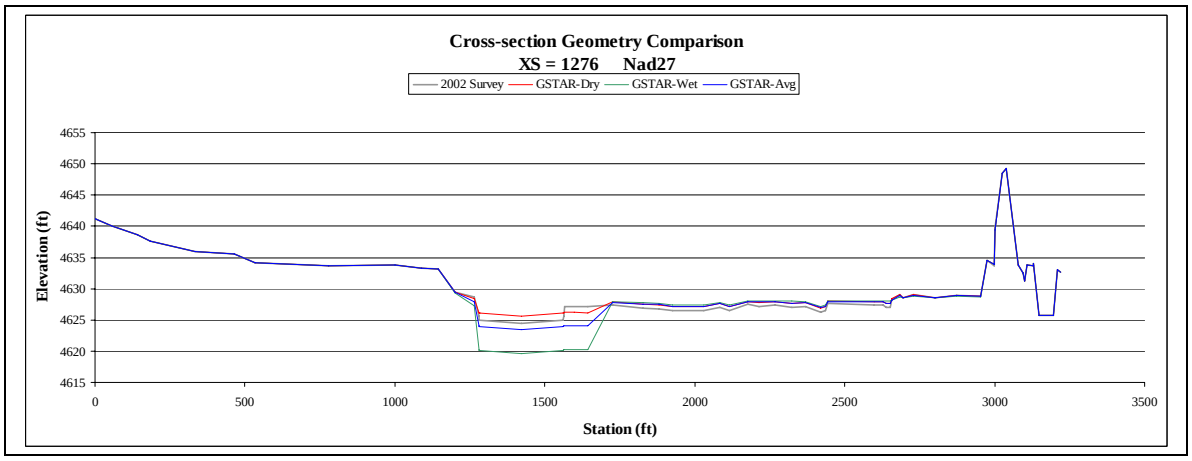

Figure 91: 20-year projected cross-section change at Agg/Deg#1276.

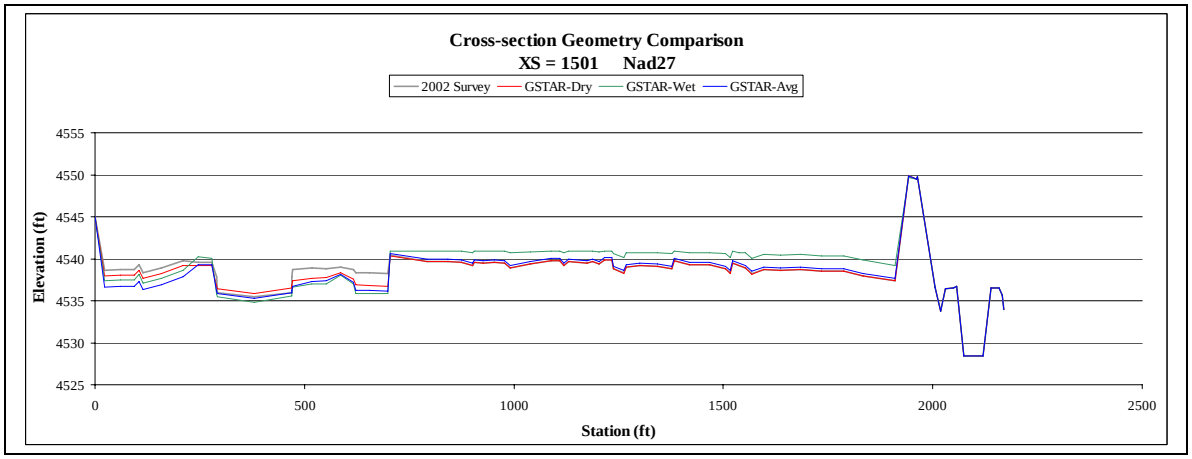

Figure 92: 20-year projected cross-section change at Agg/Deg#1501.

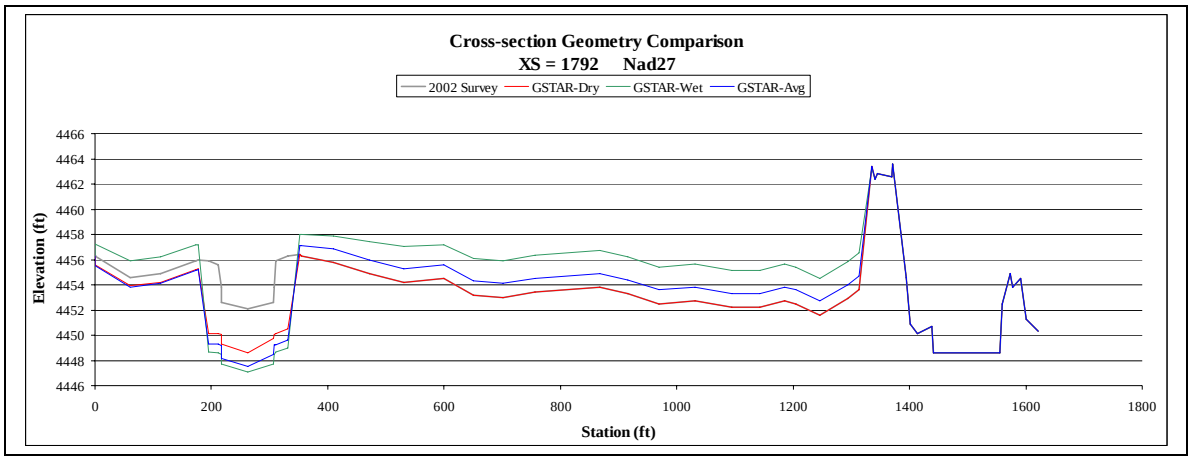

Figure 93: 20-year projected cross-section change at Agg/Deg#1792.

The large difference between the dry, average, and wet hydrology projections at the downstream end of the model (AggDeg#1792) is a result of the timing of the hydrograph. The hydrology for the wet trace has the majority of the high flows occurring at the end of the model compared to the other two traces which are near the beginning. When the flows are reversed, the upstream portion of the modeled reach produces similar results but the downstream portion of the reach experiences less erosion. If the high flows occur at the beginning of the simulation, the model has more time to recover from the high flows by the end of the simulation. By changing the timing of the flow hydrograph, the channel incision at the downstream portion of the reach is reduced by 6ft. This indicates that the bed in this reach will scour during high flows, but recover during low flows. Similarly, if the wet hydrology model is stopped prior to when the high flows occur (Figure 94), the overall results match historical data better (Figure 95 - Figure 98). From these results it is apparent that the long duration and high magnitude flows may cause extensive channel degradation and floodplain deposition.

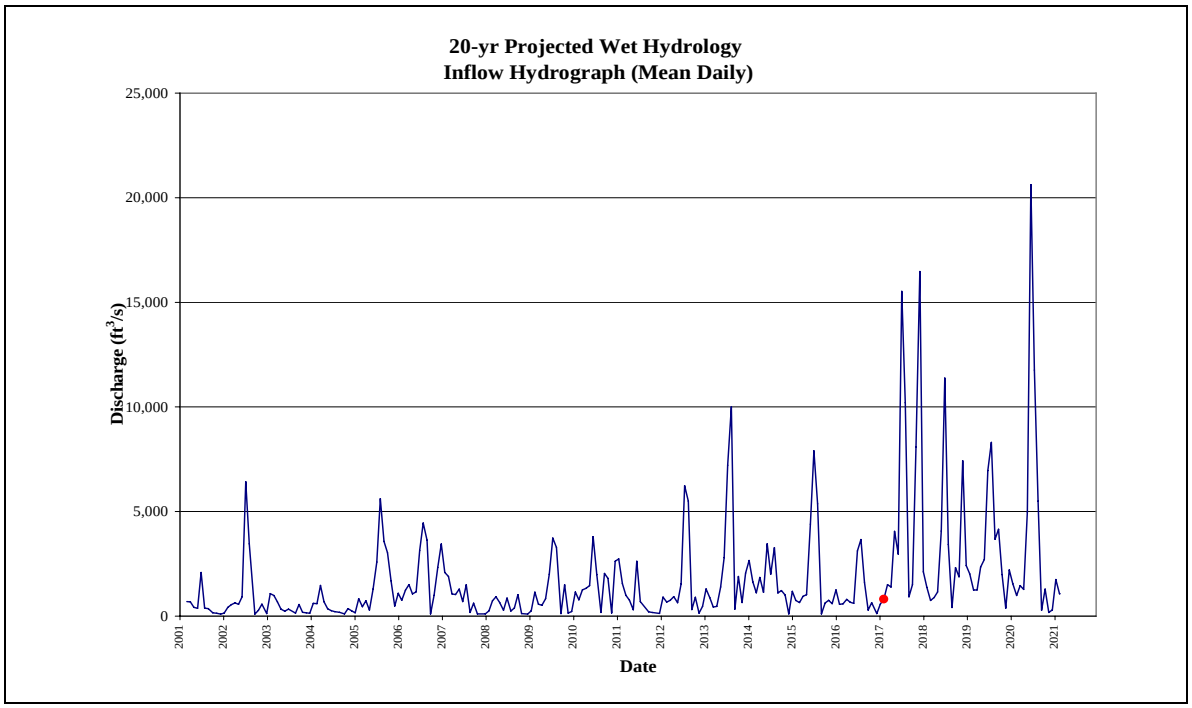

Figure 94:20-year projected wet hydrology prior to end of model high flows.

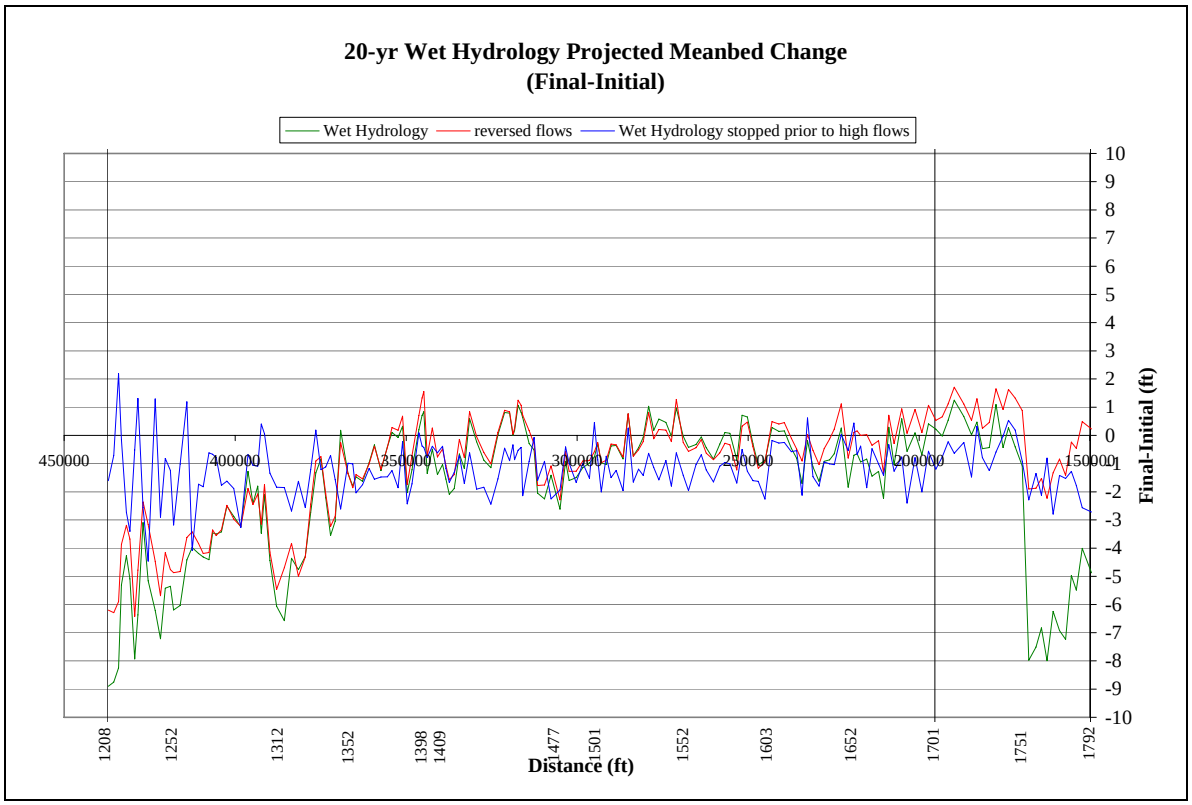

Figure 95: 20-year projected wet hydrology mean bed comparison.

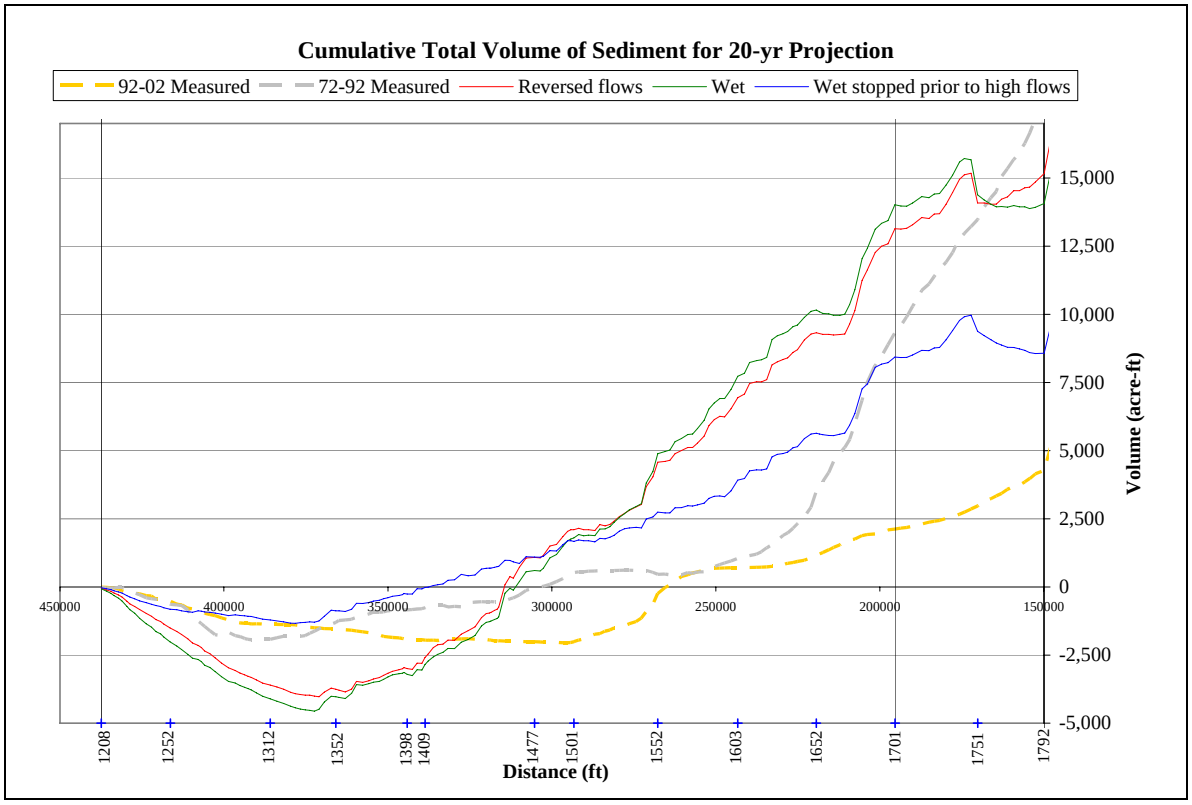

Figure 96: 20-year projected wet hydrology cumulative total sediment volume comparison.

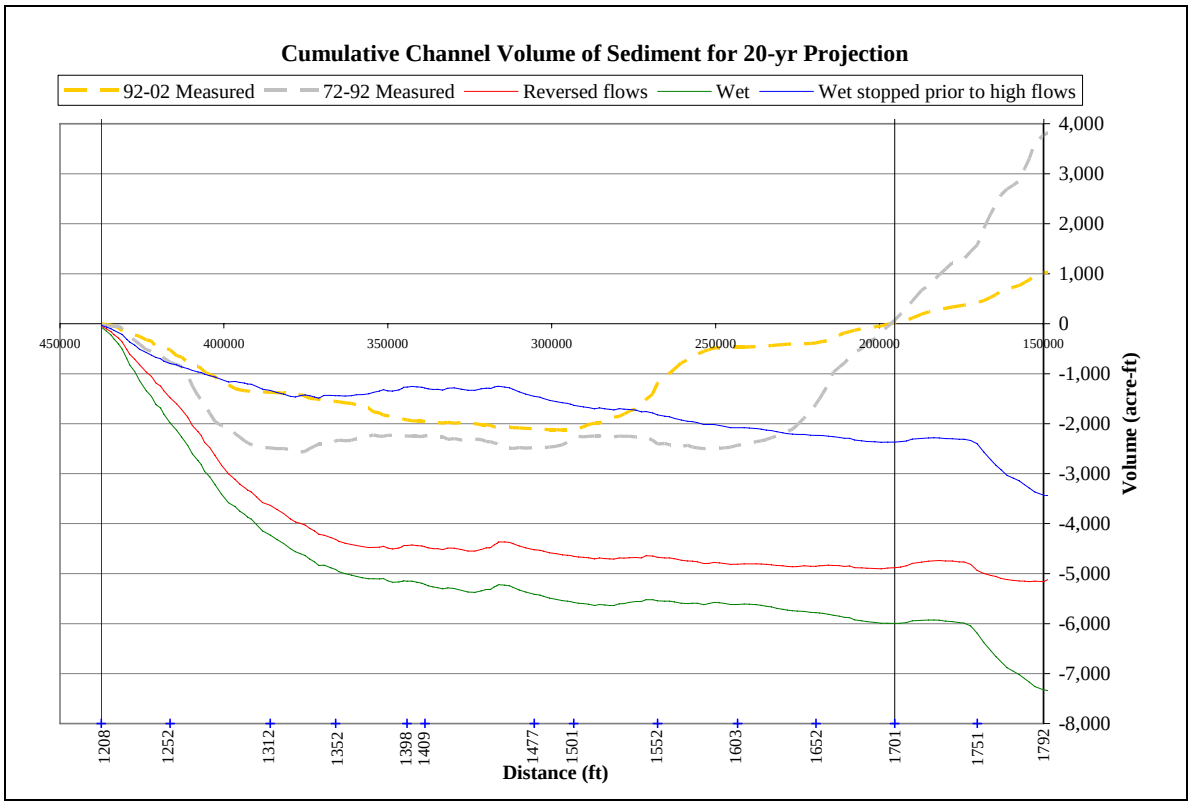

Figure 97: 20-year projected wet hydrology cumulative channel sediment volume comparison.

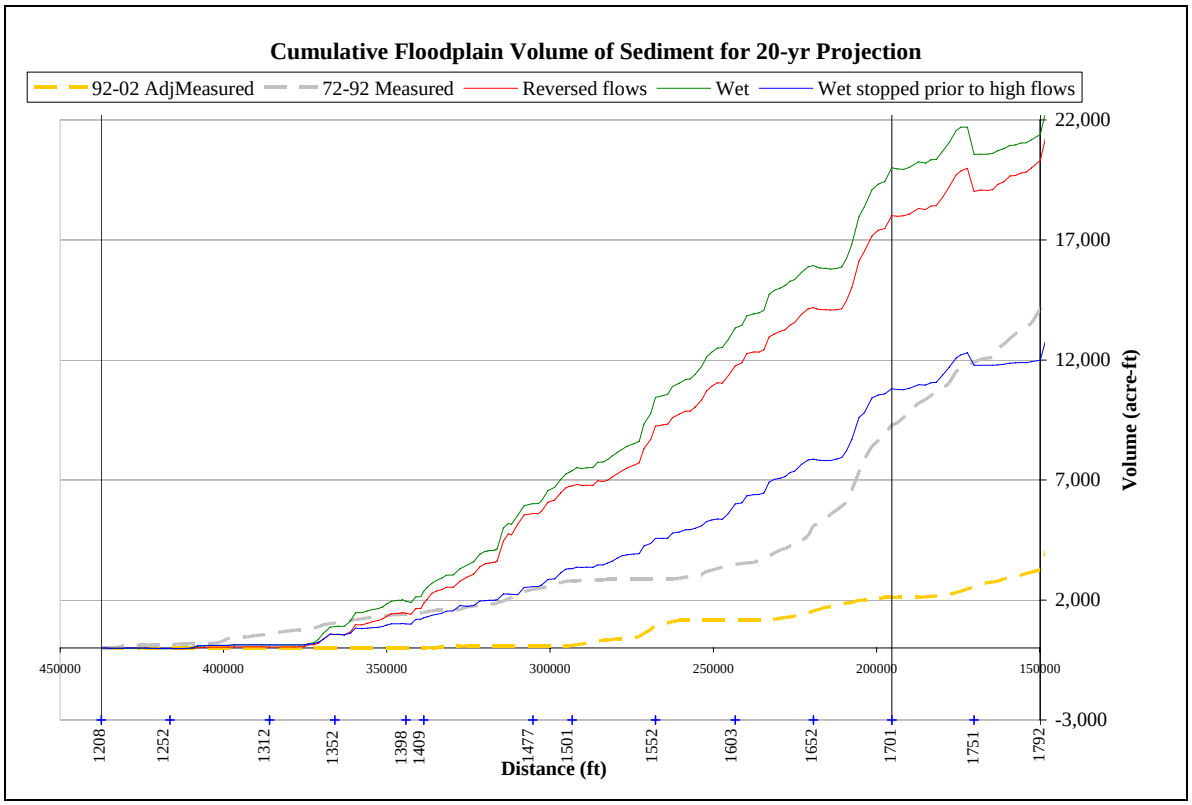

Figure 98: 20-year projected wet hydrology cumulative floodplain sediment volume comparison.

5.2 Sediment Augmentation Option

It is difficult to predict the affect of sediment augmentation because the sediment loads at the San Acacia floodway gage have not been measured above 4,000 ft^3/s. If the current loads are unknown it is difficult to predict the affect of incremental change. Since the predictive hydrology contains flows up to 21,000 ft^3/s and a large number of flows greater than 5,000 ft^3/s, therefore it is necessary to determine the incoming load for the discharges ranging from 4,000 – 21,000 ft^3/s. As described in section 5.1.3, the sediment table being used was generated by tipping the upper end of the sediment rating curve to match sediment transport capacity calculations. Augmentation of fine sediment (fine sand, silt and clay) will increase the aggradation in the floodplains in the lower reaches and augmentation of coarse sand and gravel may prevent some erosion in the upper reaches. Therefore, further work could compute the volume of gravel necessary to maintain the current bed elevations downstream of San Acacia Diversion Dam.

The results downstream of San Acacia Diversion Dam (Agg/Deg#1208 to Agg/Deg#1327) can be altered simply by changing the volume of incoming sediment and the gradation of the incoming load (Figure 99- Figure 101). The "92 Sediment" does not contain sediment data for discharges greater than 4,000 ft^3/s, whereas, the "Adjusted Sediment" contains additional sediment data based on sediment transport capacity calculations for discharges greater than 4,000 ft^3/s. Therefore, additional analysis should be conducted to better define the sediment load at these higher discharges to more accurately model the channel downstream of San Acacia Diversion Dam.

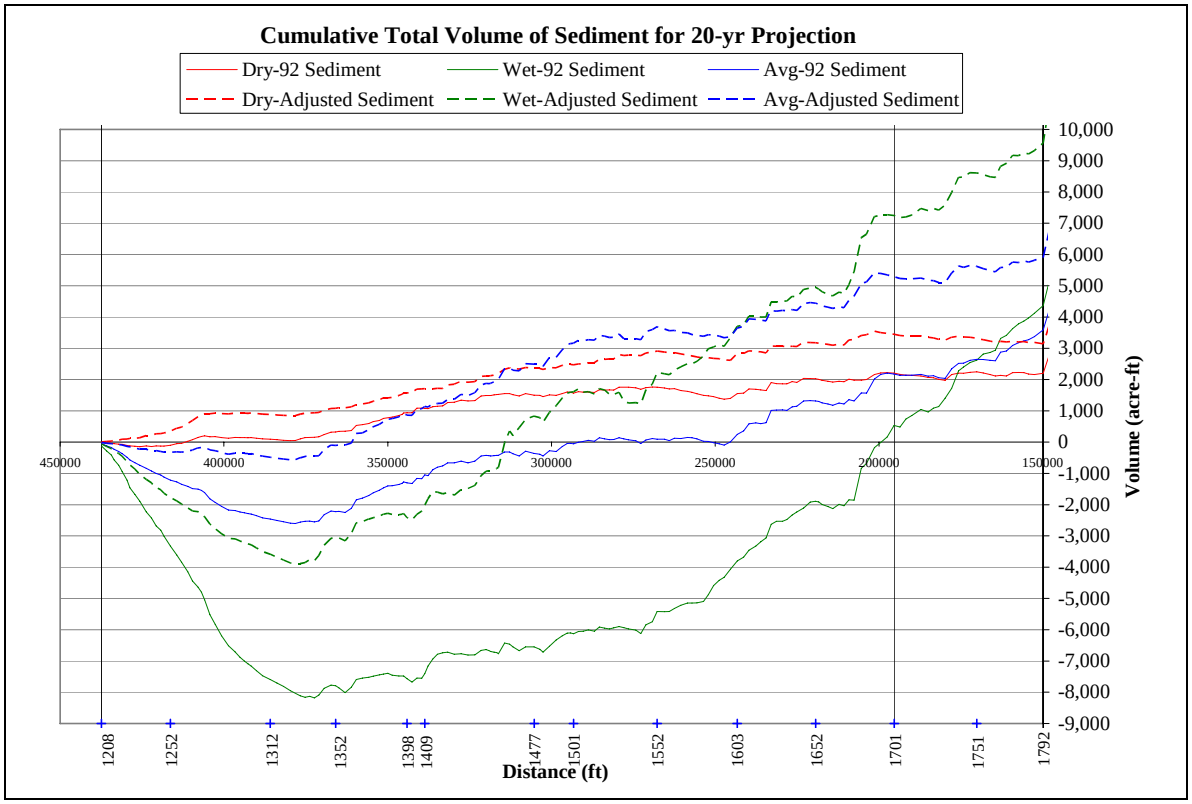

Figure 99: 20-year projected cumulative total sediment augmentation comparison.

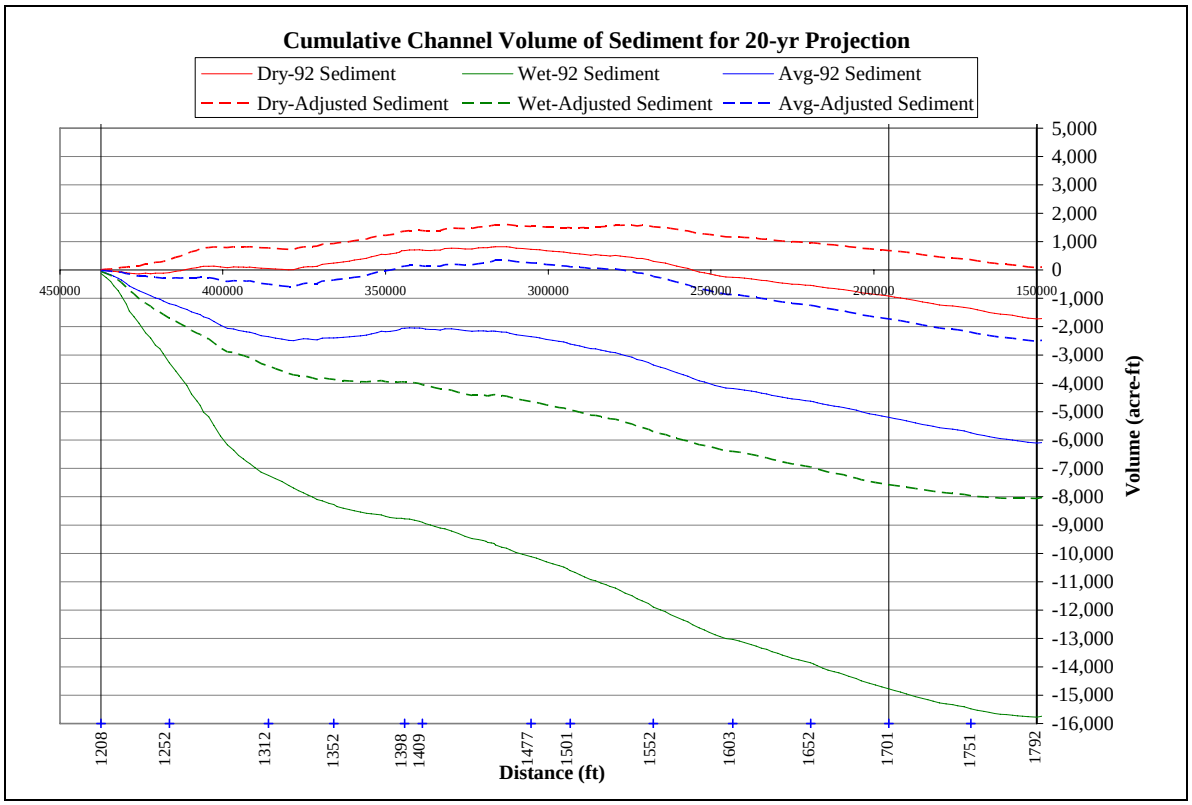

Figure 100: 20-year projected cumulative channel sediment augmentation comparison.

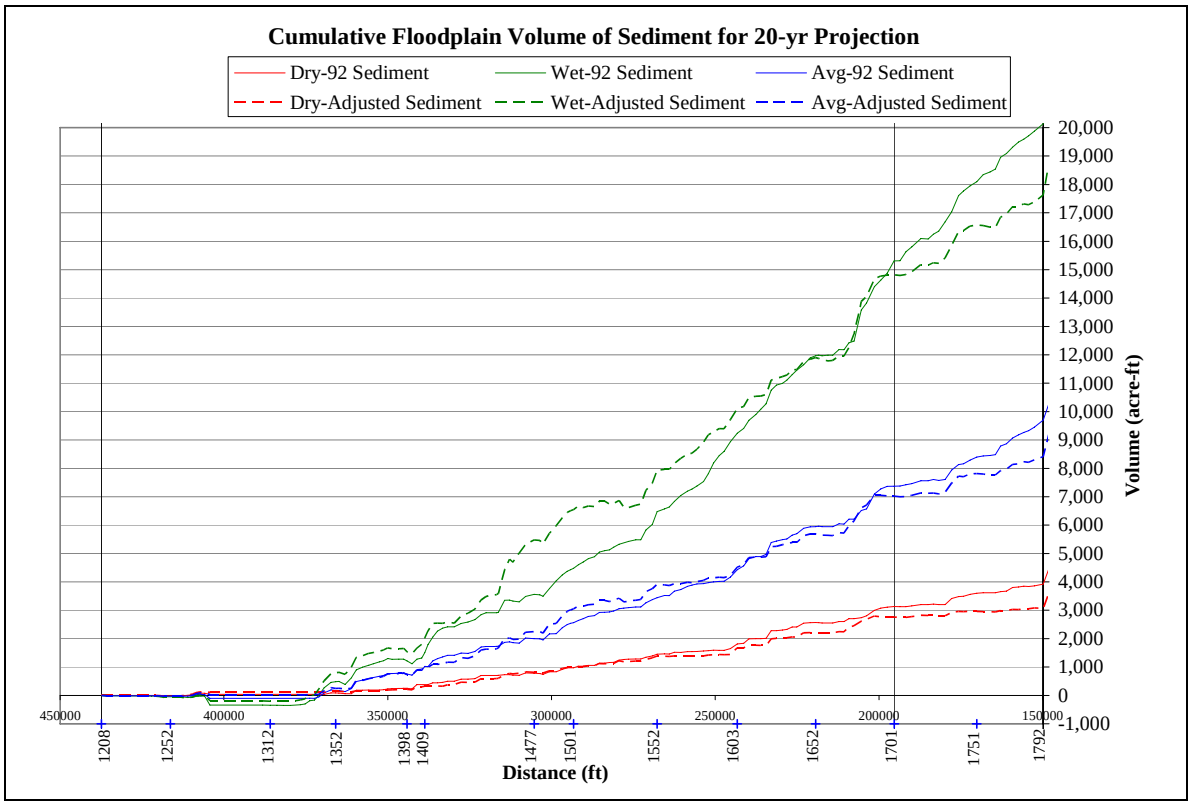

Figure 101: 20-year projected cumulative floodplain sediment augmentation comparison.

6 Conclusion

The project developed a comprehensive sediment transport model of the Middle Rio Grande from San Acacia Diversion Dam to Elephant Butte Reservoir. The model was calibrated with the data from two time periods: 1972 through 1992 and 1992 through 2002. These two periods were typical of dry and wet hydrologic conditions respectively. From the calibration results it was found that the modified GSTAR-1D model was capable of reproducing the river geometry changes caused by sediment transport. After the model was calibrated for these two time periods, the model was used to predict future sedimentation for three hydrologic regimes: wet, average, and dry. The following can be concluded:

Summary of Calibration Model Results:

- The numerical model reproduced the general shape and magnitude of the cumulative erosion and deposition in the main channel and the total cross-section for both calibration time periods; 1972 through 1992 and 1992 through 2002.
- For both calibration time periods, the numerical model reproduced the degradation in the mean bed profile downstream of San Acacia Diversion Dam as well as the aggradation in the mean bed profile near the reservoir.
- For both calibration time periods, the numerical model reproduced the cross-section geometry changes such as channel width, water surface width, thalweg elevation, and mean bed elevation fairly well. However, due to the limitations of a one-dimensional model, the model cannot predict the uneven deposition in the floodplains, main channel, or the channel meandering and migration.

Summary of 20-year Predictive No Action Model Results:

- The 20-year predictive model results are impacted by the greater magnitude and duration of peak flows encountered in the predictive hydrology and the perched system causing increased floodplain deposition.
- The 20-year predictive model produces deposition in the main channel with the dry hydrology, and main channel erosion with the average and wet hydrology just downstream of San Acacia Diversion Dam.
- Upstream of Agg/Deg#1352, additional channel erosion may take place if the future hydrology is relatively wet or many peak flows are encountered. If large flows are encountered, the coarsening of bed material may continue. Further work could define more precisely the magnitude of flows required to extend the erosion and coarsening of bed material in the upstream reach.
- Downstream of Agg/Deg# 1327, the 20-year predictive model produced similar sediment erosion in the main channel for all three hydrologic scenarios. The most likely cause of the erosion are large unregulated peak flows in the predictive hydrology. If these large flows occur, the channel capacity will most likely increase throughout the entire river.

- The 20-year predictive model produces floodplain deposition for all three hydrologic scenarios (dry, average, and wet) due to the unregulated peak flows in the predictive hydrology and the complex interaction of overbank flows in a perched channel system.
- Adjustments to the sequencing of the high flows in the wet hydrology showed that moving the high flows to the beginning of the simulation produced final 20-year results with less erosion upstream and more deposition downstream. This is a result of the channel having more time to recover from the effects of the higher flows present in the predictive hydrology.

Summary of 20-year Predictive Sediment Augmentation Model Results:

- Increasing the sand load at San Acacia Diversion Dam has the potential to stop or reverse the erosion occurring in the upper reach. For dry hydrological conditions, no additional sediment may be necessary. For average to wet hydrology, however, the increase in sand load would have to be approximately up to several thousand acre-ft. However, additional modeling of the upper reach is required to predict the volume of sediment currently entering the reach. If fine sediment is added to the system, additional floodplain deposition may occur in the downstream reach, and/or additional deposition will occur in Elephant Butte Reservoir.

Recommendations for future analysis:

- To allow proper calculation of aggradation/degradation between surveys, the potential errors in the 1992 floodplain data should be investigated more thoroughly by comparing the aerial survey data to field survey data that includes the floodplains. This would provide additional data to confirm the elevation of the floodplains.
- The overall bed changes in the predictive models differ from the historical trends due to the magnitude and duration of the unregulated discharges present in the predictive hydrology. Therefore, additional analysis of the predictive hydrology should be conducted to determine if flow regulation should be included in generating future flows.
- Collection of additional sediment data (suspended and bed material) to further define the incoming sediment rating curve, especially at higher discharges, and further define the bed material gradation variation along the reach.
- Additional research on the use of the Modified Einstein Procedure with suspended sediment field data to calculate the total sediment load on the Rio Grande.
- Additional calibration work to more closely simulate the change in channel slope and the coarsening of the river bed.
- Additional capabilities that could be introduced into the model would include: refining the sediment diffusion between the main channel and floodplains to better predict the main channel floodplain interaction in a perched system, and refinement of bed material mixing and armor layer development for Rio Grande conditions.

References

Bauer, T. R. and Hilldale, R. C., 2004. Middle Rio Grande Sediment and Substrate Data Collection. Draft. U.S. Department of the Interior, Bureau of Reclamation (Reclamation), Sedimentation and River Hydraulics Group, Denver, CO.

Bauer, T. R., 2004a. Bed Material Data Collection Trip Report, Rio Grande, New Mexico, July and August 2004. Draft. U.S. Department of the Interior, Bureau of Reclamation (Reclamation), Sedimentation and River Hydraulics Group, Denver, CO.

Bauer, T. R., 2004b. Sediment Transport Modeling in the Albuquerque Transition Zone. U.S. Department of the Interior, Bureau of Reclamation (Reclamation), Sedimentation and River Hydraulics Group, Denver, CO.

Bullard, K., 2004. Derivation of Middle Rio Grande Tributary Hydrographs. U.S. Bureau of Reclamation (Reclamation), Flood Hydrology Group, Denver, CO.

Colby, B.R., and Hembree, C.H., 1955. Computation of Total Sediment Discharge, Niobrara River near Cody, Nebraska, U.S. Geological Survey, Water-Supply, p. 1357.

Collins, K. and Ferrari, R., 2000. Elephant Butte Reservoir, 1999 Reservoir Survey. U.S. Department of the Interior, Bureau of Reclamation (Reclamation), Sedimentation and River Hydraulics Group, Denver, CO.

Collins, K., 2003. Sediment Transport Modeling of the Rio Grande from San Antonio to Elephant Butte Reservoir to Evaluate Various Temporary Channel Design Configurations (Draft) U.S. Department of the Interior, Bureau of Reclamation (Reclamation), Sedimentation and River Hydraulics Group, Denver, CO.

Daraio, J., 2003. Average Annual Watershed Soil Erosion (Washload) Estimates using the RUSLE (Revised Universal Soil Loss Equation) for Arroyos in the Rio Grande Basin. U.S. Department of the Interior, Bureau of Reclamation (Reclamation), Sedimentation and River Hydraulics Group, Denver, CO.

Engelund, F. and E. Hansen, 1972. A Monograph on Sediment Transport in Alluvial Streams, Teknisk Forlag, Copenhagen.

Gorbach, C., 1999. History and Significance of the Low Flow Conveyance Channel. WRRI Conference Proceedings 1999.

Holmquist-Johnson, C. L. and Raff, D., 2004. Bureau of Reclamation Automated Modified Einstein Procedure (BORAMEP) Program for Computing Total Sediment Discharge. Draft. U.S. Department of the Interior, Bureau of Reclamation (Reclamation), Sedimentation and River Hydraulics Group, Denver, CO.

Klawon, J. and Makar, P., 2003. Historical Terrace Mapping: Escondida Bridge to Pool of Elephant Butte Reservoir. U.S. Department of the Interior, Bureau of Reclamation (Reclamation), Sedimentation and River Hydraulics Group, Denver, CO.

Lagasse, P. F., 1980. An Assessment of the Response of the Rio Grande to Dam Construction- Cochiti to Isleta, U. S., Army Corps of Engineers Technical Report, Albuquerque, New Mexico, 133 p.

Lane, W. L., 2004. Synthetic Flows for Rio Grande Sedimentation Modeling: 2004 Update. W L Lane Consulting, Golden Colorado, August 2004.

Lara, J. M., 1972. The 1969 Elephant Butte Reservoir Sediment Survey. U.S. Department of the Interior, Bureau of Reclamation Report REC-ERC-72-13, Hydrology Branch, Denver, CO.

Lara, J. M., 1983. Elephant Butte Reservoir, 1980 Sedimentation Survey. U.S. Department of the Interior, Bureau of Reclamation (Reclamation), Sedimentation and River Hydraulics Group, Denver, CO.

Makar, P. and Bauer, T. R., 2003. Middle Rio Grande Planform Characterization and Analysis. June. U.S. Department of the Interior, Bureau of Reclamation (Reclamation), Sedimentation and River Hydraulics Group, Denver, CO.

Makar, P. and Strand, R. I., 2003. Responses of the Middle Rio Grande: San Acacia to Elephant Butte. Draft. U.S. Department of the Interior, Bureau of Reclamation (Reclamation), Sedimentation and River Hydraulics Group, Denver, CO.

Meyer-Peter, E., and R. Muller, 1948. “Formulas for Bed-Load Transport,” International Association of Hydraulic Research, 2nd Meeting, Stockholm, Sweden.

Oliver K. J., (2004). Planform interpretation of the Rio Grande from Velarde to the Narrows of Elephant Butte - Geographic Information Database of the Historic River Channel for 1908 - 2001. U. S. Department of the Interior, Bureau of Reclamation (Reclamation), Technical Service Center, Remote Sensing and GIS Group, Denver, CO.

Orvis, C. J., 1989. Elephant Butte Reservoir, 1988 Sedimentation Survey. U.S. Department of the Interior, Bureau of Reclamation (Reclamation), Sedimentation and River Hydraulics Group, Denver, CO.

Reclamation, 2003. Geomorphologic Assessment of the Rio Grande San Acacia Reach, Technical Report, River Analysis Team, Bureau of Reclamation (Reclamation), Albuquerque, New Mexico, USA.

Sailer, M, and Young, C., 2002. Sedimentation studies of aggradation or degradation in the Middle Rio Grand project. Draft. U.S. Department of the Interior, Bureau of Reclamation (Reclamation), Sedimentation and River Hydraulics Group, Denver, CO.

Samad, M. A., Baird, D. C., and Montoya, F. P., 1996. Calibration of Sediment Transport Model for the upper End of Elephant Butte Reservoir. U.S. Department of the Interior, Bureau of Reclamation (Reclamation), Sedimentation and River Hydraulics Group, Denver, CO.

Smith, K, 2003. Bureau of Reclamation (Reclamation), Albuquerque Area Office News Release on Temporary Channel Construction, Construction Progress Update, December.

Strand, R. I., and Pemberton, E. L., 1982. Reservoir Sedimentation, Technical Guideline for Bureau of Reclamation (Reclamation).

U.S. Army Corps of Engineers (USACE), 2004. Hydrologic Engineering Center-River Analysis System User's Manual, Version 3.1, Hydrologic Engineering Center, Davis, California.

U.S. Bureau of Reclamation (Reclamation), (1950-1997). Project History Reports for the Middle Rio Grande Project.

U.S. Bureau of Reclamation (Reclamation), 1969. Guide for Application of Total Sediment Load Computer Program – Psands. Sedimentation Branch, Division of Project Investigations, Office of Chief Engineer, Denver, Colorado.

U.S. Bureau of Reclamation (Reclamation), 1982. Project Data Book.

U.S. Geological Survey (USGS), 1895-2002. Surface Water Records, Water Resources Data, New Mexico.

Vermeyen, T., 1995. Erosional and Depositional Characteristics of Cohesive Sediments Found in Elephant Butte Reservoir, New Mexico. Technical Report R-95-15., Water Resources Services, Technical Service Center, Bureau of Reclamation (Reclamation), Denver, CO.

Yang C. T., 1984. Unit Stream Power Equation for Gravel, Journal of Hydraulic Engineering, ASCE, vol. II 0, no. 12.

Yang, C. T., 1973. Incipient motion and sediment transport. J. Hydraulics Div., ASCE, 99:1679-1704.

Yang, C.T., Huang, J., Greimann, B.P., 2004. “User’s Manual for GSTAR-1D 1.0 (Generalized Sediment Transport for Alluvial Rivers – One Dimension version 1.0),” Draft publication of Bureau of Reclamation (Reclamation), Denver, CO.

Appendix A – Chronology of significant Rio Grande events

-provided electronically in PDF format on the enclosed disk under the File: *Appendix A – Chronology of Significant Rio Grande Events.pdf.*

Appendix B – Water and sediment discharge data

-provided electronically in PDF format on the enclosed disk under the File: *Appendix B – Water and Sediment Discharge Data.pdf.*

Appendix C – Historical cross-section plots

-provided electronically in PDF format on the enclosed disk under the File: *Appendix C – Historical XS Plots.pdf.*

Appendix D – Historical planform plots

-provided electronically in PDF format on the enclosed disk under the File: *Appendix D – Historical Planform Plots.pdf.*

Appendix E – 1972-1992 calibration cross-section plots

-provided electronically in PDF format on the enclosed disk under the File: *Appendix E – 1972-1992 Calibration XS Plots.pdf.*

Appendix F – 1992-2002 calibration cross-section plots

-provided electronically in PDF format on the enclosed disk under the File: *Appendix F – 1992-2002 Calibration XS Plots.pdf.*

Appendix G – Predicted future cross-section plots

-provided electronically in PDF format on the enclosed disk under the File: *Appendix G – 2002-2022 Predicted XS Plots.pdf.*